

# Geology of the Northern Norrbotten ore province, northern Sweden

Paper 6 (13)

Editor: Stefan Bergman



**SGU**

Sveriges geologiska undersökning  
Geological Survey of Sweden



Rapporter och meddelanden 141

# **Geology of the Northern Norrbotten ore province, northern Sweden**

Editor: Stefan Bergman

Sveriges geologiska undersökning  
2018

ISSN 0349-2176  
ISBN 978-91-7403-393-9

**Cover photos:**

*Upper left:* View of Torneälven, looking north from Sakkaravaara, northeast of Kiruna. **Photographer:** Stefan Bergman.

*Upper right:* View (looking north-northwest) of the open pit at the Aitik Cu-Au-Ag mine, close to Gällivare. The Nautanen area is seen in the background. **Photographer:** Edward Lynch.

*Lower left:* Iron oxide-apatite mineralisation occurring close to the Malmberget Fe-mine. **Photographer:** Edward Lynch.

*Lower right:* View towards the town of Kiruna and Mt. Luossavaara, standing on the footwall of the Kiruna apatite iron ore on Mt. Kiirunavaara, looking north. **Photographer:** Stefan Bergman.

**Head of department, Mineral Resources:** Kaj Lax

**Editor:** Stefan Bergman

**Layout:** Tone Gellerstedt och Johan Sporrang, SGU

**Print:** Elanders Sverige AB

Geological Survey of Sweden  
Box 670, 751 28 Uppsala  
phone: 018-17 90 00  
fax: 018-17 92 10  
e-mail: sgu@sgu.se  
www.sgu.se

# Table of Contents

<b>Introduktion (in Swedish)</b> .....	<b>6</b>
<b>Introduction</b> .....	<b>7</b>
<b>1. Regional geology of northern Norrbotten County</b> .....	<b>9</b>
References .....	14
<b>2. Geology, lithostratigraphy and petrogenesis of c. 2.14 Ga greenstones in the Nunasvaara and Masugnsbyn areas, northernmost Sweden</b> .....	<b>19</b>
Abstract .....	19
Introduction .....	20
Regional setting of Norrbotten greenstone belts .....	21
Geology of the Nunasvaara and Masugnsbyn greenstone successions .....	23
Petrogenesis of the greenstones: Preliminary U-Pb geochronology, litho-geochemistry and Sm-Nd isotopic results .....	52
Summary and conclusions .....	68
Acknowledgements .....	69
References .....	70
<b>3. Stratigraphy and ages of Palaeoproterozoic metavolcanic and metasedimentary rocks at Käymäjärvi, northern Sweden</b> .....	<b>79</b>
Abstract .....	79
Introduction .....	80
General geology .....	80
Structure and stratigraphy of the Käymäjärvi area .....	81
Sample description .....	89
Analytical methods .....	90
Analytical results .....	91
Discussion .....	96
Conclusions .....	100
Acknowledgements .....	101
References .....	101
<b>4. Petrological and structural character of c. 1.88 Ga meta-volcanosedimentary rocks hosting iron oxide-copper-gold and related mineralisation in the Nautanen–Aitik area, northern Sweden</b> .....	<b>107</b>
Abstract .....	107
Introduction .....	108
Regional setting .....	108
Geology of the Nautanen–Aitik area .....	110
Structural geology and deformation .....	132
Summary and Conclusions .....	144
Acknowledgements .....	144
References .....	145
<b>5. Age and lithostratigraphy of Svecofennian volcanosedimentary rocks at Masugnsbyn, northernmost Sweden – host rocks to Zn-Pb-Cu- and Cu ±Au sulphide mineralisations</b> .....	<b>151</b>
Abstract .....	151
Introduction .....	152
Geological overview .....	153
Discussion and preliminary conclusions .....	194
Acknowledgements .....	197
References .....	198

<b>6. Folding observed in Palaeoproterozoic supracrustal rocks in northern Sweden</b> .....	<b>205</b>
Abstract .....	205
Introduction .....	205
Geological setting .....	207
Structural geological models .....	209
Geophysical data .....	212
Discussion and Conclusions .....	251
References .....	255
<b>7. The Pajala deformation belt in northeast Sweden:</b>	
<b>Structural geological mapping and 3D modelling around Pajala</b> .....	<b>259</b>
Abstract .....	259
Geological setting .....	259
Structural analysis .....	263
2D regional geophysical modelling and geological interpretation .....	272
Local and semi-regional 3D models .....	274
Discussion .....	280
Conclusions .....	283
References .....	284
<b>8. The Vakko and Kovo greenstone belts north of Kiruna:</b>	
<b>Integrating structural geological mapping and geophysical modelling</b> .....	<b>287</b>
Abstract .....	287
Introduction .....	287
Geological setting .....	289
Geophysical surveys .....	291
Results .....	296
Discussion .....	306
Conclusions .....	308
References .....	309
<b>9. Geophysical 2D and 3D modelling in the areas around</b>	
<b>Nunasvaara and Masugnsbyn, northern Sweden</b> .....	<b>311</b>
Abstract .....	311
Nunasvaara .....	312
2D modelling of profile 1 and 2 .....	316
Masugnsbyn .....	321
Regional modelling .....	329
Conclusion .....	338
References .....	339
<b>10. Imaging deeper crustal structures by 2D and 3D modelling of geophysical data.</b>	
<b>Examples from northern Norrbotten</b> .....	<b>341</b>
Abstract .....	341
Introduction .....	341
Methodology .....	342
Geological setting .....	342
Results .....	345
Conclusion .....	358
Outlook .....	358
Acknowledgements .....	358
References .....	359

<b>11. Early Svecokarelian migmatisation west of the Pajala deformation belt, northeastern Norrbotten province, northern Sweden</b>	<b>361</b>
Abstract	361
Introduction	362
Geology of the Masugnsbyn area	362
Discussion	372
Conclusions	374
Acknowledgements	375
References	376
<b>12. Age and character of late-Svecokarelian monzonitic intrusions in northeastern Norrbotten, northern Sweden</b>	<b>381</b>
Abstract	381
Introduction	381
Geological setting	382
Analytical methods	387
Analytical results	388
Discussion	393
Conclusions	396
Acknowledgements	396
References	397
<b>13. Till geochemistry in northern Norrbotten –regional trends and local signature in the key areas</b>	<b>401</b>
Abstract	401
Introduction	401
Glacial geomorphology and quaternary stratigraphy of Norrbotten	403
Samples and methods	406
Results and discussion	407
Conclusions	426
Acknowledgements	427
References	427

# Introduktion

Stefan Bergman & Ildikó Antal Lundin

Den här rapporten presenterar de samlade resultaten från ett delprojekt inom det omfattande tvärvetenskapliga Barentsprojektet i norra Sverige. Projektet initierades av Sveriges geologiska undersökning (SGU) som ett första led i den svenska mineralstrategin. SGU fick ytterligare medel av Näringsdepartementet för att under en fyraårsperiod (2012–2015) samla in nya geologiska, geofysiska och geokemiska data samt för att förbättra de geologiska kunskaperna om Sveriges nordligaste län. Det statligt ägda gruvbolaget LKAB bidrog också till finansieringen. Projektets strategiska mål var att, genom att tillhandahålla uppdaterad och utförlig geovetenskaplig information, stödja prospekterings- och gruvindustrin för att förbättra Sveriges konkurrenskraft inom mineralnäringen. Ny och allmänt tillgänglig geovetenskaplig information från den aktuella regionen kan hjälpa prospekterings- och gruvföretag att minska sina risker och prospekteringskostnader och främjar därigenom ekonomisk utveckling. Dessutom bidrar utökad geologisk kunskap till en effektiv, miljövänlig och långsiktigt hållbar resursanvändning. All data som har samlats in i projektet lagras i SGUs databaser och är tillgängliga via SGU.

Syftet med det här delprojektet var att få en djupare förståelse för den stratigrafiska uppbyggnaden och utvecklingen av de mineraliserade ytbergarterna i nordligaste Sverige. Resultaten, som är en kombination av ny geologisk kunskap och stora mängder nya data, kommer att gynna prospekterings- och gruvindustrin i regionen i många år framöver.

Norra Norrbottens malmprovins står för en stor del av Sveriges järn- och kopparmalmsproduktion. Här finns fyra aktiva metallgruvor (mars 2018) och mer än 500 dokumenterade mineraliseringar. Fyndigheterna är av många olika slag, där de viktigaste typerna är stratiforma kopparmineraliseringar, järnformationer, apatitjärnmalm av Kirunatyp och epigenetiska koppar-guldmineraliseringar. En vanlig egenskap hos de flesta malmer och mineraliseringar i Norr- och Västerbotten är att de har paleoproterozoiska vulkaniska och sedimentära bergarter som värdbergart. För undersökningarna valdes ett antal nyckelområden med bästa tillgängliga blottningsgrad. De utvalda områdena representerar tillsammans en nästan komplett stratigrafi i ytbergarter inom åldersintervallet 2,5–1,8 miljarder år.

Rapporten består av tretton kapitel och inleds med en översikt över de geologiska förhållandena, som beskriver huvuddragen i de senaste resultaten. Översikten följs av fyra kapitel (2–5) som huvudsakligen handlar om litostratigrafi och åldersbestämningar av ytbergarterna. Huvudämnet för de därpå följande fem kapitlen (6–10) är 3D-geometri och strukturell utveckling. Därefter kommer två kapitel (11–12) som fokuserar på U-Pb-datering av en metamorf respektive intrusiv händelse. Rapporten avslutas med en studie av geokemin hos morän i Norra Norrbottens malmprovins (kapitel 13).

# Introduction

Stefan Bergman & Ildikó Antal Lundin

This volume reports the results from a subproject within the Barents Project, a major programme in northern Sweden. The multidisciplinary Barents Project was initiated by SGU as the first step in implementing the Swedish National Mineral Strategy. SGU obtained additional funding from the Ministry of Enterprise and Innovation to gather new geological, geophysical and till geochemistry data, and generally enhance geological knowledge of northern Sweden over a four-year period (2012–2015). The state-owned iron mining company LKAB also helped to fund the project. The strategic goal of the project was to support the exploration and mining industry, so as to improve Sweden's competitiveness in the mineral industry by providing modern geoscientific information. Geological knowledge facilitates sustainable, efficient and environmentally friendly use of resources. New publicly available geoscientific information from this region will help exploration and mining companies to reduce their risks and exploration costs, thus promoting economic development. All data collected within the project are stored in databases and are available at SGU.

This subproject within the Barents Project aims to provide a deeper understanding of the stratigraphy and depositional evolution of mineralised supracrustal sequences in northernmost Sweden. The combined results in the form of new geological knowledge and plentiful new data will benefit the exploration and mining industry in the region for many years to come.

The Northern Norrbotten ore province is a major supplier of iron and copper ore in Sweden. There are four active metal mines (March 2018) and more than 500 documented mineralisations. A wide range of deposits occur, the most important types being stratiform copper deposits, iron formations, Kiruna-type apatite iron ores and epigenetic copper-gold deposits. A common feature of most deposits is that they are hosted by Palaeoproterozoic metavolcanic or metasedimentary rocks. A number of key areas were selected across parts of the supracrustal sequences with the best available exposure. The areas selected combine to represent an almost complete stratigraphic sequence.

This volume starts with a brief overview of the geological setting, outlining some of the main recent achievements. This is followed by four papers (2–5) dealing mainly with lithostratigraphy and age constraints on the supracrustal sequences. 3D geometry and structural evolution are the main topics of the next set of five papers (6–10). The following two contributions (11–12) focus on U-Pb dating of a metamorphic event and an intrusive event, respectively. The volume concludes with a study of the geochemical signature of till in the Northern Norrbotten ore province (13).

**Authors, paper 6:**

*Susanne Grigull*

Geological Survey of Sweden,  
Department of Physical Planning,  
Uppsala, Sweden

*Robert Berggren*

Geological Survey of Sweden,  
Department of Mineral Resources,  
Uppsala, Sweden

*Johan Jönberger*

Geological Survey of Sweden,  
Department of Mineral Resources,  
Uppsala, Sweden

*Cecilia Jönsson*

Geological Survey of Sweden,  
Department of Mineral Resources,  
Uppsala, Sweden

*Fredrik Hellström*

Geological Survey of Sweden,  
Department of Mineral Resources,  
Uppsala, Sweden

*Stefan Luth*

Geological Survey of Sweden,  
Department of Mineral Resources,  
Uppsala, Sweden

## 6. Folding observed in Palaeoproterozoic supracrustal rocks in northern Sweden

Susanne Grigull, Robert Berggren, Johan Jönberger,  
Cecilia Jönsson, Fredrik Hellström & Stefan Luth

### ABSTRACT

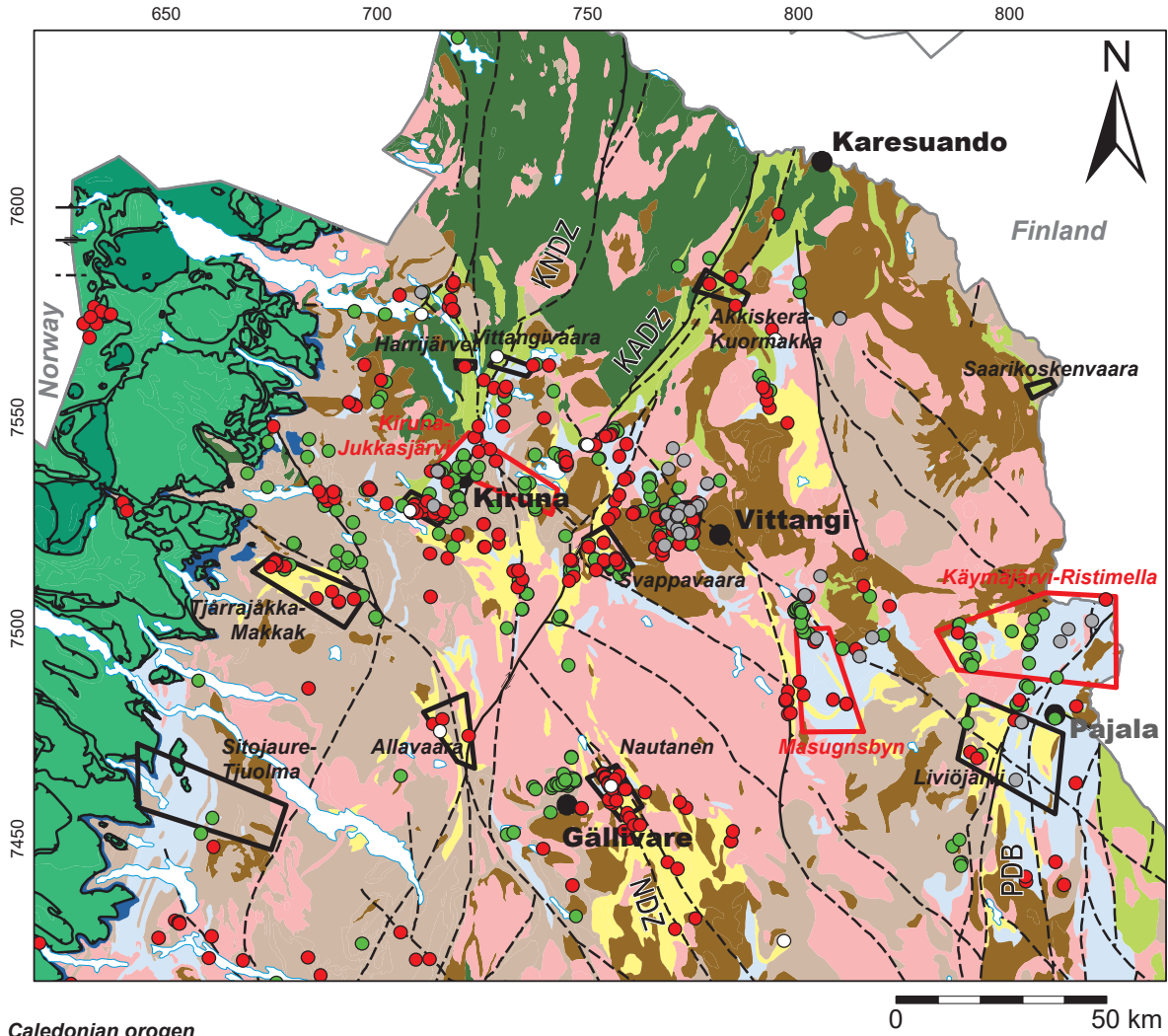
Despite the abundance of iron ore and sulphide deposits in the northern Fennoscandian Shield and a long history of mining in northern Sweden, the structural geological development of the area is poorly understood. In this paper, available and newly acquired geological and geophysical data are integrated and interpreted with particular emphasis on characterising the folding history in supracrustal rocks in these parts of the northern Fennoscandian Shield. The collection and integration of geological and geophysical data concentrate on key areas north of Kiruna, south of Masugnsbyn and north of Pajala. The Kiruna key area lies to the west of a major dextral-reverse shear zone: the Karesuando–Arjeplog deformation zone (KADZ), while the other areas lie to the east of the zone. A comparison of the folding history between these areas shows that the rocks to the west have been subject to fewer folding phases than those to the east.

### INTRODUCTION

During the late Palaeoproterozoic (2.0–1.8 Ga), the Fennoscandian Shield was subject to the polycyclic Svecokarelian (or Svecofennian) orogeny. During the orogeny strain in the northern Fennoscandian Shield was partitioned into localised deformation zones and zones occupying the space between these shear zones (Fig. 1).

Structural geological studies of the northern Fennoscandian Shield addressing deformation in the Kiruna area and within the Kiruna–Naimakka deformation zone (KNDZ) were mainly undertaken by, e.g., Vollmer et al. (1984), Witschard (1984), Forsell (1987), Wright (1988), Talbot & Koyi (1995) and Bergman et al. (2001). Work specifically addressing deformation in the Pajala area and within the Pajala deformation belt was carried out by, e.g. Berthelsen & Marker (1986), Henkel (1991), Kärki et al. (1993), Olesen & Sandstad (1993), Bergman et al. (2006), Niiranen et al. (2007) and Luth et al. (2015).

Bergh et al. (2010, 2012) studied the deformation history in tectonic windows exposing Palaeoproterozoic deformation zones in Norway. Lahtinen et al. (2015a) present a new model for the tectonic evolution of Fennoscandia from detailed structural studies in the Palaeoproterozoic Martimo belt in Finland.



**Caledonian orogen**

- Margin to the continent Baltica
- Terranes from outboard of the continent Baltica

**Platformal sedimentary cover rocks on the Fennoscandian Shield**

- Ediacaran-Cambrian cover rocks on the Fennoscandian Shield

**Syn-orogenic rocks of the 2.0–1.8 Ga orogen**

- Mostly non-metamorphic GSDG-GP and subordinate GDG intrusive suites, supracrustal rocks (1.8 Ga)
- Variably metamorphosed GSDG-GP and subordinate GDG intrusive suites, supracrustal rocks (1.88 or 1.87–1.83 Ga)
- Metamorphosed GDG intrusive suite (1.90–1.88 or 1.87 Ga)
- Metamorphosed volcanic rock, carbonate rock and skarn (1.91–1.86 Ga)
- Metamorphosed clastic sedimentary and volcanic rocks

**Archaean (3.2–2.7 Ga) and Palaeoproterozoic (2.5–2.0 Ga), pre-orogenic rocks of the 2.0–1.8 Ga orogen**

- Metamorphosed sedimentary rock, basic-ultrabasic volcanic rock and gabbro (2.44–2.0 Ga)
- Metamorphosed supracrustal rock, orthogneiss, granitoid and dioritoid (3.20–2.65 Ga) reworked after a c. 2.7 Ga event

- Graphite deposit
- Precious metal deposit
- Sulphide deposit
- Iron ore deposit
- Thrust fault
- Strike-slip fault
- - - Deformation zone, unspec.

Figure 1. Simplified geological map of northern Norrbotten, modified from the 1:1 000 000 bedrock geological map of Sweden (Bergman et al. 2012). The black and red polygons show the key areas that were studied during the Barents project. The key areas marked in red are those from which the majority of the information on folding was derived for this study. KNDZ: Kiruna–Naimakka deformation zone, KADZ: Karesuando–Arjeplog deformation zone, NDZ: Nautanen deformation zone, PDB: Pajala deformation belt, GSDG: Granite-syenitoid-dioritoid-gabbroid, GP: Granite-pegmatite, GDG: Granitoid-dioritoid-gabbroid.

Bergman et al. (2001) and Lahtinen et al. (2015b) conclude that rocks of the Fennoscandian Shield have been affected by at least two, and locally three or four, folding phases. However, the timing between them is poorly constrained and it is difficult to interpret the relationships between ductile folding phases and localised deformation observed in major crustal scale shear zones such as the Kiruna–Naimakka deformation zone, the Karesuando–Arjeplog deformation zone, the Nautanen deformation zone, and the Pajala deformation belt (Fig. 1). But it is important to understand the relationship between various deformation phases in order to establish the structural architecture and tectonic evolution of the northern Fennoscandian Shield. Where possible, the work carried out for this paper aims to clarify the ductile deformation history of the Palaeoproterozoic rocks before formation of the high strain deformation belts. Integrating available data with newly acquired geophysical and geological data, this paper focuses on unravelling the folding patterns and phases observed in the Kiruna–Jukkasjärvi, Masugnsbyn, and Käymäjärvi–Ristimella key areas.

## GEOLOGICAL SETTING

The supracrustal rocks of northern Norrbotten can be divided into rocks that were deposited before or during the approximately 2.0–1.8 Ga orogeny (Fig. 1; see also Bergman 2018). Pre-orogenic rocks include deformed Archaean basement rocks and overlying younger, predominantly mafic volcanic and volcanoclastic-sedimentary successions as well as carbonate rocks collectively known as the Karelian greenstone group (e.g. Martinsson et al. 2016). In the key areas west of the Karesuando–Arjeplog deformation zone (KADZ in Fig. 1) the greenstones are assigned to the Kiruna greenstone group, whereas in the eastern key areas greenstones are defined as the Veikkavaara greenstone group. The Kiruna greenstone group is thought to have been deposited in a failed rift setting (Martinsson 2004), whereas the Veikkavaara greenstone group was more likely deposited at the margins of a rift (Martinsson et al. 2016).

Younger, syn-orogenic, supracrustal rocks overlie the Karelian greenstones and consist of intermediate to felsic volcanic rocks, and (epi)clastic sediment successions (e.g. Kurravaara conglomerate, Porphyrite group, Pahakurkio group, Kalixälv group, Sammakkovaara group, Kiirunavaara group). These rocks are assumed to have formed along an active continental margin during a period of NE-directed subduction under the Archaean craton, and related accretion of volcanic arc complexes (Nironen 1997, Korja et al. 2006, Lahtinen et al. 2009, Martinsson et al. 2016 and references therein).

Both pre- and syn-orogenic rocks are intruded by numerous syn- and post-orogenic magmatic suites, which locally led to contact metamorphism and metasomatic alterations within the intruded rocks. All supracrustal rocks have undergone metamorphism, and metamorphic grades range from greenschist to upper amphibolite facies, seemingly increasing in grade from west to east. Where the protolith to the metamorphic rocks is still discernible, the prefix “meta” is included when referring to the rock type. Metamorphic terminology is used for the metamorphic rock types where the protolith is unknown.

The stratigraphy of the key areas addressed in this paper has been described in various SGU reports. Grigull & Antal Lundin (2013) and Grigull & Jönberger (2014) provide a summary for the Kiruna area; Hellström & Jönsson (2014) for the Masugnsbyn area; and Luth & Jönsson (2014), Luth et al. (2015), Grigull et al. (2014), Grigull & Berggren (2015) for the areas south and north of Pajala. Figure 2 illustrates the generalised, correlated lithostratigraphy for the key areas in relation to each other (Martinsson 1995). The lithostratigraphic sequences used for the Kiruna, Masugnsbyn, and Käymäjärvi–Ristimella key areas are described in more detail in the respective sections below.

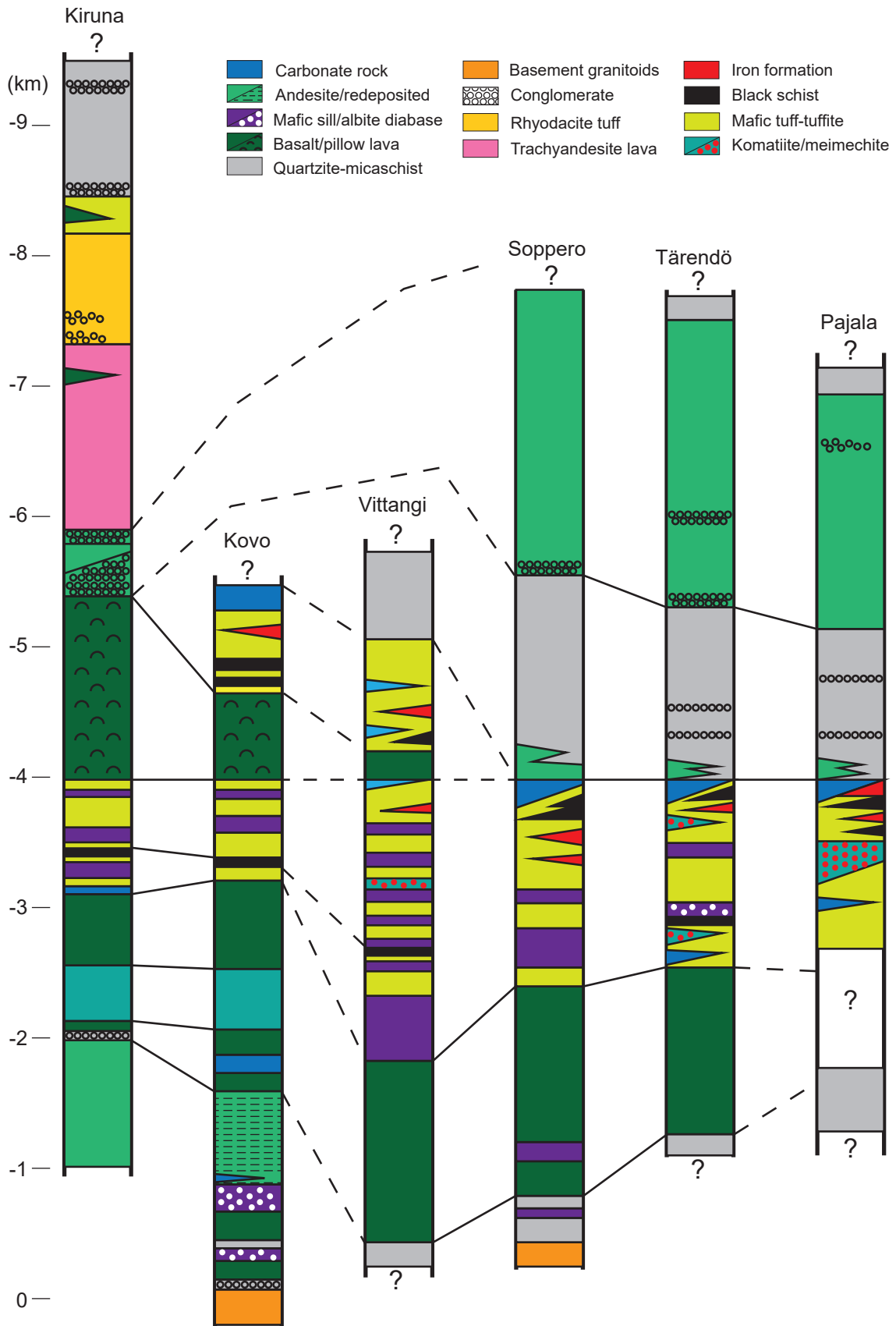


Figure 2. Correlated lithostratigraphic columns for Palaeoproterozoic supracrustal rocks in northern Norrbotten. After Martinsson (1995).

## STRUCTURAL GEOLOGICAL MODELS

### Kiruna–Jukkasjärvi key area and Pussijärvi

#### *Lithostratigraphy*

The current understanding of the geological units and lithostratigraphy in the Kiruna–Jukkasjärvi key area is largely based on Geijer (1910), Offerberg (1967), Witschard (1984), Forsell (1987), Martinsson (1997), Bergman et al. (2001), Martinsson (2004), and Martinsson et al. (2016). Martinsson et al. (2016) provide the most recent stratigraphic overview of the supracrustal and intrusive rocks in northern Norrbotten. In this report the stratigraphic sequence and terminology proposed by Martinsson et al. (2016) are adapted specifically for the rocks in the Kiruna key area. In the Kiruna area, and up to Kurravaara village, the entire stratigraphic succession from the Kovo group through to the Hauki quartzite can be observed. A simplified stratigraphic column is shown in Figure 3.

To the northeast of lake Mikonjärvi, the oldest supracrustal rocks in the Kiruna area occur as a thin sliver of conglomerate belonging to the Kovo group and unconformably overlying an Archaean granite intrusion. This conglomerate is overlain by most of the Kiruna greenstone group, starting with predominantly amygdaloidal basalts and conglomerates belonging to the Såkevaratjah formation (200–400 m), followed by ultrabasic rocks of the Ädnamvare formation (500 m), and a thick package of amygdaloidal basaltic lava flows of the Pikse formation (500–1000 m). The Pikse formation is overlain by the economically important, sulphide-bearing Viscaria formation (600 m), which predominantly consists of graphite-bearing tuffites, mafic sills, and some carbonate rocks. For the sake of simplicity, the reinterpreted map for the Kiruna area in Figure 3 does not display rocks older than the Viscaria formation. The reader is referred to Martinsson (1997) for a description of those rocks. The Viscaria formation is followed by an approximately 1500 m thick sequence of basaltic pillow lavas interrupted by thinner tuffitic units belonging to the Peuravaara formation. From Lake Kirkkoväärtijärvi up to Lake Linkaluoppal, the Peuravaara formation is followed by graphitic schists, iron-rich metasedimentary rocks, and dolomitic rocks of the Linkaluoppal formation (min. 700 m). The Linkaluoppal formation is missing in the Kiruna area and up to Kurravaara township. Here, conglomeratic to sandy metasedimentary rocks belonging to the Kurravaara conglomerate (see below) directly overlay pillow lavas of the Peuravaara formation, indicating at least a local unconformity between the pre-orogenic Kiruna greenstone group and the overlying syn-orogenic units (see also Martinsson 1997).

The Kurravaara conglomerate is clast-supported with a sandy matrix. The clasts are well-rounded, and the concentration of Kiruna greenstone group-derived clasts is high at the bottom. Towards the top most clasts are derived from volcanic rocks of the Porphyrite group (e.g. Martinsson & Perdahl, 1995). The Porphyrite group predominantly occurs east of Kiruna, and it is suggested that it was deposited contemporaneously with the Kurravaara conglomerate (Martinsson & Perdahl 1995, Kumpulainen 2000, Martinsson 2004, Martinsson et al. 2016). The volcanic rocks of the Porphyrite group do not occur in the Kiruna key area.

The Kurravaara conglomerate is mainly covered by metavolcanic rocks of the Kiirunavaara group, which is divided into three formations (Martinsson 2004). The Hopukka formation mainly consists of andesitic to trachyandesitic metavolcanic rocks, followed by rhyodacitic rocks and occasionally conglomerates of the Luossavaara formation. The Luossavaara formation forms the hanging wall to the Kiirunavaara and Luossavaara magnetite ore deposits. It is followed by the Matojärvi formation which predominantly consists of felsic tuffite, basalt, reworked volcanoclastic metasedimentary rocks and clastic metasedimentary rocks such as metagreywacke and phyllite. The Matojärvi formation forms the hanging wall to hematite ore deposits such as Rektorn, Henry and Nukutus. It is also the hanging wall to the Lappmalmen ore body that does not crop out, but can be interpreted as a displaced part of the Rektorn ore body due to late horst and graben type brittle faulting (Parák 1975).

Although the lower part of the Kiirunavaara group is lithologically similar to the rocks of the Por-

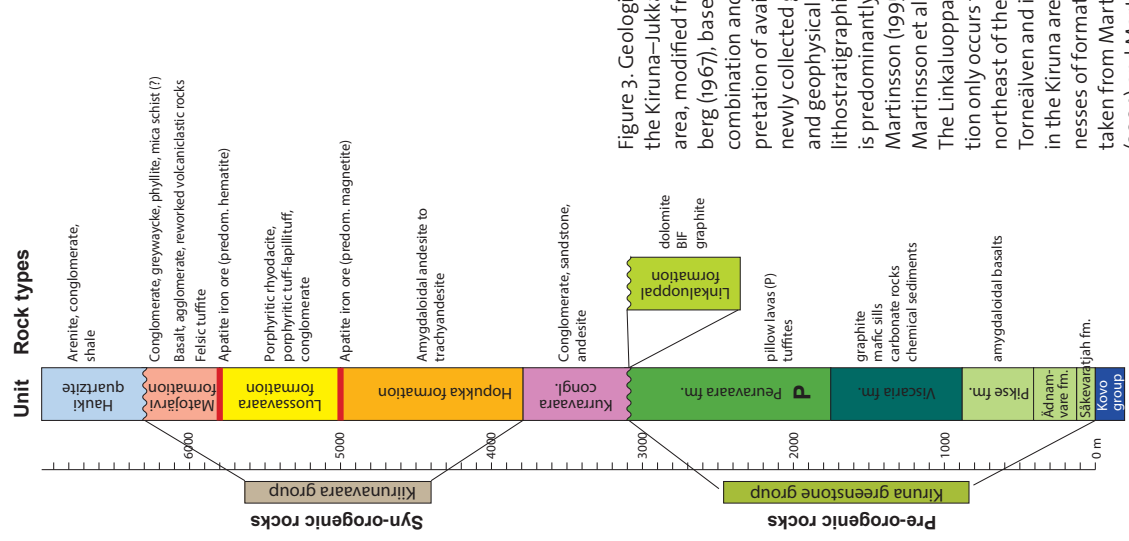
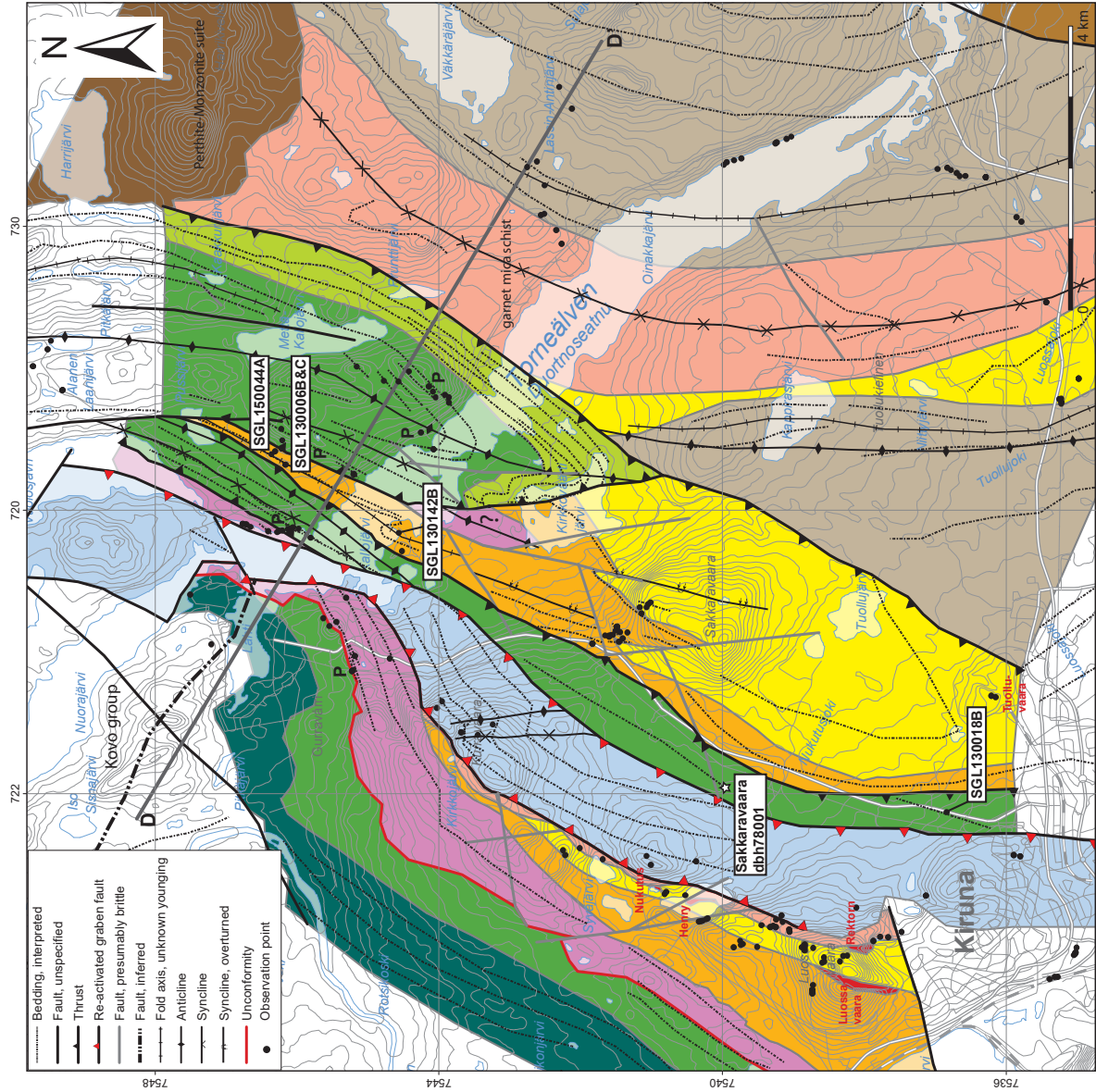


Figure 3. Geological map of the Kiruna–Jukkasjärvi key area, modified from Offerberg (1967), based on the combination and reinterpretation of available and newly collected geological and geophysical data. The lithostratigraphic column is predominantly based on Martinsson (1995) and Martinsson et al. (2016). The Linkaluoppal formation only occurs to the northeast of the river Torneälven and is eroded in the Kiruna area. Thickneses of formations are taken from Martinsson et al. (2004) and Martinsson et al. (2016).

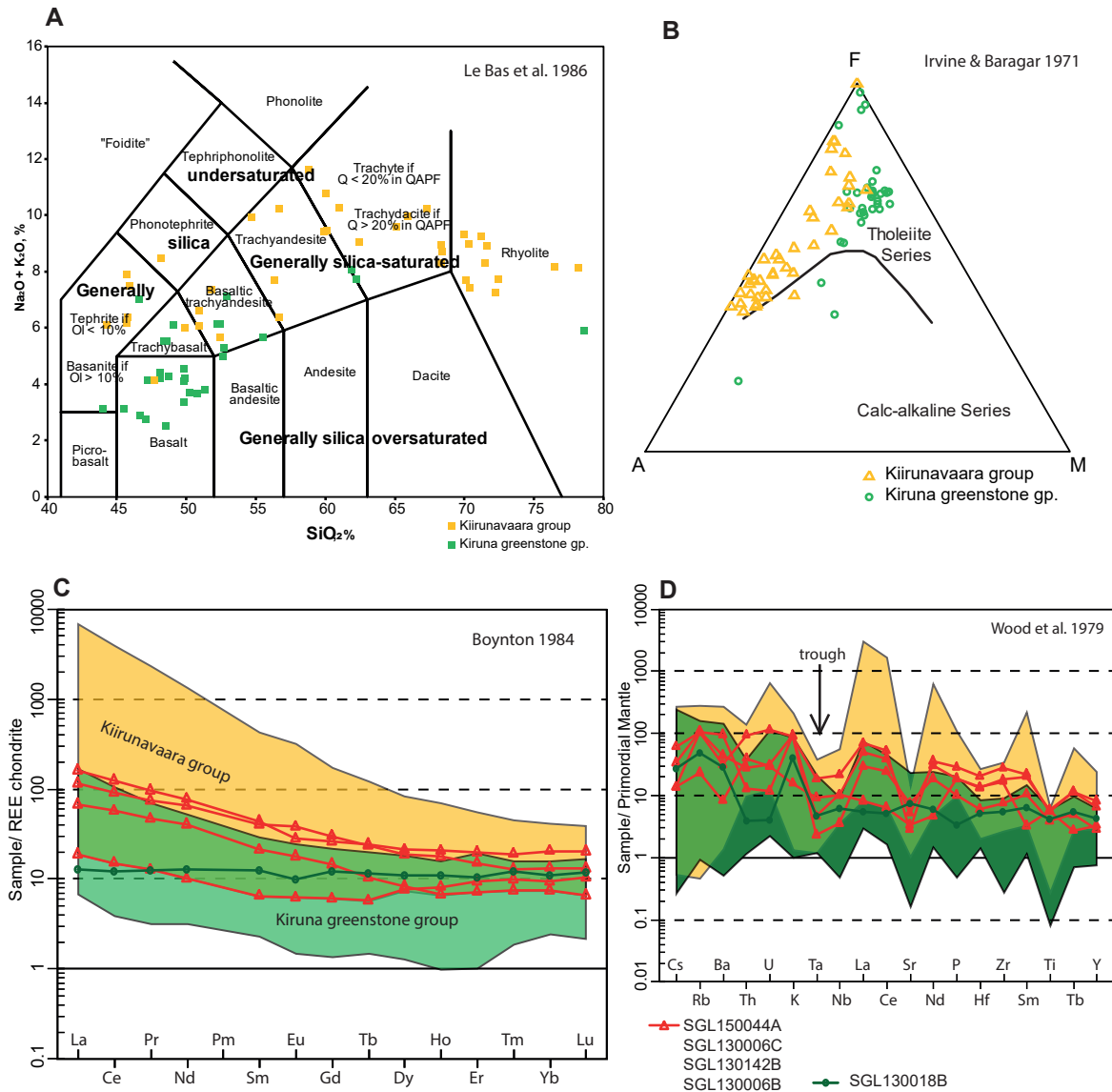


Figure 4. Whole-rock geochemistry results for rocks from the Kiruna greenstone group (KGG) compared with the syn-orogenic rocks of the younger Kiirunavaara group. **A.** TAS classification diagram after Le Bas et al. (1986). **B.** AFM discrimination diagram after Irvine & Baragar (1971). **C.** REE from mafic rocks normalised to chondrite (Boynton 1984). **D.** Spider diagram of incompatible trace elements from mafic rocks normalised to primordial mantle (Wood et al. 1979).

phyrite group, they are chemically distinct. The Kiirunavaara group rocks exhibit a tholeiitic or slightly alkaline and partly bimodal geochemical character, whereas the Porphyrite group rocks have a calc-alkaline chemical composition (e.g. Martinsson & Perdahl, 1995).

Unconformably overlying the Kiirunavaara group are quartzites, metaarenites and, locally, conglomerate lenses of the Hauki quartzite extending in a long band at least from Kiruna up to the Vittangivaara key area (cf. Luth et al. 2018a). The clasts of the conglomerate predominantly consist of Kiirunavaara group material (Martinsson 2004), suggesting a local source. The contact with the underlying units is presumed to be tectonic.

Lithochemically, the rocks of the Kiruna greenstone group and the younger syn-orogenic rocks are distinctly different (Martinsson & Perdahl 1995). Figure 4 shows the lithochemical characteristics of pre-orogenic mafic rocks of the Kiruna greenstone group and the syn-orogenic rocks of the

Kiirunavaara group in the Kiruna area. The rocks of the Kiirunavaara group are generally trachyandesitic to rhyolitic. Basalts occur very rarely, whereas the Kiruna greenstone group rocks are of a predominantly basaltic composition (Fig. 4A). The metavolcanic rocks of the Kiirunavaara group plot in the tholeiitic field in an AFM diagram (Fig. 4B). This distinguishes them from the predominantly calc-alkaline metavolcanic rocks of the Porphyrite group (Martinsson et al. 2016, Martinsson et al. 2018). One of the characteristics that can be used to distinguish between these two groups is the steep negative slope towards heavier rare earth elements in the Kiirunavaara group, whereas the Kiruna greenstone group exhibits a relatively shallow slope (Fig. 4C). An additional characteristic of the Kiirunavaara group is a depletion of high field strength elements (HFS elements) Ta and Nb compared with other incompatible elements. This depletion is not observed in the Kiruna greenstone group (Fig. 4D).

## GEOPHYSICAL DATA

### Introduction

The area was investigated by airborne geophysical surveys made by LKAB in 1960, 1973 and 1983. The airborne geophysical information includes magnetic, radiometric and electromagnetic data (both slingram and VLF). Ground gravity measurements have been acquired over the area with regional coverage of approximately 1–1.5 km station spacing. A compilation of the petrophysical properties of the rocks in the area is presented in Figure 5 and Table 1. Several parts of the area have also been surveyed with ground magnetic or slingram measurements. More information on these previous geophysical investigations is found in Grigull & Antal Lundin (2013).

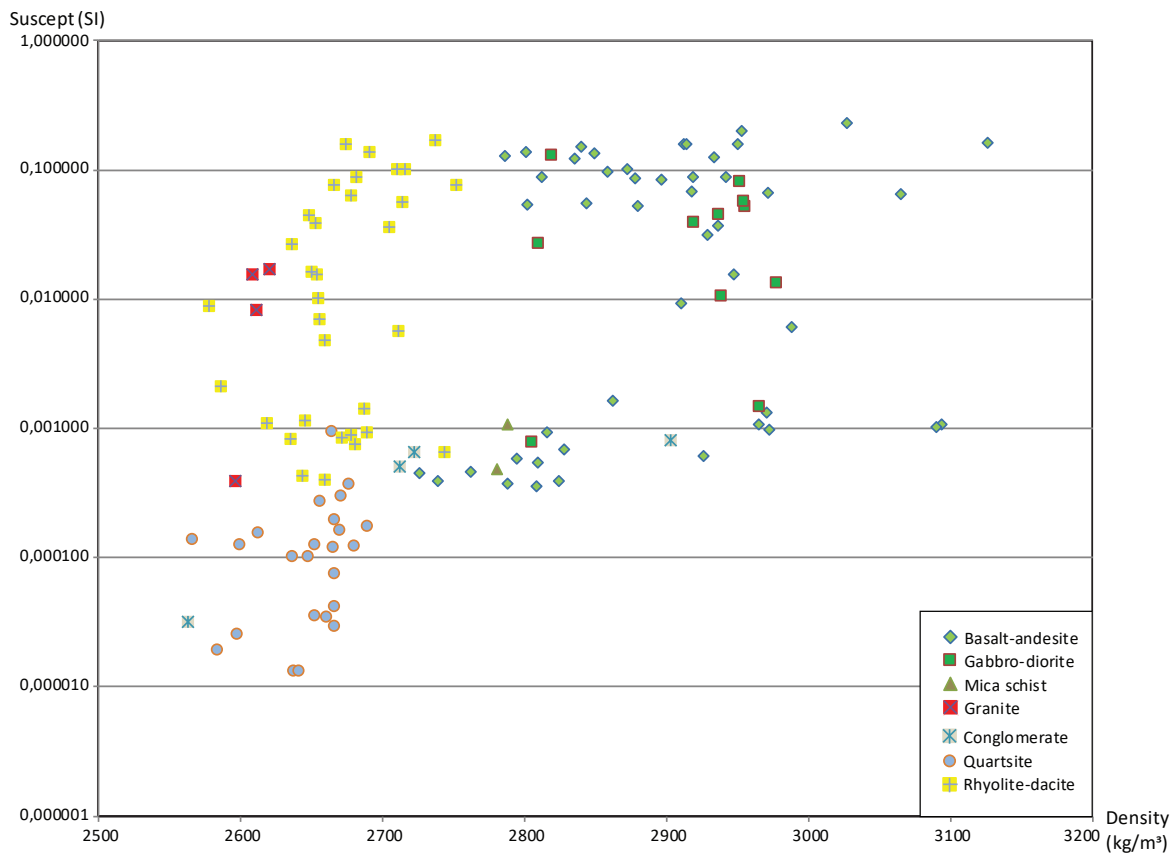


Figure 5. Petrophysical properties of the lithologies in the area, expressed graphically as magnetic susceptibility (SI unit) v density (kg/m³). The total number of petrophysical samples is 131.

Intrusive rocks in the northwestern part of the area shown in Figure 6–8 are Archaean basement. These intrusions vary between granites and gabbros. On the gravity map (Fig. 6) the area is seen as a low anomaly, which indicates that the more felsic intrusive rocks predominate. In the north-central part of the area there is a low-gravity anomaly that coincides with a low magnetic anomaly (Fig. 6 and 7). This area coincides with the Hauki quartzite, extending in a north-south direction. According to the gravity map, the low anomaly is also relatively pronounced between the two major positive anomalies on both sides of the river Torneälven (Fig. 6). Thus, it is possible that the quartzite is coherent throughout this low-gravity anomaly.

Table 1. Petrophysical information on the rock types in the area.

Rock type	No. of samples	Density (SI) mean	Density (SI) Std. dev.	Susceptibility $\times 10^{-5}$ (SI) min	Susceptibility $\times 10^{-5}$ (SI) max	Susceptibility $\times 10^{-5}$ (SI) median	Q-value min	Q-value max	Q-value median
Basalt-andesite	50	2893	93	36	23 206	5403	0.00	29.61	0.45
Gabbro-diorite	12	2916	64	77	12 860	3915	0.01	2.31	0.86
Mica schist	2	2784	*	49	106	*	0.02	0.02	*
Granite	4	2609	10	40	1694	1184	0.01	0.66	0.37
Conglomerate	4	2725	139	3	80	58	0.02	0.10	0.04
Quartzite	24	2647	32	1	94	12	0.00	0.03	0.00
Rhyolite-dacite	35	2671	39	40	16 780	1025	0.02	16.73	0.34

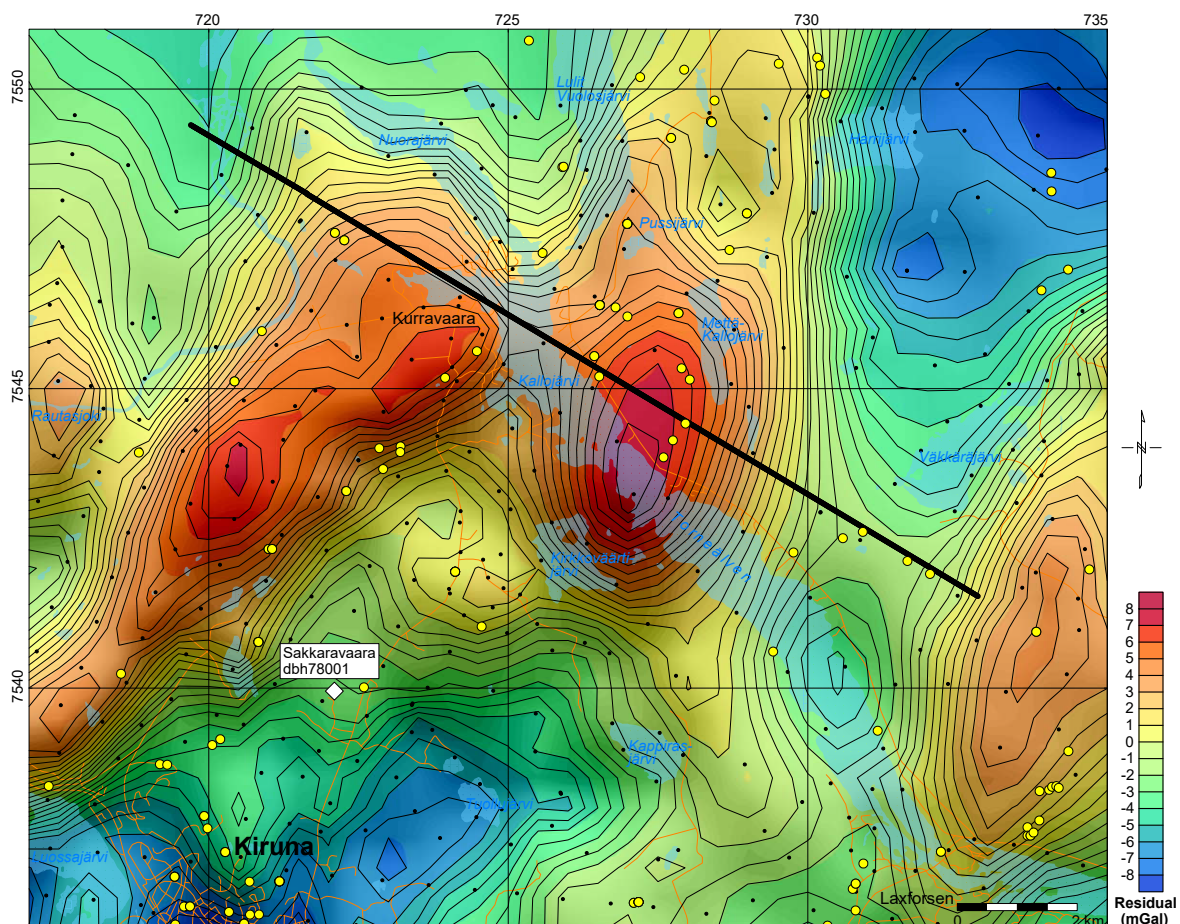


Figure 6. Residual gravity field, expressed as the difference between the Bouguer anomaly and an analytical continuation upwards to 3 km. The black dots represent measurement points. The yellow circles represent acquired petrophysical samples. The black line represents the extent of the regional interpreted geological profile presented in Figure 14A.

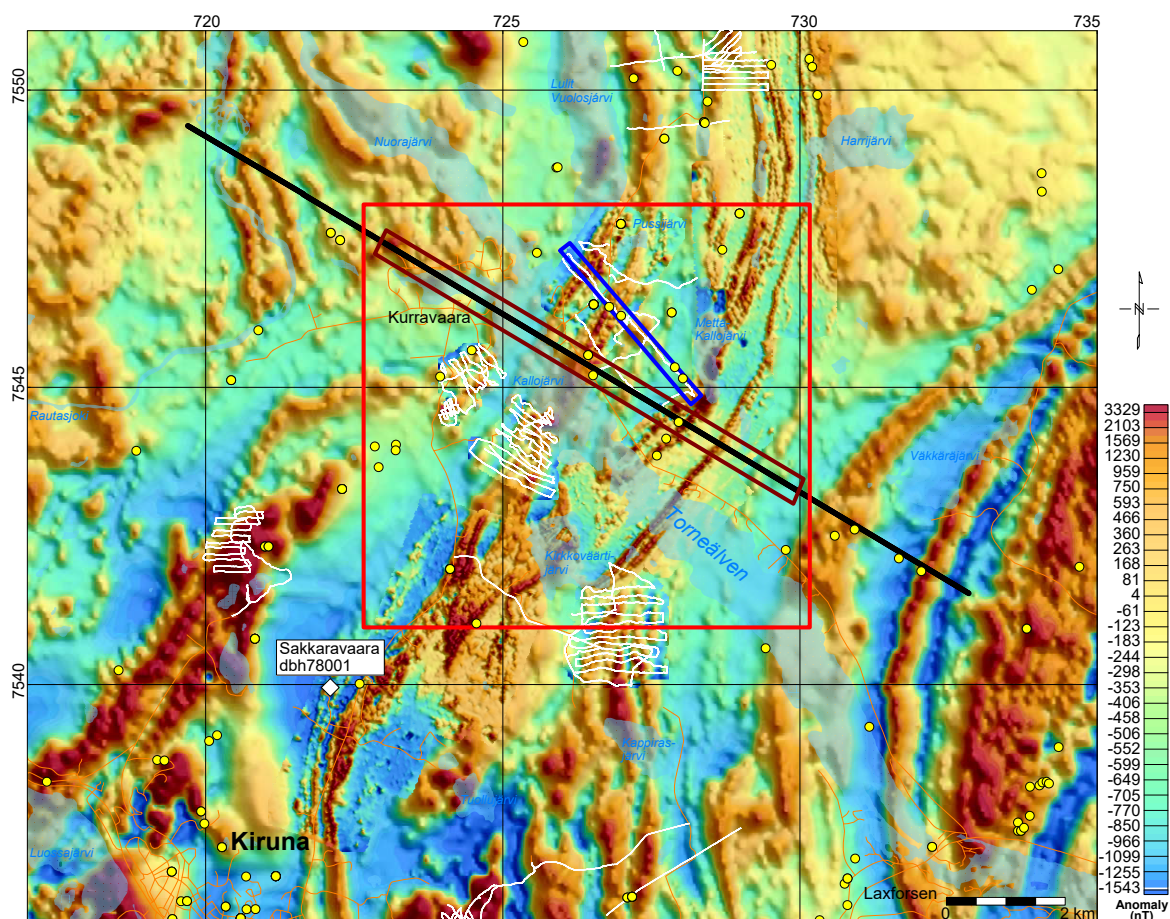


Figure 7. Magnetic anomaly map. The data from the airborne measurements are overlain by data from ground magnetic surveys. The yellow circles represent acquired petrophysical samples. The white lines represent newly acquired ground profiles by magnetometer. The black line represents the extent of the interpreted regional geological profile, shown in Figure 14A. The red polygon shows the extent of a 3D VOXI model and the brown box surrounding the central part of the regional profile represents the extent of the cross-section derived from that 3D VOXI model, and shown in Figure 15. The blue box marks the interpreted ground magnetic profile presented in Figure 16.

A rock sequence dominated by greenstones belonging to the Kiruna greenstone group occurs east of the Hauki quartzite. This gives rise to a positive anomaly in the gravity data. Sharp variations in the content of magnetic minerals are visible in the banded magnetic signature obtained from previously acquired ground magnetic surveys. Strong conductive horizons in the eastern part of the greenstone sequence, which consist of graphite horizons, are seen in the slingram data (Fig. 8). Intercalated within the greenstones are intermediate metavolcanic rocks belonging to the Kiirunavaara group, which produce a generally high-magnetic pattern, continuing to the south. A granite intrusion occurs in the northeastern part of the area, which is seen as a relatively homogeneous, low-magnetic area corresponding to a pronounced gravity low (Fig. 6).

The gravity low continues to the south and coincides with both relatively high-magnetic and low-magnetic areas. The lithology of this area is dominated by felsic metavolcanic rocks with relatively low densities. The felsic metavolcanic rocks are situated between mica schist to the west, and mafic to intermediate metavolcanic rocks to the east. The mica schist continues to the south, where it gives rise to a moderate gravity high. Several high-magnetic bands, striking in a north-south direction, occur in the central-southern part of the area. The bands are produced by alternating sequences of felsic metavolcanic rocks of rhyolitic to dacitic composition. Further west is an area with a lower magnetic signature. This area coincides with a pronounced gravity low, and the lithology in this part is metavolcanic rock

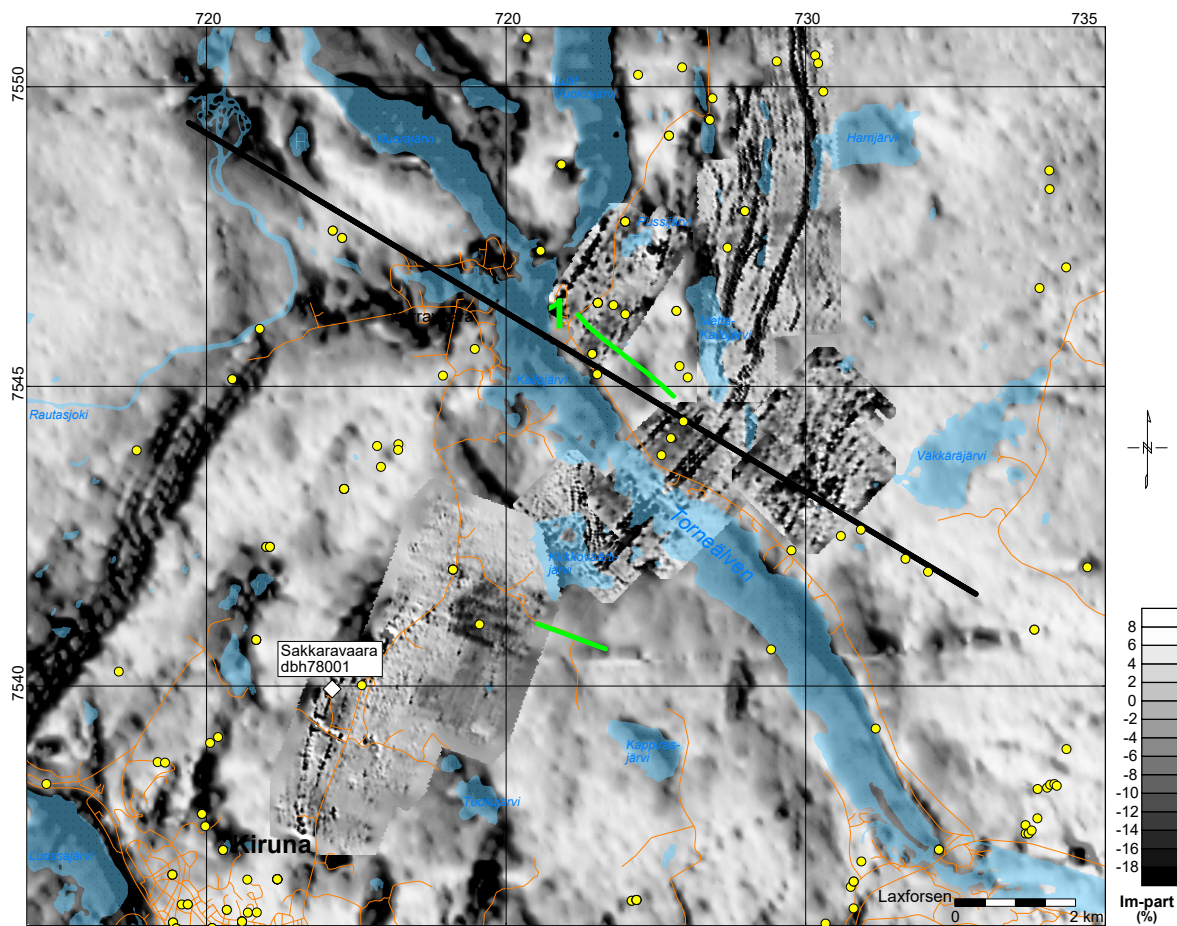


Figure 8. Slingram data from airborne measurements, overlain by data from ground-measured slingram surveys. The data displayed is the quadrature portion of the slingram data. The yellow circles represent acquired petrophysical samples. The green lines represent the extent of ground profiles with VLF instruments and the result from the profile labelled “1” is presented in Figure 17. The black line represents the extent of the regional interpreted geological profile, shown in Figure 14A.

of a rhyolitic composition. West of this area is a high-magnetic structure, oriented north-south, which consists of intermediate metavolcanic rock. The relatively broad, low-magnetic area to the west consists of Hauki quartzite.

A positive gravity anomaly occurs west of Torneälven, extending to the southwest and coinciding with a low-magnetic area. The lithology is dominated by mafic metavolcanic rocks, while to the south-east there is a strong high-magnetic area caused by felsic to intermediate metavolcanic rocks.

### *Structural inventory*

Although several studies of the tectonic development of the Kiruna area exist (e.g. Vollmer et al. 1984, Witschard 1984, Forsell 1987, Wright 1988, Talbot and Koyi 1995), there is no generally accepted structural model. Moreover, the structural framework around Kurravaara township and Lake Pussijärvi (Fig. 3) to the northeast of Kiruna is poorly understood. Here, the rocks have been affected by deformation within the Kiruna–Naimakka deformation zone (Bergman et al. 2001, Fig. 1), and the structures by which the Kiirunavaara group and the Kiruna greenstone group are connected with the rocks north and northeast of Torneälven are unclear (see also Luth et al. 2018a). A new structural geological model has therefore been developed with particular emphasis on the area around Kurravaara township and Pussijärvi, linking the model to the relatively well-understood Kiruna area.

Between Mt Luossavaara and Kurravaara township, bedding planes dip moderately to steeply mainly to the east to southeast and younging is consistently to the east for rocks both of the Kiirunavaara group and the Kurravaara conglomerate (Fig. 9A, B; cf. Martinsson et al. 2016, Wright 1988). Axial-planar cleavage and foliation planes are generally subvertical or dip steeply to the east-southeast. Cleavage and foliation dip is steeper than, or similar to, bedding in most locations (Fig. 9A). Bedding/cleavage intersection lineations and mineral lineations plunge steeply to moderately and usually trend roughly southwards. Other lineation orientations also occur and are not easily explained (Fig. 9A, B). A possible cause is non-cylindrical folding, resulting in warped fold axes with depressions and culminations. The foliation density in the Kurravaara conglomerate increases and steepens close to the contact with the Hauki quartzite. Wherever a strong foliation in the Kurravaara conglomerate could be observed, the clasts are strongly stretched into a prolate geometry and sometimes even boudinaged parallel to the bedding/cleavage intersection lineations. This may indicate shearing parallel to the foliation, but needs further investigation.

Direct evidence of folding was observed at very few locations. In a tephrite of the Matojärvi formation in the hanging wall of the Rektorn iron ore deposit, mineralised veins are folded into west-vergent, overturned meso-scale folds (Fig. 10A). These folds are interpreted to be parasitic to the regional fold structure. Bedding/cleavage intersection lineations at the Rektorn quarry plunge approximately 60 degrees to the south and south-southeast. Close to the contact with the Hauki quartzite, quartz veins cutting through sheet silicate-rich metavolcanic rocks belonging to the Matojärvi formation were folded pygmatically (Fig. 10B). A clear foliation has developed parallel to the axial plane of the pygmatic folds. The metavolcanic rock contains many circular quartz blasts which may be quartz-filled amygdyles. Strain shadows around the quartz blasts are symmetrical, and the rock is affected by pressure solution enhancing the foliation. The axial plane of the pygmatic folds dips 65 degrees to the southeast. A mineral lineation was measured at 107/70, a more or less plunging dip of the axial planar foliation and parallel to the plunge of the fold axis. Folds were also observed in rocks of the Kiirunavaara group at Sakkaravaara (Fig. 9C) and in quartzites of the Hauki quartzite on Mt. Kurravaara (Fig. 9D). The Hauki quartzite is folded into upright, open folds plunging approximately 45 degrees to the south-west.

The rocks of the Kiirunavaara group are cut off by an east-dipping fault and brought into contact with the Hauki quartzite (Fig. 3). Mafic rocks to the east of the Hauki quartzite have been interpreted as belonging to the Kiirunavaara group on some maps (Offerberg 1967, Bergman et al. 2001), and as belonging to the Kiruna greenstone group on others (Forsell 1987). No isotope dates are available for these rocks, however. During this project, a sample of a mafic metavolcanic rock was taken (SGL130018A in Fig. 3) that exhibits a lithochemical signature matching other mafic rocks belonging to the Kiruna greenstone group (Fig. 4C and 4D). Additionally, graphite-bearing schist is reported from a drill hole at Sakkaravaara, west of the road to Kurravaara (dbh 78001 in Fig. 3). In the Kiruna area, graphite has so far only been described as occurring in the greenstones. The graphite layer is a good electrical conductor, creating a relatively clear electromagnetic anomaly on the slingram anomaly map (Fig. 8). In the geological model presented here, a strip of rocks up to 900 m wide to the east of the Hauki quartzite is therefore attributed to the Kiruna greenstone group.

The rocks between Kiruna and Kurravaara to the west of the fault between the Kiirunavaara group and the Hauki quartzite occupy the upright western limb of a regional-scale, west-vergent, probably overturned syncline. It is unclear whether the folds observed in the Hauki quartzite were formed synchronously with this syncline or post-date this folding event.

To the northeast of Kurravaara township on the northeastern side of the river Torneälven, previous geological maps show only greenstones, cut off by a major NW–SE striking fault running more or less parallel to Torneälven (e.g. Offerberg 1967). However, based on work carried out for the Barents Project, several observations indicate that both the Kurravaara conglomerate and the Kiirunavaara group extend

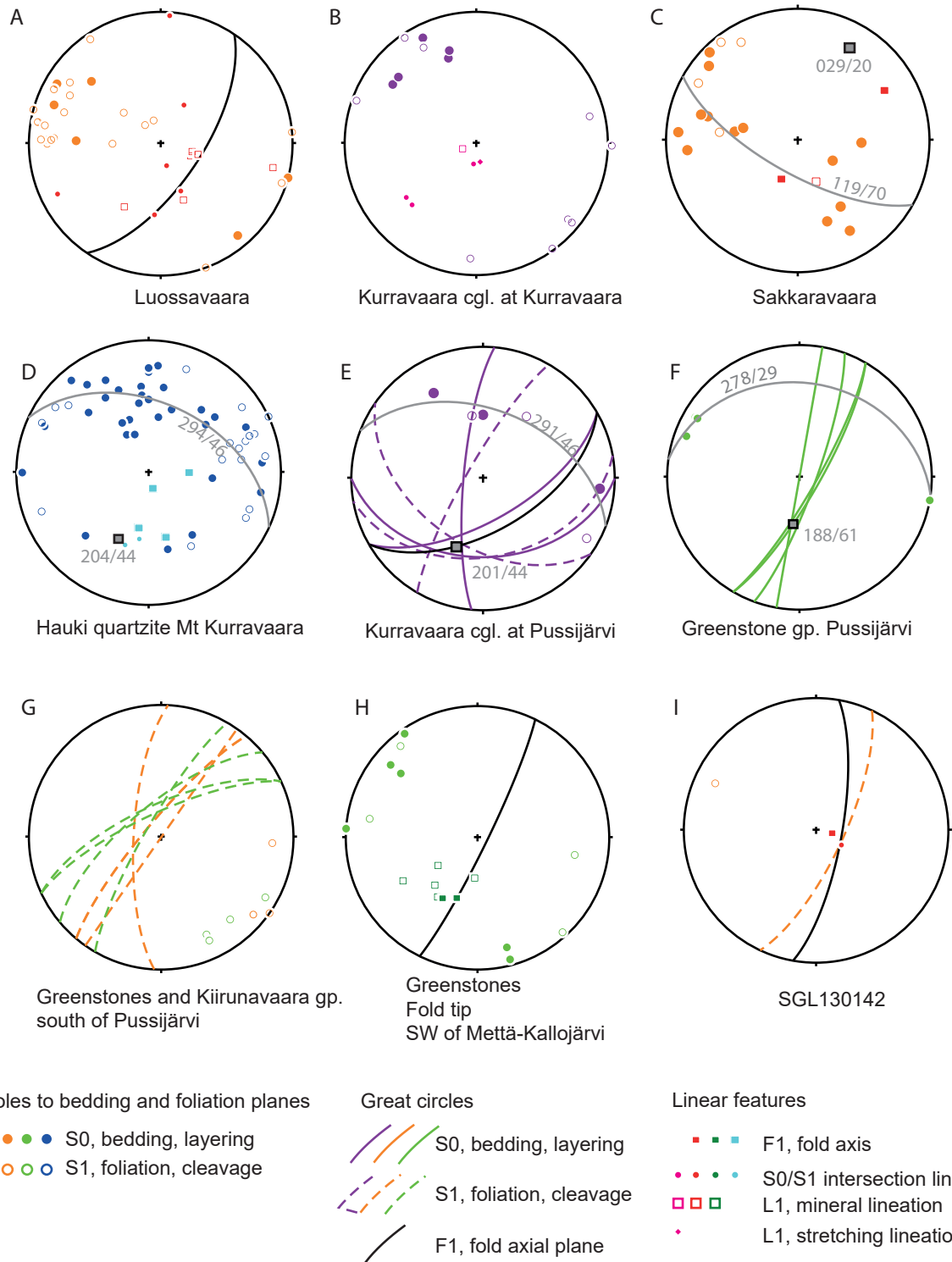


Figure 9. Stereographic projections (lower hemisphere) of structural geology data in the Kiruna–Pussijärvi area. Green: Kiruna greenstone group. Purple and pink: Kurravaara conglomerate. Red and orange: Kiirunavaara group. Blue: Hauki quartzite. Grey: Cylindrical best-fit great circles and poles to these.



Figure 10. **A.** West-vergent parasitic folds observed in the hanging wall to the Rektorn iron ore deposit. (SWEREF99 TM: N7537660, E719979). **B.** Ptygmatically folded quartz vein in amygdaloidal metavolcanic rock of the Matojärvi formation close to the contact with the Hauki quartzite. The axial plane to the fold dips approximately 65 degrees to the southeast and a mineral lination plunges approximately 70 degrees to the E-SE. (SWEREF99 TM: N7539147, E720193).



Figure 11. Conglomerate attributed to the Kurravaara conglomerate (SWEREF99 TM: N7546700, E725797). **A.** The conglomerate is clast-supported and contains sandy layers. **B.** Porphyritic clast with large plagioclase phenocrysts, probably belonging to the Porphyrite group (same location as A.). **C.** Kink fold in strongly-foliated and migmatized paragneiss, thought originally to have been Kurravaara conglomerate (SWEREF99 TM: N7546253, E725711). **D.** Stereographic projection (lower hemisphere) of structural data collected from the kink folds in C.

further to the north of Torneälven. A conglomerate was found along the northern shore (Fig. 3) and could be followed in small outcrops downstream for at least 200 metres. It is a clast-supported conglomerate with a sandy matrix and intercalated sandy layers (Fig. 11A). The conglomerate mainly contains mafic to intermediate volcanic clasts, but also chert clasts. One clast exhibits large plagioclase phenocrysts (Fig. 11B), typical of metavolcanic rocks from the Porphyrite group. This conglomerate was therefore attributed to the Kurravaara conglomerate. About 100 m to the east of that relatively well-preserved conglomerate, a rapid increase in deformation and metamorphic grade is marked by a penetrative, closely-spaced foliation grading into a mica-rich paragneiss even further east. The protolith of the paragneiss is unclear, but is here interpreted as belonging to the Kurravaara conglomerate. At a later stage the gneissic foliation has been affected by lower grade kink folds (Fig. 11C). The same gneissic band may thereby exhibit both Z- and S-shaped kink folds, indicating that the rocks were shortened in parallel with the gneissic foliation. The axial planes to the kink folds dip moderately to steeply to the east and north, i.e. they are nearly perpendicular to each other (Fig. 11D). But this was the only location where such kink folds were observed, and they are therefore difficult to interpret without further field work.

Approximately 50 m east of where the kink folds were observed, near-pristine pillow lavas of the Kiruna greenstone group occur and are thought to belong to the Peuravaara formation. Bedding planes and foliations in both the pillow lavas and the strongly-foliated part of the conglomerate dip moderately to steeply to the southeast (Fig. 9F and 11). The greenstones, consisting of pillow lavas and intercalated



Figure 12. Basaltic trachyandesite attributed to the Kiirunavaara group (SWEREF99 TM: N7546305, E726830). Samples SGL150044A, SGL130006C, SGL130006B were retrieved from this area. For exact localities refer to the map in Figure 3.

tuffite layers, can be followed towards the east for approximately 750 metres. Further to the east, the rock type changes into a strongly-foliated intermediate metavolcanic rock with a strong positive magnetic anomaly (cf. Fig. 7). This rock is characterised by round quartz-filled nodules and feldspar porphyroclasts (Fig. 12).

The lithostratigraphic position of this rock is unclear. However, lithogeochemical analyses of three samples taken several hundred metres apart (cf. Fig. 3) indicate that these rocks are basaltic trachyandesites with a REE and trace element signature typical of the syn-orogenic rocks of the Kiirunavaara group (Fig. 4C and 4D). Hence, the rock may not be a part of the Kiruna greenstone group, but may instead belong to the Kiirunavaara group. Axial length ratios of what is interpreted as flattened pumice pieces were measured on both a horizontal and a vertical surface, and resulted in a maximum flattening strain of approximately 10 on both surfaces, assuming the pumice pieces were originally spheroidal. Despite the development of a penetrative foliation, and the relatively high strain, no stretching or mineral lineations were observed, and strain shadows formed around round quartz nodules are symmetrical. It is therefore assumed that the foliation is due to strong co-axial deformation. To the east of these strongly foliated rocks, further pristine pillow lavas occur as part of the Peuravaara formation. These pillow lavas can be traced approximately 2.3 km eastwards. The new geological model of the Kurravaara–Pussijärvi area suggests an extension of the Kurravaara conglomerate and the Kiirunavaara group further to the north. The northwest–southeast-striking deformation zone proposed in older maps (e.g. Offerberg 1967) probably does not exist. This conclusion is supported by newly acquired ground magnetic data southeast of Lake Kirkkoväärtijärvi showing no displacement of highly magnetic anomalies (Fig. 7).

The Kiruna greenstone group contains rock types that can be used as geophysical markers, such as

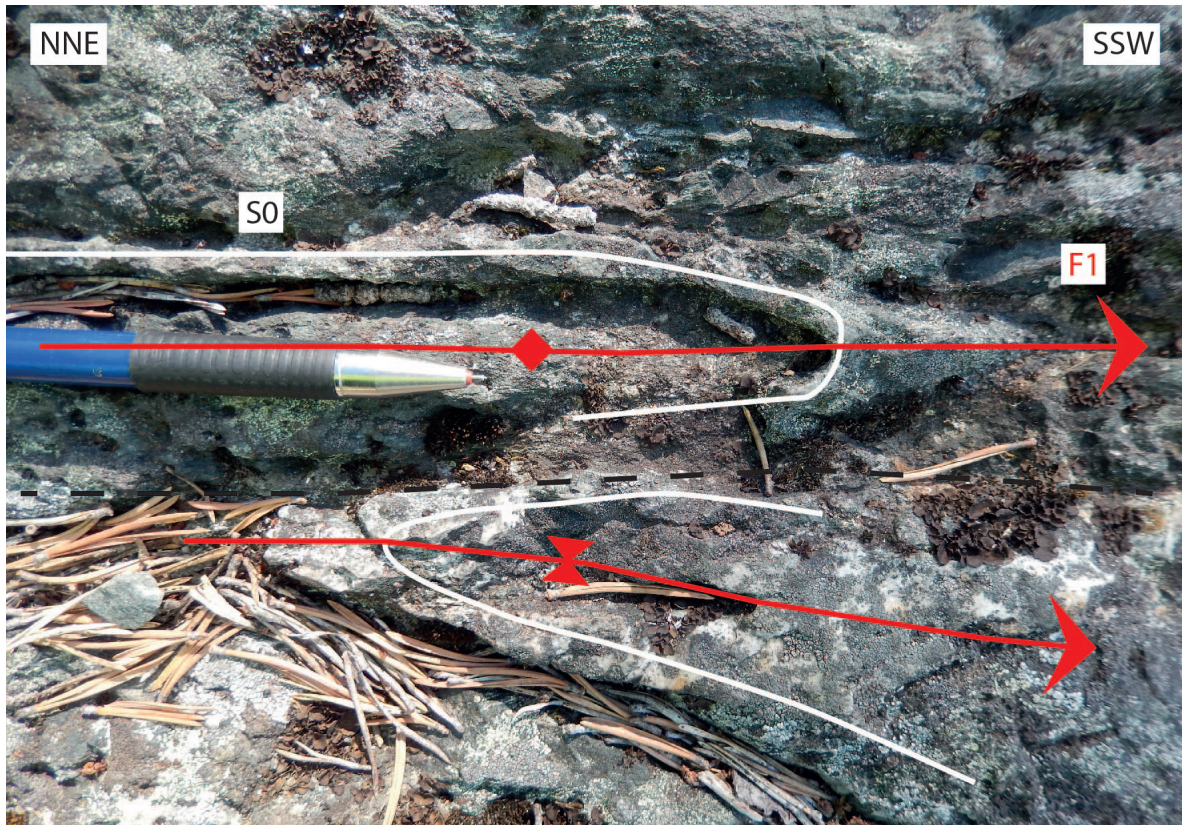


Figure 13. Small-scale folding observed in pillow basalts belonging to the Peuravaara formation of the Kiruna greenstone group. Top section. (SWEREF99 TM: N7544069, E726864).

graphite horizons in the Viscaria formation, and also laterally continuous graphite horizons and a banded iron formation (BIF) in the upper part of the Linkaluoppal formation. The graphite horizons and the BIF belonging to the Linkaluoppal formation can be traced on magnetic and electromagnetic maps (Fig. 7 and 8) and are interpreted to occur in the western limb of an approximately north-south-trending syncline ranging approximately from Vittangivaara in the north (cf. Luth et al. 2018a; not included in Fig. 3) to approximately 1.5 km north of lake Harrijärvi in the south (Fig. 3), where the core of the syncline is cut off to the east by an intrusion belonging to the Perthite monzonite suite. North of Torneälven, the corresponding anticline to the west is cored by pillow lava basalts of the Peuravaara formation. Further north, diorites and graphite layers of the Viscaria formation crop out (e.g. Martinsson 1999), indicating that, regionally speaking, younging is to the east and south, and that one of the major structures in the area is a slightly west-vergent, locally overturned, south-south-west-plunging anticline ranging at least from Alanen Laanijärvi in the north to Lake Kirkkoväärtijärvi in the south. Meso-scale folding close to the hinge of that anticline in the south has been observed in drill cores during an excessive drilling program to the northeast of Lake Kirkkoväärtijärvi (Gustafsson & Carlson 1992, Kallosalmi drilling project, prospecting report PRAP92013), and in pillow lavas belonging to the Peuravaara formation on the northeastern shore of Torneälven (Fig. 13). Here, a fold axial plane was measured dipping steeply towards the southeast. Fold axes and mineral lineations plunge approximately 65 degrees towards the southwest (Fig. 9H). In the eastern limb of the anticline, bedding mainly dips steeply towards the southeast, and only locally towards the northwest. In a very few outcrops younging is reliably indicated by chert fillings between some pillows or by the shape of the pillows themselves. However, younging in both directions was observed within the eastern limb of the anticline, and this is interpreted as representing parasitic folding within the actual fold limb.

## *2D modelling based on magnetic and gravity data*

In order to resolve the folding patterns in the area, a geological cross-section marked D-D' in Figure 3 was developed, based on geophysical modelling and geological data. Several ground measurements were made, primarily by magnetometer, at a number of key locations to achieve a more detailed picture of the geometries of the bedrock structures. The coverage of these newly acquired magnetometer profiles is shown in Figure 7.

The area mainly consists of greenstones; the magnetic properties of these rocks differ significantly over small distances. On the gravity map the centre of the fold gives rise to a strong positive anomaly (Fig. 6). Petrophysical analyses of samples from this area show that the densities of these lithologies are mainly between 2 900 and 3 100 kg/m<sup>3</sup>.

The interpreted regional geological model in Figure 14A is based on geophysical information from ground gravity data and airborne magnetic measurements. Figure 14B shows the geological model for the Kovo and Vakko zones described in Luth et al. (2016, 2018a). The model has been constructed by forward modelling with “Potent” software, using the potential field data together with petrophysical information on the various rock types to constrain the model. In areas with sparse petrophysical information, especially in the northwestern part of the profile, the rocks have been assigned the properties shown in Table 1. The background properties for the density and magnetic susceptibility of the subsurface have been specified at 2 700 kg/m<sup>3</sup> and  $100 \times 10^{-5}$  SI units.

In the west the profile starts within the Archaean granitoid. The petrophysical samples available from this lithology have an average density of 2 670 kg/m<sup>3</sup> and susceptibility of  $1\,000 \times 10^{-5}$  SI units. East of the granitoid is a vast area of mainly mafic to intermediate rocks. The low- to moderate-magnetised rocks in this area have been visualised in Figure 14A in light green, while the higher magnetised rocks are shown in darker green. Closest to the granitoid is an elliptical magnetic structure on the magnetic anomaly map (Fig.7). No petrophysical information is available from this structure, so density and magnetic susceptibility have been assumed to be 2 860 kg/m<sup>3</sup> and  $10\,000 \times 10^{-5}$  SI units, respectively. In order to fit the observed magnetic data with the modelled data, the structure could be represented as a near-isoclinal syncline. The behaviour of the gravity field indicates that the granitoid dips under the more dense mafic to intermediate rocks.

Very little petrophysical information is available between 2 000 m and 5 000 m along the profile. One sample was obtained from the low-magnetic metavolcanic rocks with a density of 2 860 kg/m<sup>3</sup> and a susceptibility of  $200 \times 10^{-5}$  SI units. Four samples were analysed from the more highly magnetised metavolcanic rocks whose average properties are 2 900 kg/m<sup>3</sup> and  $12\,400 \times 10^{-5}$  SI units. These properties have been assigned to the lithologies and, based on the shape of the magnetic field, it is possible that the highly magnetised lithologies are folded across the outline of the profile. No petrophysical data exists between 5 000 m and 6 000 m along the profile. To achieve a good fit between observed data and calculated response, density and susceptibility values of 2 900 kg/m<sup>3</sup> and  $2\,000 \times 10^{-5}$  SI units have here been assigned to the subsurface.

Just west of the Hauki quartzite, at 6 000 m along the profile, one petrophysical sample from the metavolcanic rock was obtained, having a density of 2 970 kg/m<sup>3</sup> and a susceptibility of  $6\,500 \times 10^{-5}$  SI units. Based on the shape of the magnetic field curve, it is likely that the metavolcanic rock dips beneath the quartzite. The quartzite is not exposed at the extent of the profile, but its existence is indicated by both the magnetic and gravity data. On the magnetic map, a smooth, low-anomaly area and a local gravity low between the positive anomalies to the northwest and southeast indicate less dense bedrock. Petrophysical samples from the quartzite in the vicinity have an average density of 2 650 kg/m<sup>3</sup> and susceptibility of  $20 \times 10^{-5}$  SI units. By applying these physical properties to the quartzite, the modelled depth extent is roughly 300 m at the eastern side.

A highly magnetised metavolcanic rock occurs east of the quartzite. Both in situ measurements of susceptibility and petrophysical laboratory measurements have been carried out and give densities in

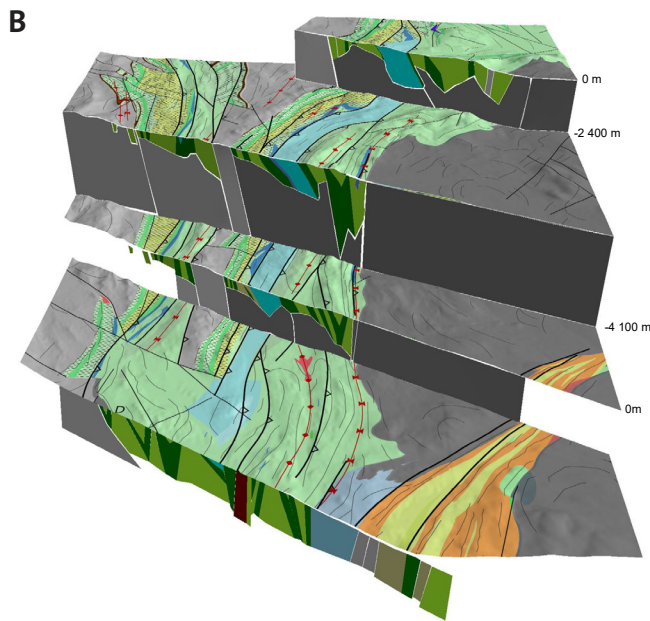
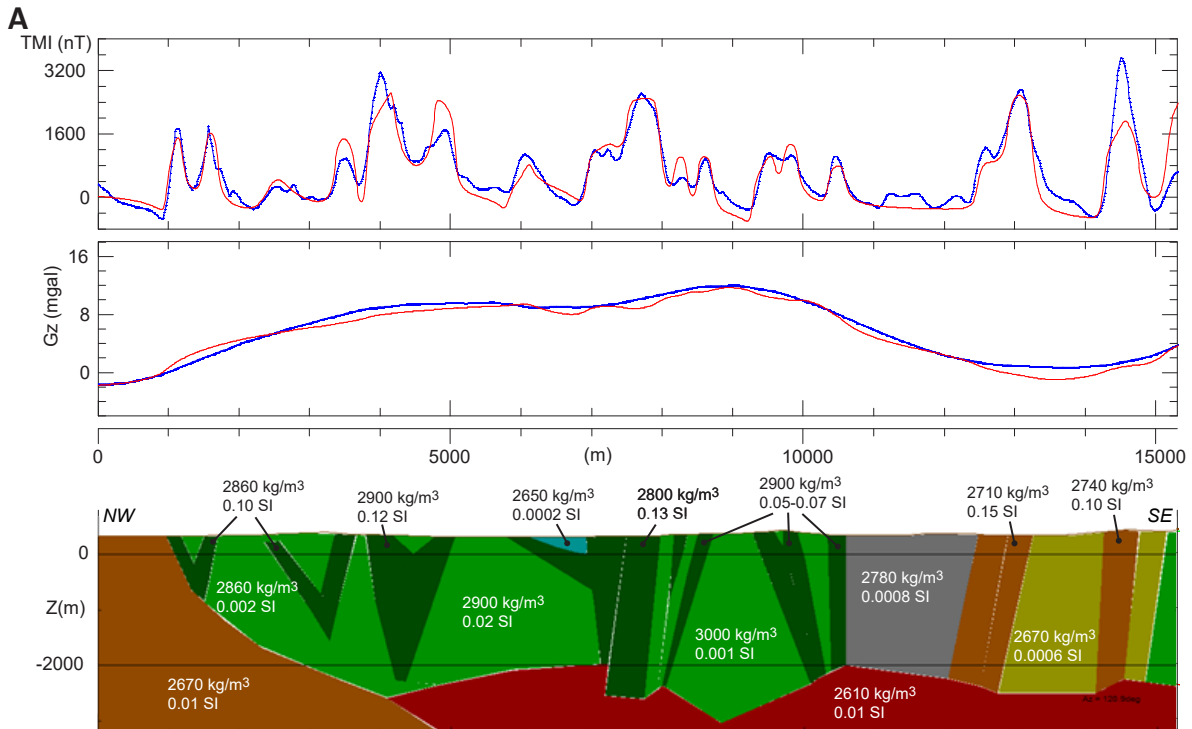


Figure 14. **A.** Modelled regional geological 2D model based on magnetic data from airborne measurements and ground gravity data. The cross-section is displayed from northwest (left side) to southeast (right side). The upper diagram shows the variation in the magnetic field; the diagram in the middle shows the gravity field. Blue lines in these diagrams are recorded data; red lines are the response from the model. The extent of the profile is outlined by the black line in Figure 3 and Figure 6–8.

**B.** 2.5D geological model based on the geological models of the Vakko and Kovo zones to the north (cf. Luth et al. 2018a). Visualisation in GOCAD software.

the range of 2 800–2 900 kg/m<sup>3</sup> and susceptibilities in the range of 8 000–12 900 × 10<sup>-5</sup> SI units. The highest magnetised lithology dips towards the northwest, and can be seen in the cross-section from the VOXI model (Fig. 15). A low-magnetic mafic metavolcanic rock occurs to the east. This has been sampled at two locations, giving an average density of 3 000 kg/m<sup>3</sup> and susceptibility of 120 × 10<sup>-5</sup> SI units.

Narrow high-magnetic bands surrounding the low-magnetic core can be observed in the vicinity of the anticline. Samples have been obtained on the eastern side and these have an average density and susceptibility of 2 900 kg/m<sup>3</sup> and 7 000 × 10<sup>-5</sup> SI units, values that have also been assigned to the high-

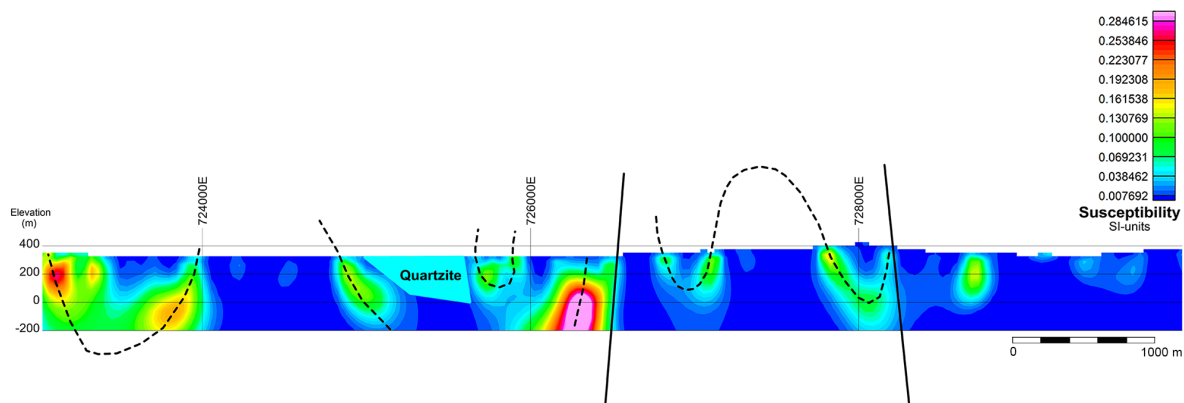


Figure 15. Cross-section derived from a 3D VOXI model along the central part of the regional 2D model in Figure 7. This model is based on data from airborne magnetic measurements.

magnetic bands on the western side of the low-magnetic core. The centre of the anticline consists of low-magnetic mafic metavolcanic rock with a higher density of  $3\,000\text{ kg/m}^3$ . The susceptibility of the low-magnetic metavolcanic rocks in this area is approximately  $100 \times 10^{-5}$  SI units.

A mica schist occurs east of the anticline, shown in light grey in the profile in Figure 14A. This rock is thought to belong to the Matojärvi formation and is seen as an orange-coloured area on the bedrock map (Fig. 3). It has an average density of  $2\,780\text{ kg/m}^3$ . The less dense rock is reflected in the gravity data, which is lower in the mica schist than in the core of the anticline. The gravity field continues to decrease to the east over the felsic metavolcanic rocks, which have densities in the range  $2\,670\text{--}2\,740\text{ kg/m}^3$ . When comparing the gravity and magnetic signatures, the more rhyolitic sequences (yellow in Fig. 14A) coincide with low-magnetic areas, whereas the dacitic rocks (orange in Fig. 14A) are heterogeneously magnetised and give rise to high magnetic anomalies. This is supported by both field observations and petrophysical analysis, which state that the susceptibilities for the rhyolite are less than  $100 \times 10^{-5}$  SI units, while the susceptibility for the dacitic rocks is in the range  $5\,000\text{--}15\,000 \times 10^{-5}$  SI units. According to the geophysical data, these metavolcanic rocks dip quite steeply. To the east lies a highly magnetised andesite which has been sampled for petrophysical analysis at several locations. These samples have an average density of  $2\,910\text{ kg/m}^3$  and susceptibility of  $14\,000 \times 10^{-5}$  SI units.

Both granitic and gabbroic intrusive rocks occur to the east of these metavolcanic rocks, with granite predominating north of them. Petrophysical samples acquired from this granite have an average density of  $2\,610\text{ kg/m}^3$ . In the central and eastern part of the profile, it is assumed that the felsic intrusions underlie the supracrustal rocks.

### *3D modelling based on airborne magnetic data*

Several 3D models have been made of the area. The data input was primarily magnetic data from airborne measurements, but modelling was also based on ground gravity data and data from ground magnetic measurements. 3D models have been constructed by inversion in the VOXI module, an extension of the Geosoft package. The main aim was to achieve an image of the geometries at depth of the various lithologies. One result of the 3D modelling is presented as a cross-section (Fig. 15). It is based on magnetic data from airborne measurements and shows the variations in magnetic susceptibility in the sub-surface down to 200 m below sea level. The 3D model, from which this cross-section is derived, covers an area of  $7\text{ km} \times 7\text{ km}$  surrounding the anticline at Pussijärvi (Fig. 7). The cell size of the volume pixels (voxels) is  $50\text{ m} \times 50\text{ m}$  in the horizontal direction and  $25\text{ m}$  in the vertical direction. The voxels gradually increase in size with depth, causing decreased resolution. The lateral extent of the

cross-section represents the central part of the regional profile in Figure 14A and is marked as a brown box in the magnetic anomaly map (Fig. 7).

Before the model was inverted, the magnetic susceptibilities of the sub-surface were constrained to keep the inversion within pre-defined boundaries. Available susceptibility information from previous and newly acquired petrophysical samples was used to constrain the model, along with in situ measurements of susceptibilities on outcrops. 19 petrophysical samples from this area, which have a magnetic susceptibility span in the range  $30\text{--}13000 \times 10^{-5}$  SI units, were used. In situ measurements of susceptibility on outcrops were conducted at 16 locations; eight measurements are normally made for each rock type and at each location. As the maximum value from these in situ measurements is  $33\,000 \times 10^{-5}$  SI units, the constraints for the 3D model were set from  $-10 \times 10^{-5}$  to  $35\,000 \times 10^{-5}$  SI units so as to include the paramagnetic properties that could occur, particularly due to quartzite.

A high-magnetic structure, which can be interpreted as a syncline, occurs in the western part of the cross-section (Fig. 15). A highly magnetic structure dips towards the southeast just west of the quartzite. In the middle of the cross-section is a strong, highly magnetic structure that dips to the northwest. The latter corresponds well with the structural measurements in this area, which show that the dip of the foliation is approximately 70–80 degrees to the northwest. Further east, on the eastern flank of the anticline, is a relatively highly magnetic feature, the orientation of which corresponds well to structural information measured on outcrops. The structural measurements show that the foliation dips towards the southeast, at approximately 65–85 degrees, and becomes steeper to the southeast.

### *2D modelling based on ground magnetic data*

The interpreted geological cross-section (Fig. 16) is based on the ground magnetic profile highlighted with a blue box in the magnetic anomaly map (Fig. 7). The main aim was to achieve an image of the geometrical properties of the highly magnetised structures along the extent of the profile. The model is constrained by either the magnetic properties of the petrophysical samples acquired along the profile, or in situ susceptibility measurements on outcrops. The depth extent of the lithologies is adopted from the regional geological profile shown in Figure 14A.

In the geological model in Figure 16, the less magnetised rocks are shown in light green and the higher magnetised rocks in dark green. It is evident from the ground magnetic data that the supracrustal rocks in the Kiruna greenstone group are heterogeneously magnetised.

In situ measurements of magnetic susceptibilities in the northwestern part of the profile show that the magnetisation of metavolcanic rocks varies from 40 to  $13\,000 \times 10^{-5}$  SI units. The behaviour of measured magnetic data in the area indicates that the geometries of these magnetised layers dip to the southeast beneath a broader low-magnetic portion of metavolcanic rock with a susceptibility of less than  $100 \times 10^{-5}$  SI units.

To the southeast is an area of roughly 1 km showing rapid variations in magnetic field. Field observations show that the magnetic susceptibility of the more magnetised layers is around  $12\,000 \times 10^{-5}$  SI units, so the thin layers giving rise to the positive magnetic anomalies have been assigned susceptibilities of between  $10\,000$  and  $15\,000 \times 10^{-5}$  SI units. Between these are lithologies with considerably lower magnetisation; measurements of  $100 \times 10^{-5}$  SI units have been recorded on the greenstones in this area. The geometries of the greenstones are steep, dipping to the northwest. Considering the geometries observed to the northwest, this observation suggests the presence of a syncline.

The lithologies continue to show this steep, northwestward dip until the relatively large, low-magnetic area in the southeastern part of the profile. Both in situ measurements and petrophysical sampling show this area to have a susceptibility of  $100 \times 10^{-5}$  SI units.

Lithologies are more magnetised at the southeastern end of the profile. Field observations close to the profile show magnetic susceptibility values of up to  $7\,000 \times 10^{-5}$  SI units. But to fit the model to the magnetic measurements, the greenstones must be assigned values of  $8\,000\text{--}10\,000 \times 10^{-5}$  SI units. Signature

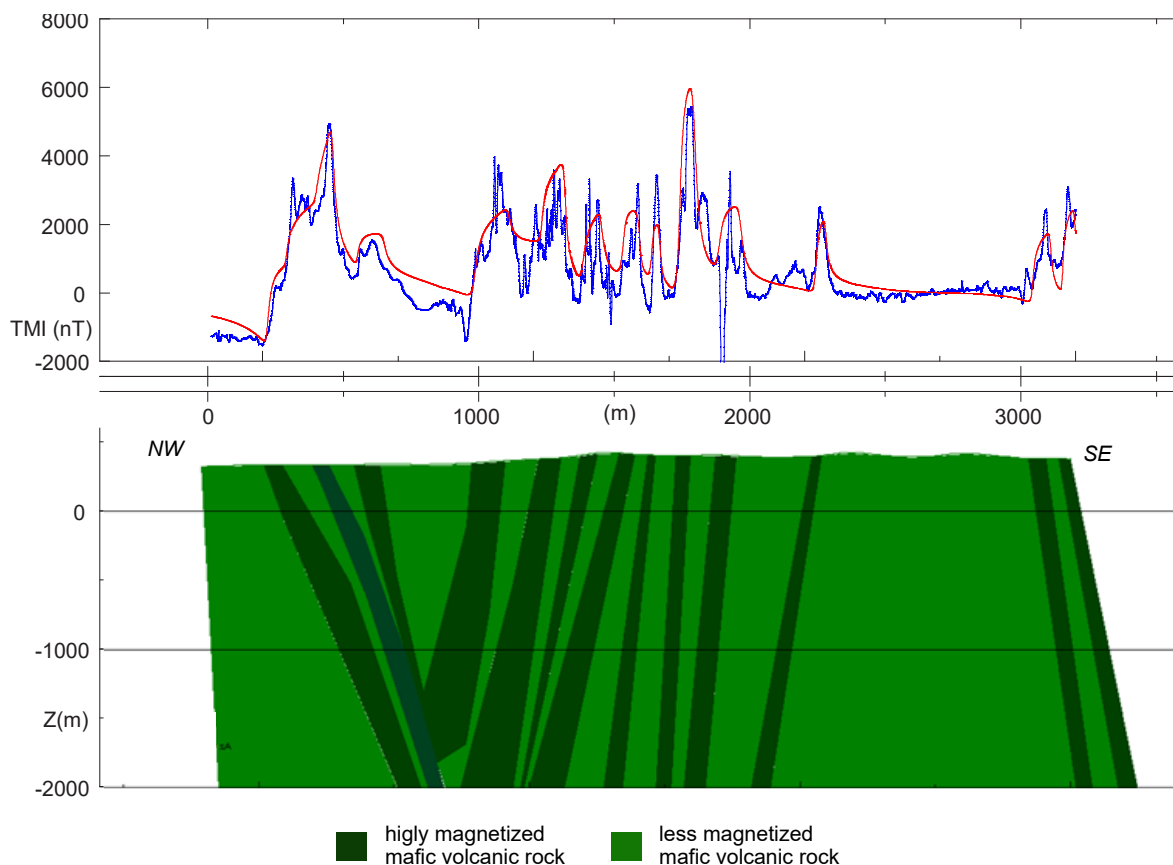


Figure 16. Forward modelled geological cross-section based on ground magnetic measurements along the profile marked in Figure 7 by the blue box. A syncline to the west and an anticline to the east are indicated in the model.

of the magnetic field shows that these highly magnetised greenstones dip to the southeast, indicating that they make up the eastern limb of an anticline.

Ground measurements along a profile with a VLF instrument have also been carried out in the area. The extent of this profile is marked in Figure 8 as the green line labelled “1”. The result of this measurement is displayed as a resistivity cross-section in Figure 17. The VLF profile is located a short distance southwest of the profile measured by magnetometer (the geological interpretation is presented in Fig. 16). The majority of the lithologies seen in Figure 16 were crossed by this VLF profile.

The most striking feature in the resistivity cross-section is a narrow conductive zone, roughly 600–700 m from the western end. This could represent a brittle fault just east of the syncline interpreted from the magnetic data in Figure 16.

On a regional scale, the rocks of the Kiruna greenstone group, the Kurravaara conglomerate, and the Kiirunaavaara group are all deformed into a series of synclines and anticlines with large amplitudes (–600 m) and wavelengths of hundreds of metres to 1–2 kilometres. Fold axes plunge predominantly to the south to southwest (Fig. 9), although north-plunging folds also occur. Fold axial traces can be followed for several kilometres, deflected slightly around younger and older magmatic intrusions due to rheology differences between the usually coarse-grained intrusive rocks and the finer-grained volcanic-metasedimentary rocks. Cleavage has developed in most rocks, but varies distinctly between rocks that appear nearly pristine and rocks that are pervasively foliated, and even partially migmatized. Foliation planes are usually lined with chlorite or biotite. With the exception of small-scale, subordinate kink folds in migmatitic mica-rich paragneiss south of Pussijärvi, no evidence of more than one folding event was found. Grigull & Lundin (2014), Talbot & Koyi (1995) and Forsell (1987) suggest that an

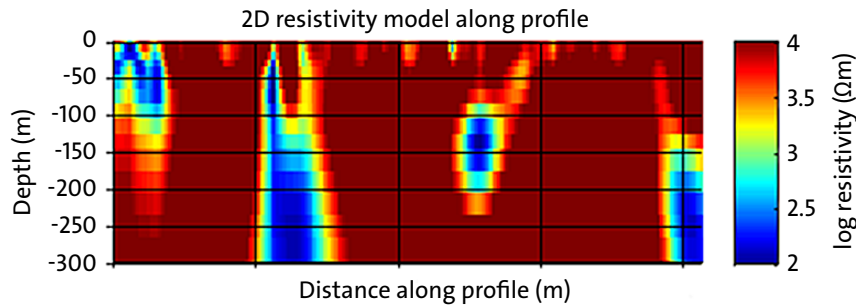


Figure 17. Inversion model based on VLF measurements along the profile labelled “1” (Fig. 8). The cross-section displays the apparent resistivity in the ground at shallow depth.

(isoclinal) folding phase preceded the folding described above. After thorough interpretation of existing and newly collected geoscientific data, no convincing evidence of this event could be detected, however. The structural model derived from the results of the Barents Project therefore predicts only one folding phase due to NW–SE to E–W-directed shortening and later or contemporaneous displacement of these folds along several thrusts and brittle faults. This model is supported by the studies of Vollmer et al. (1984) and Wright (1988). In the present geological model (Fig. 3 and 14), it is suggested that the Hauki quartzite was deposited into a graben that formed during a period of extension, cutting into the underlying rocks and partially reusing old structures, locally cutting them at an acute angle. Regional-scale folding of the Hauki quartzite is inferred from outcrop-scale open folds and cleavage-bedding relationships, indicating continued E–W compression and graben inversion after sediment deposition. Although direct evidence of thrusting was not observed in the field, placement of stratigraphically older rocks onto younger rock units requires westward-directed thrusting, corresponding to an overall east–west-directed compressional stress regime (cf. Luth et al. 2018a).

## Masugnsbyn key area

### *Lithostratigraphy*

The Masugnsbyn area features metavolcanic and metasedimentary rocks of predominantly basaltic composition corresponding to the Veikkavaara greenstone group (VGG) to the east, and metasedimentary, partially migmatized rocks of the Pahakurkio (PHG) and Kalixälv group (KÄG) to the west and south (Padget 1970, Niiniskorpi 1986; Fig. 18A). A simplified lithostratigraphic column is shown in Figure 18B. For a detailed description of the lithostratigraphic units, the reader is referred to Lynch et al. (2018) and Hellström et al. (2018); see also summary review of geological and geophysical information of the Masugnsbyn area by Hellström & Jönsson (2014). The following brief description of lithological units of the Masugnsbyn area mainly follows Padget (1970) and Niiniskorpi (1986).

The Veikkavaara greenstone group (VGG) contains predominantly basaltic greenstone at the base, a thin middle unit of pelitic schists and quartzite, and at the top volcanoclastic, basaltic tuffs with laterally extensive graphite horizons. The upper part of the VGG contains a banded iron formation and at the top lenses of marble that are locally dolomitic, e.g. the Masugnsbyn dolomite, which is currently quarried. The Veikkavaara greenstones have an overall high-magnetic signature and form a V-shaped fold, which can also be observed in the gravity data (Fig. 19 and 20). The greenstone sequence is clearly outlined as a high-magnetic, banded sequence, where alternating high and low magnetic anomalies probably reflect depositional features. Graphite-bearing layers in the upper part of the Veikkavaara greenstones are good electrical conductors and can therefore be traced from electromagnetic

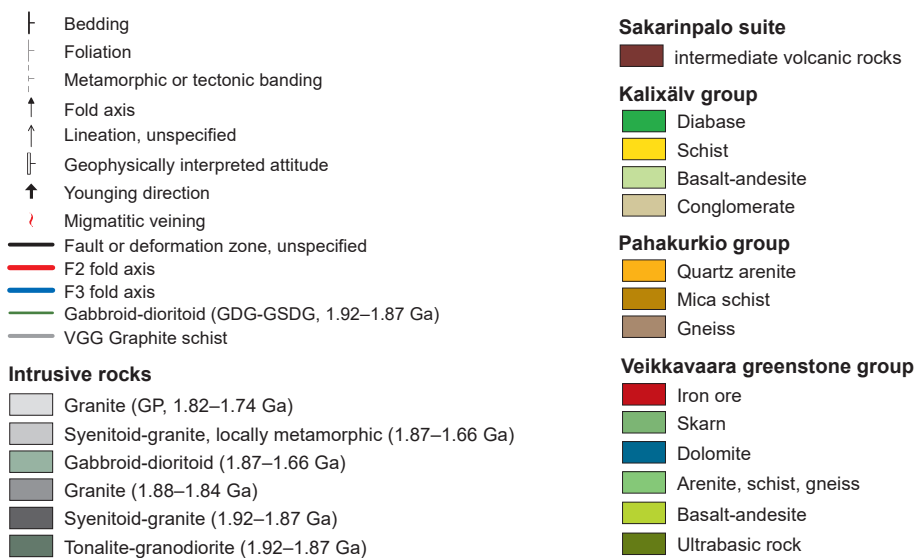
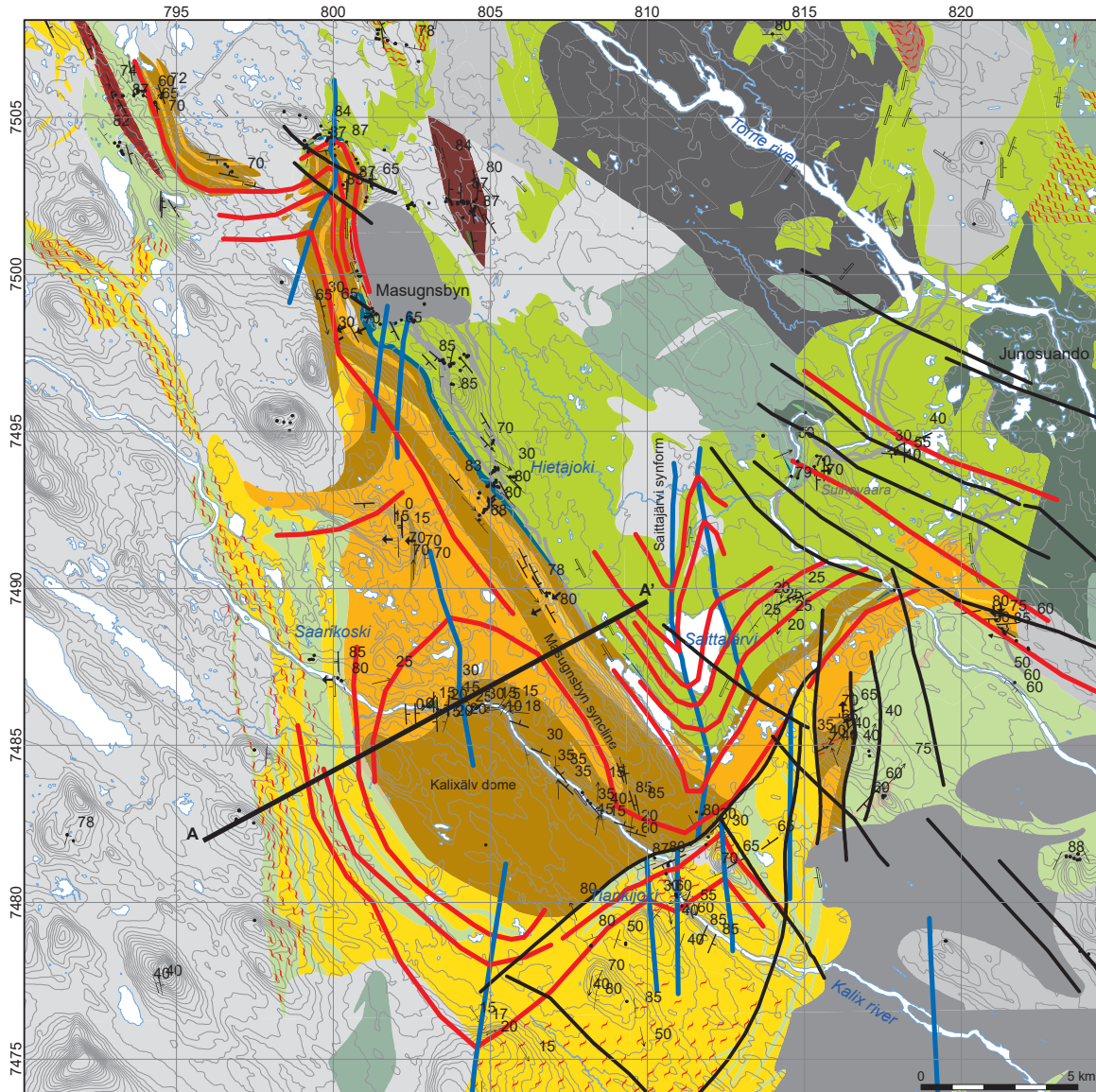


Figure 18. A. Geological map of the southern part of the Masugnbyn key area (see also Hellström et al., 2018). Profile A-A' refers to a qualitative cross-section presented in Figure 28. Fold axial traces of the folding phase F2 are marked in red; F3 fold axial traces are marked in blue. Small black dots mark recent outcrop observations.

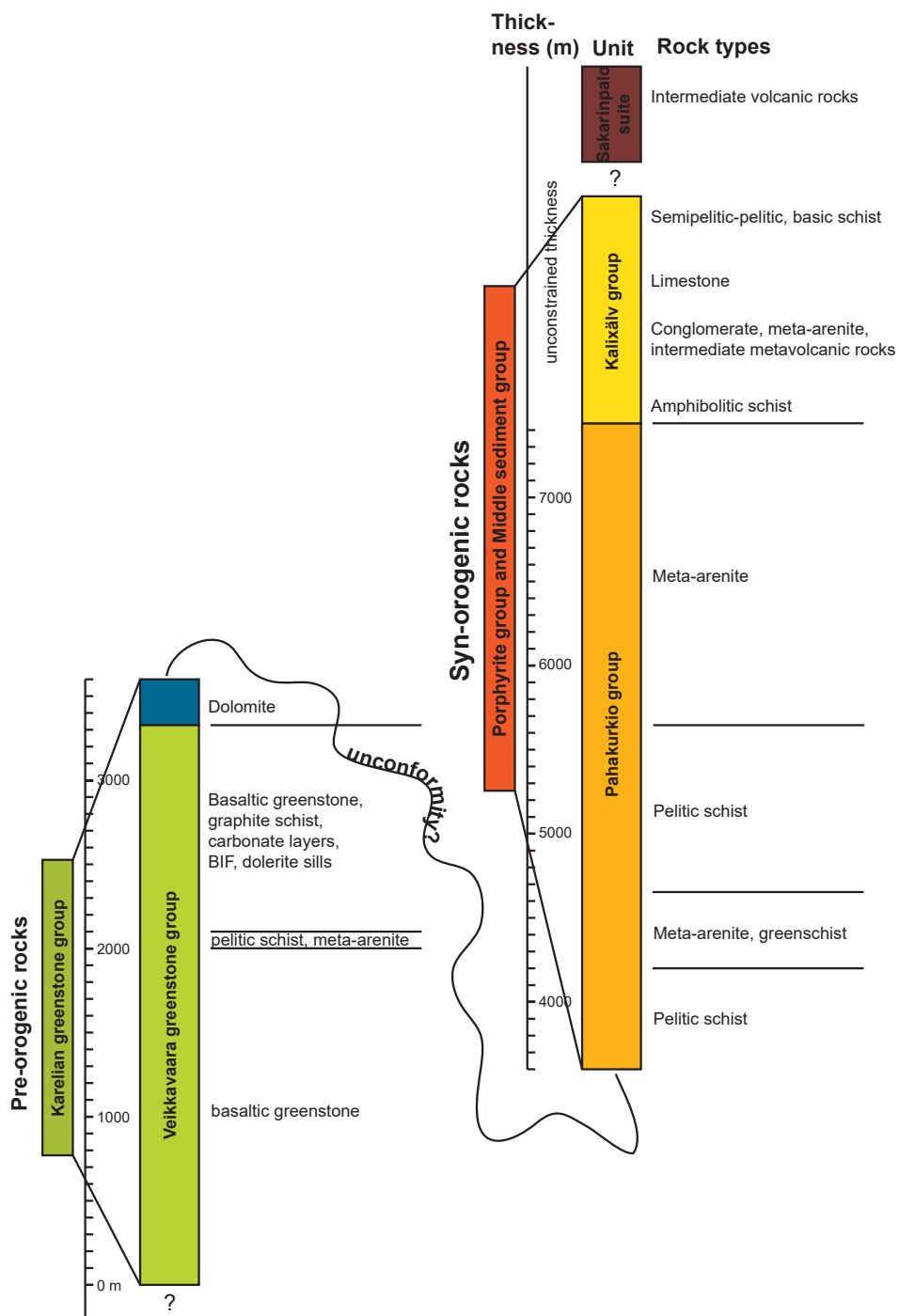


Figure 18. **B.** Simplified lithostratigraphic column of the southern Masugnsbyn area based on a combination of geological data from Padget (1970), Niiniskorpi (1986) and Hellström & Jönsson (2014).

maps such as VLF (Very Low Frequency) and slingram maps over approximately the same distance (Fig. 21, cf. Hellström & Jönsson 2014).

The Pahakurkio group overlies the rocks of the Veikkavaara greenstone group. The contact between these two units is not exposed, so it is unclear whether the contact is conformable. The Pahakurkio group consists of a sequence of clastic metasedimentary rocks and has been divided into four lithological units. From bottom to top, these are pelitic schist, metaarenite (arkosic sandstone), andalusite-

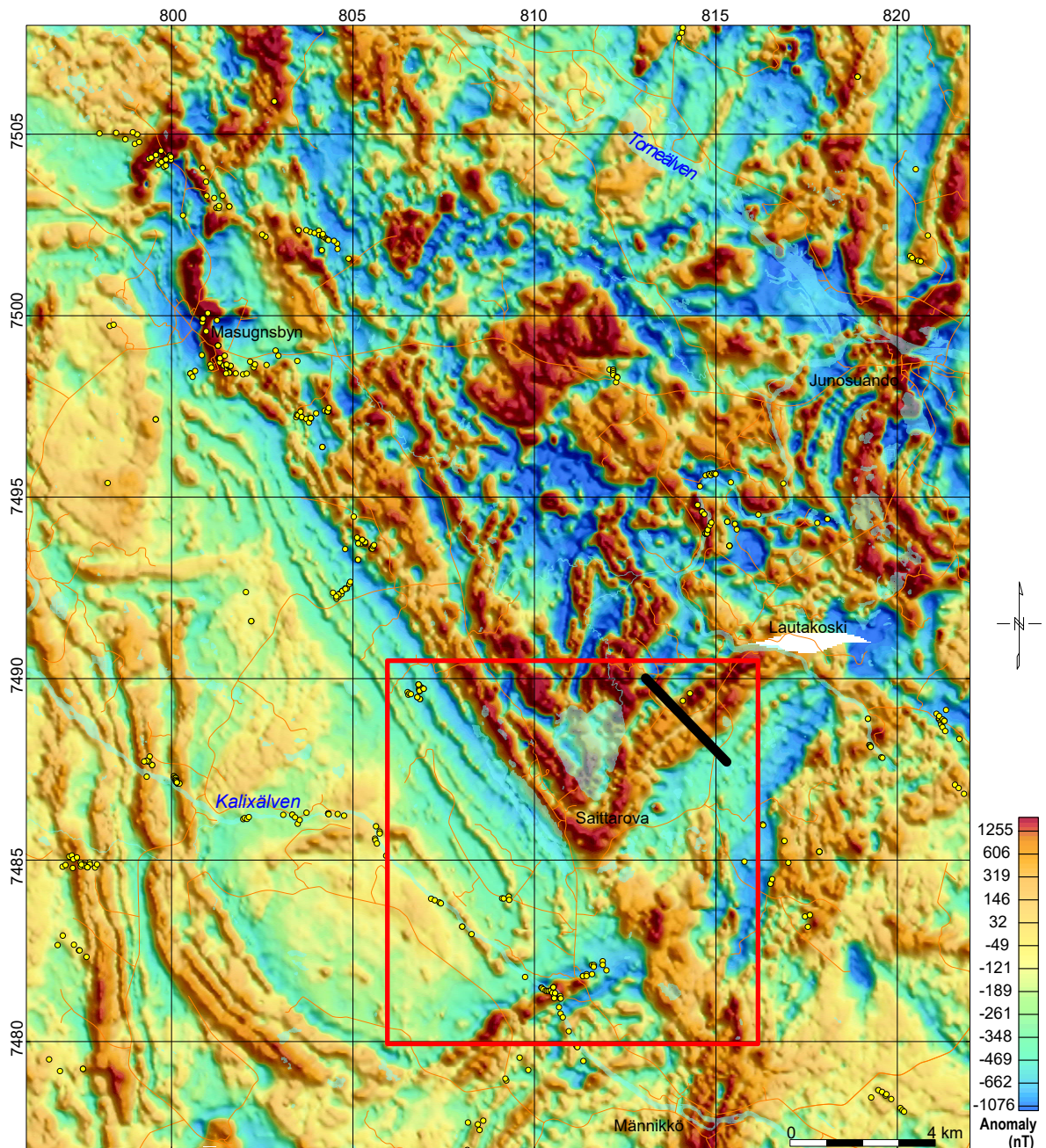


Figure 19. Residual magnetic anomaly map based on data from airborne measurements. Yellow circles represent acquired petrophysical samples. The red polygon outlines the area of the 3D VOXI model and the black line in its upper right-hand corner shows the extent of the cross-section derived from it (Fig. 27). Note the high-magnetic signature of the mafic rocks of the greenstone group.

bearing pelitic schist and a second unit of metaarenite. The arenites are often cross-bedded, allowing the determination of younging directions, which are consistently to the west. The rocks of the Pahakurkio group have an overall low magnetic signature, but there are higher-magnetic conformable layers consisting of strongly scapolite-altered intermediate rocks, which, judging from the aeromagnetic map, have a considerable lateral extent (Fig. 19). Graphite schists and carbonate rocks may also occur within the Pahakurkio group, which makes it difficult to distinguish these rocks from the VGG.

Rocks of the Kalixälv group are exposed to the west and south of the Pahakurkio group sedimentary pile. On the aeromagnetic map, the unit is characterised by alternating high and low-magnetic

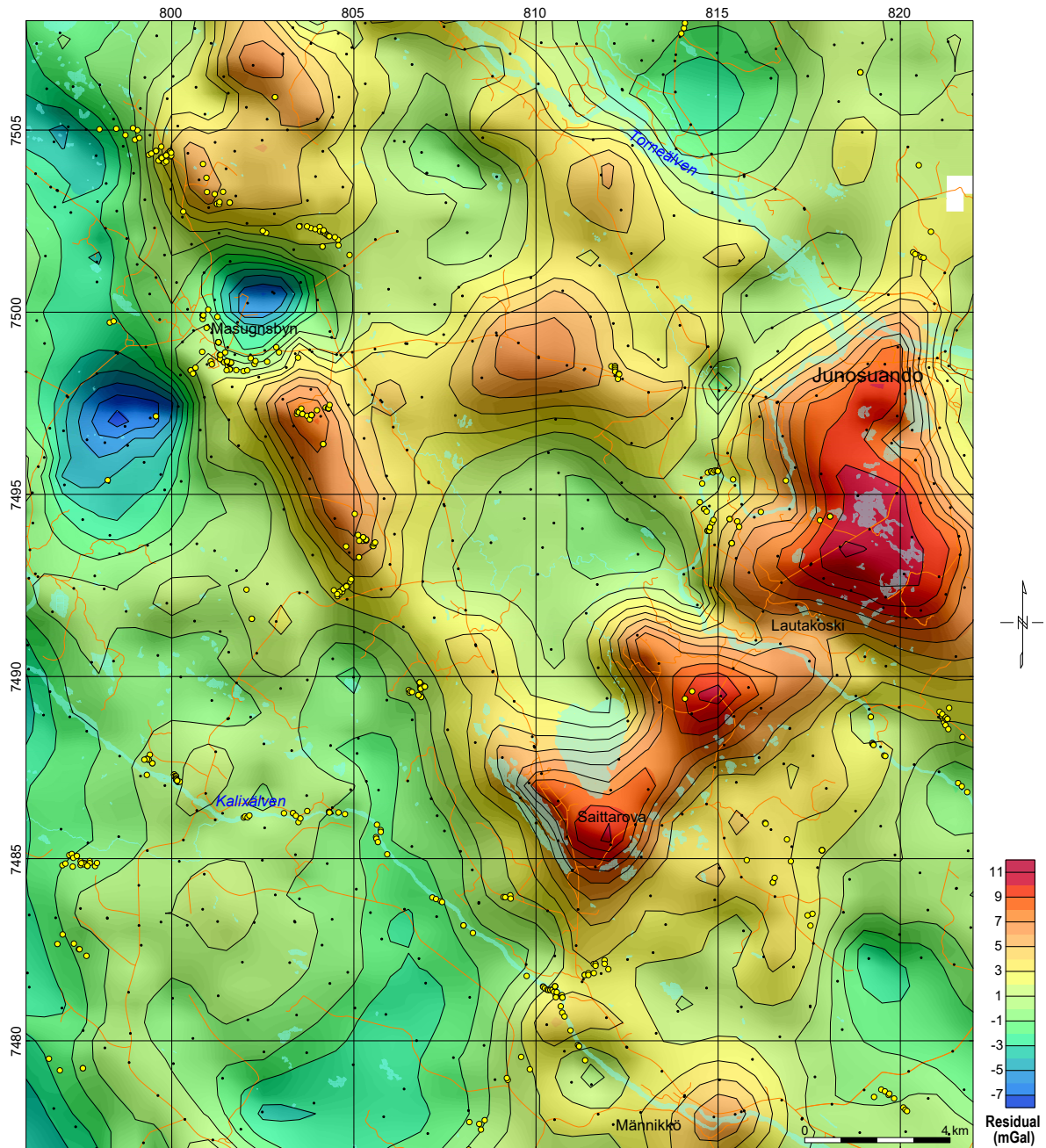


Figure 20. Residual gravity anomaly. Yellow circles represent acquired petrophysical samples and black dots are measurement sites. The dense mafic rocks of the greenstone group generate positive gravity anomalies, while the lighter metasedimentary rocks of the Pahakurkio and Kalixälven group are negative features on the gravity map

bands caused by alternating layers of metavolcanic rocks and pelitic to arenitic metasedimentary rocks, respectively. An approximately 20–30 m thick basal conglomerate is overlain by amphibole-bearing metaarenite, followed by mica schist, quartzites and layers of meta-andesite, but the bedrock crops out poorly. To the west and southwest, an increasing degree of migmatization affects the metasedimentary rocks, so the natural, upper stratigraphic limit for the group is not known. The transition from the Pahakurkio to Kalixälven group is not well understood, and an interpretation of structures is difficult, due not least to the similar lithologies of both groups (pelitic and arenitic metasedimentary rocks).

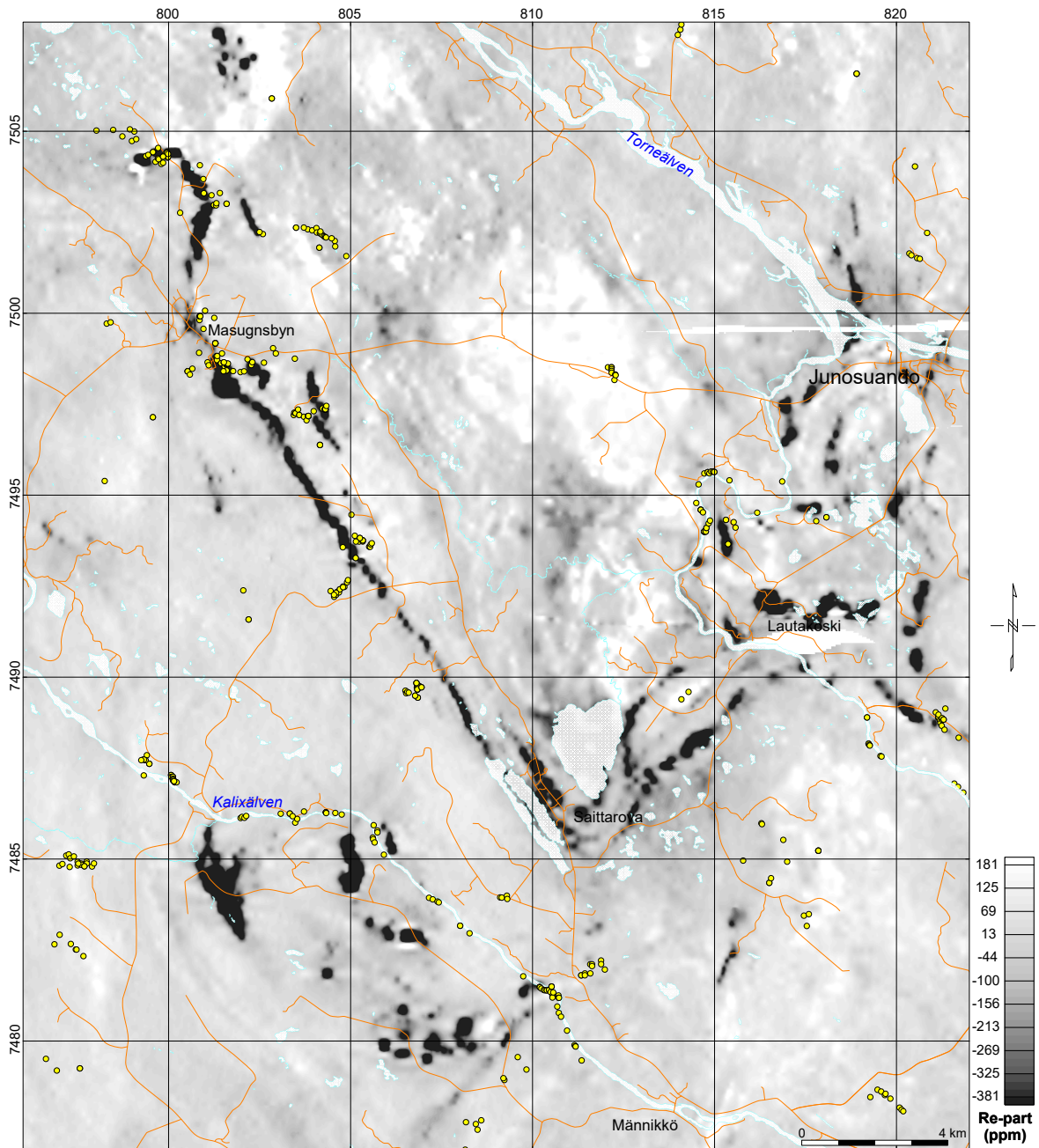


Figure 21. Slingram anomaly map based on data from airborne measurements. In-phase component. Yellow circles represent acquired petrophysical samples. The darker colours show metasedimentary rocks that are rich in graphite and therefore good electrical conductors.

### *Structural inventory*

The deformational record is best preserved in sedimentary rocks of the Pahakurkio group. During a first deformation phase (D1), a gneissic foliation (S1) with foliation-parallel migmatitic veins formed locally in these rocks. It is therefore assumed that all rocks in the area were deformed to some extent during D1. It is, however, unclear whether folding occurred during D1. The first observed folds F2 are attributed to a second deformation event D2, since they fold the migmatitic foliation S1.

Structural geological data from Lake Saittajärvi (cf. Fig. 18A) northwestwards to at least Masugnsbyn show that both metasedimentary rocks of the Pahakurkio group and graphite and dolomite layers



Figure 22. Stereographic projection (lower hemisphere) of structural data at Hietajoki. Note that both bedding and foliation dip steeply to the northeast. However, younging is consistently to the southwest (see text).

of the Veikkavaara greenstone group dip steeply towards the northeast (Fig. 22), whilst younging is consistently to the southwest, i.e. positioning younger under older rocks (Fig. 18A; see also Kumpulainen 2000). These structural data suggest that the rocks in this approximately 16 km long NW–SE oriented band from Masugnsbyn to Saittajärvi occupy an overturned F2 fold limb formed during a second deformation phase D2.

At Suinavaara (cf. Fig. 18A), rocks of the Veikkavaara greenstone group crop out and display a hinge zone of an F2 fold. Here, fold axes plunge 40 degrees towards the southeast. Folding is disharmonic and a well-developed axial planar foliation striking northwest–southeast truncates the original layering (Fig. 23A). The truncation is interpreted to be a consequence of dissolution along the foliation planes perpendicular to the original shortening direction. On a regional scale, this process creates pinnate fold hinges and apparent offsets of the greenstone layers visible on outcrop scale (Fig. 23A) and as magnetic lows on the aeromagnetic map (Fig. 19).

Strong coaxial deformation during F2 is also inferred from, e.g., chocolate tablet boudinage of competent layers in siltstones of the Pahakurkio group at Hietajoki (Fig. 23B, cf. Fig. 18A) and isoclinal F2 folding of greenstone layers observed just south of Masugnsbyn (Fig. 23B).

Direct geological evidence of a second folding phase (F2) affecting the rocks at least in the southern part of the Masugnsbyn key area can be found in outcrops along the river Kalixälven near the estuary of the Tiankijoki river (cf. Fig. 18A). Here, fold interference patterns can be observed in arenitic to pelitic metasedimentary rocks of the Kalixälven group. A gneissic foliation (S1) developed in these rocks during D1. At some locations, the original bedding (S0) is still discernible, and S1 crosscuts S0. Migmatite veins run parallel to this gneissic foliation and were tightly to isoclinally folded during folding phase F2, belonging to a second deformation phase D2. Parasitic folds belonging to the F2 folding phase are locally discernible (Fig. 24A–C). During folding phase F2, compression was oriented N–S, and an axial planar foliation S2 developed locally.

Sillimanite platelets grew parallel to S2 and were folded by a later folding event (F3) during a third deformation phase (D3). Some of the F3 fold hinges are infilled by migmatitic veins (Fig. 24B) and a non-pervasive, spaced cleavage (S3) developed parallel to the kink fold axial planes (Fig. 24B & C).

Recent radiometric isotope dating of the migmatitic rocks along the river Kalixälven yielded metamorphic ages of 1.88–1.86 Ga (Bergman et al. 2006, Hellström 2018). U–Pb SIMS analyses of metamorphic, low-Th/U zircon rims from a sillimanite-cordierite-bearing migmatite (cf. Fig. 24C), were dated at  $1878 \pm 3$  Ma (Hellström 2018). This age is interpreted to date migmatitisation and also puts constraints on the age of folding of supracrustal rocks. The 20 Ma age difference between the zircon rim age obtained and the monazite age of Bergman et al. (2006) possibly reflects resetting of the U–Pb isotopic system in monazite, i.e. 20 million years after the migmatitisation event dated by U–Pb in zircon.

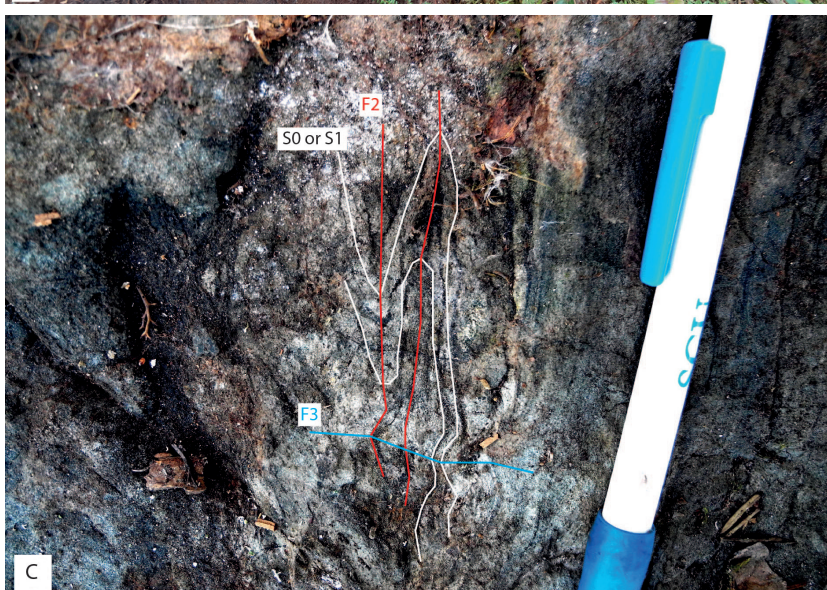


Figure 23. **A.** Disharmonic folds in basaltic volcaniclastic meta-sedimentary rocks of the Veikkavaara greenstone group at Suinavaara (SWEREF99 TM: N7494097, E815614). A southeast-plunging fold axis is marked by the pencil. Note the thinning of the fold limbs in the top left-hand corner of the photograph and the truncation of original bedding by the axial planar cleavage. **B.** Boudinage of competent layers parallel to S<sub>0</sub> in siltstones of the Pahtakurkio group. The interboudin space is filled with quartz. S<sub>1</sub> is recognisable in the finer-grained layers, shallowly dipping to the northeast. Hietajoki (SWEREF99 TM: N7492325, E804671). **C.** Isoclinal folds (F<sub>2</sub>) in mafic volcaniclastic metasedimentary rocks of the Veikkavaara greenstones. Kink folds (F<sub>3</sub>) occur orthogonal to F<sub>2</sub>. Pahtajoki (SWEREF99 TM: N7502177, E802368).

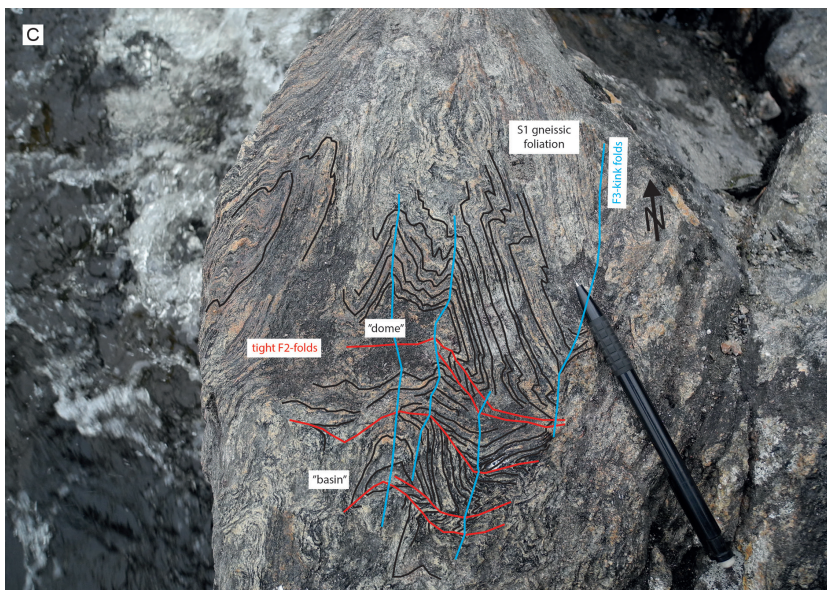
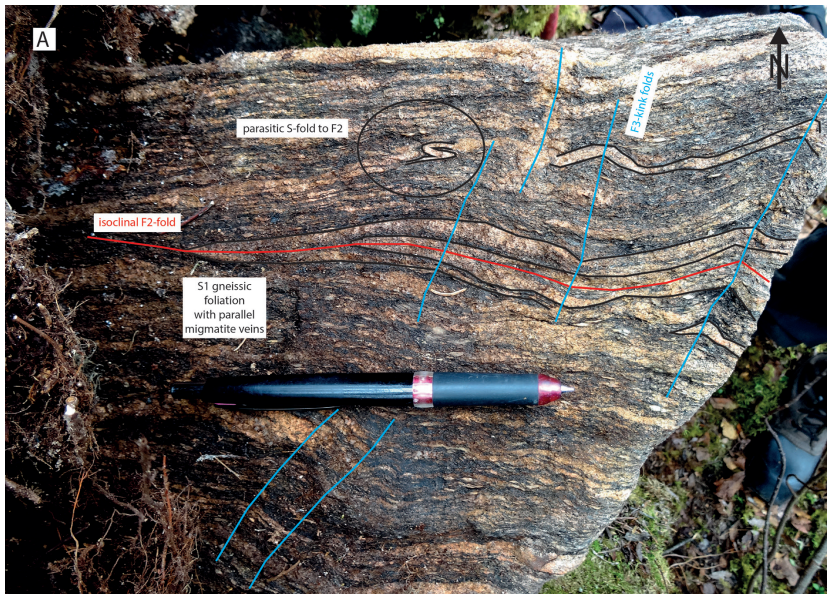


Figure 24. Fold interference patterns in migmatitic pelitic rocks of the Kalixälven group on the shore of the river Kalixälven (SWEREF99 TM: N7480220, E810924). Tight to isoclinal F2 folds are refolded by open kink folds (F3). **A.** Note the small S fold, which is incompatible with the F3 folding and must therefore be a parasitic fold to F2. **B.** Increased amplitude and decreased wavelength of F3 folds. The F3 fold hinge is infilled by a migmatitic vein. North is up. **C.** Small-scale “basin and dome” structure created by depressions and culminations of the F3 folds. This fold interference pattern is thought to roughly represent the regional-scale structural pattern in the Masugnbyn area.

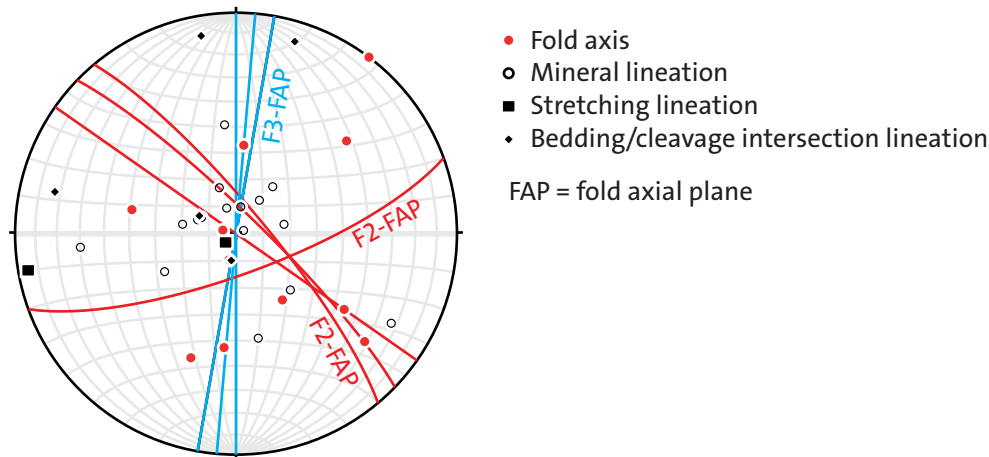


Figure 25. Stereographic projection (lower hemisphere) of fold axial planes, fold axes, and related lineations for the Masugnsbyn area. Three predominant fold orientations can be seen. The two fold axial plane orientations of F2 are interpreted as being due to reorientation of F2 folds during F3 kink folding around vertically or steeply dipping fold axes. No distinction was drawn between greenstones and syn-orogenic rocks.

Plotting axial planes and fold axes for the entire Masugnsbyn key area in a stereographic projection shows three main fold axial plane orientations (Fig. 25).

The relationship between F2 and F3 folding can be seen impressively in high-resolution magnetic data available for an area just north of Masugnsbyn (Fig. 26). Here, the magnetic banding created by the different lithologies in the Pahakurkio group can be used to trace entire layers. The fold interference pattern is evident immediately and matches the proposed two more or less orthogonal folding events that have affected the area.

On the current bedrock map at a scale of 1:50 000 (Padget 1970), the large-scale, V-shaped structure at Lake Saittajärvi in the centre of Figure 18A is interpreted to be an anticline cored by greenstones. However, a 3D model of airborne magnetic data on that area reveals that the limbs of this structure dip towards each other (Fig. 27,) suggesting that the structure is instead a north-plunging synformal anticline. The eastern limb and the core of the synform are poorly exposed and it is difficult to verify the proposed structural model. A cross-section across the eastern part of the 3D model supports the theory that the rocks in the eastern limb of the synform had been folded prior to its formation (Fig. 22B). This is consistent with the structural data collected from the western limb of the V-shaped structure near Hietajoki and Masugnsbyn.

Both the structural observations and the geophysical modelling results suggest two phases of folding. During F2 compression was oriented N–S, resulting in isoclinal to tight E–W trending folds. During F3 compression was oriented E–W and resulted in open kink or crenulation folds with steeply to shallowly north and south-plunging fold axes. F3 fold axial planes dip steeply. Fold interference patterns were created by refolding of the F2 fold axial planes (Fig. 24 A–C). F3 folds are less pervasive and have somewhat more variable amplitudes and wavelengths than the F2 folds. Their effect is mostly observed in the hinge zones of what has been interpreted as regional-scale F3 folds. The dominant large-scale synform mentioned earlier is therefore a synform that folds bedding (S0), migmatitic banding (S1) and F2 folds around a steeply north-plunging fold axis. The hinge of this regional-scale F3 synform lies close to lake Saittajärvi. Here, a large positive slingram anomaly can be observed (Fig. 21), but it is unclear whether this relates to the water body of the lake or to a potential enrichment in graphite. Although some of the F3 fold hinges are infilled by migmatitic veins, the kink folding style during F3 indicates colder metamorphic conditions during the second folding phase than during the isoclinal F2 folding.

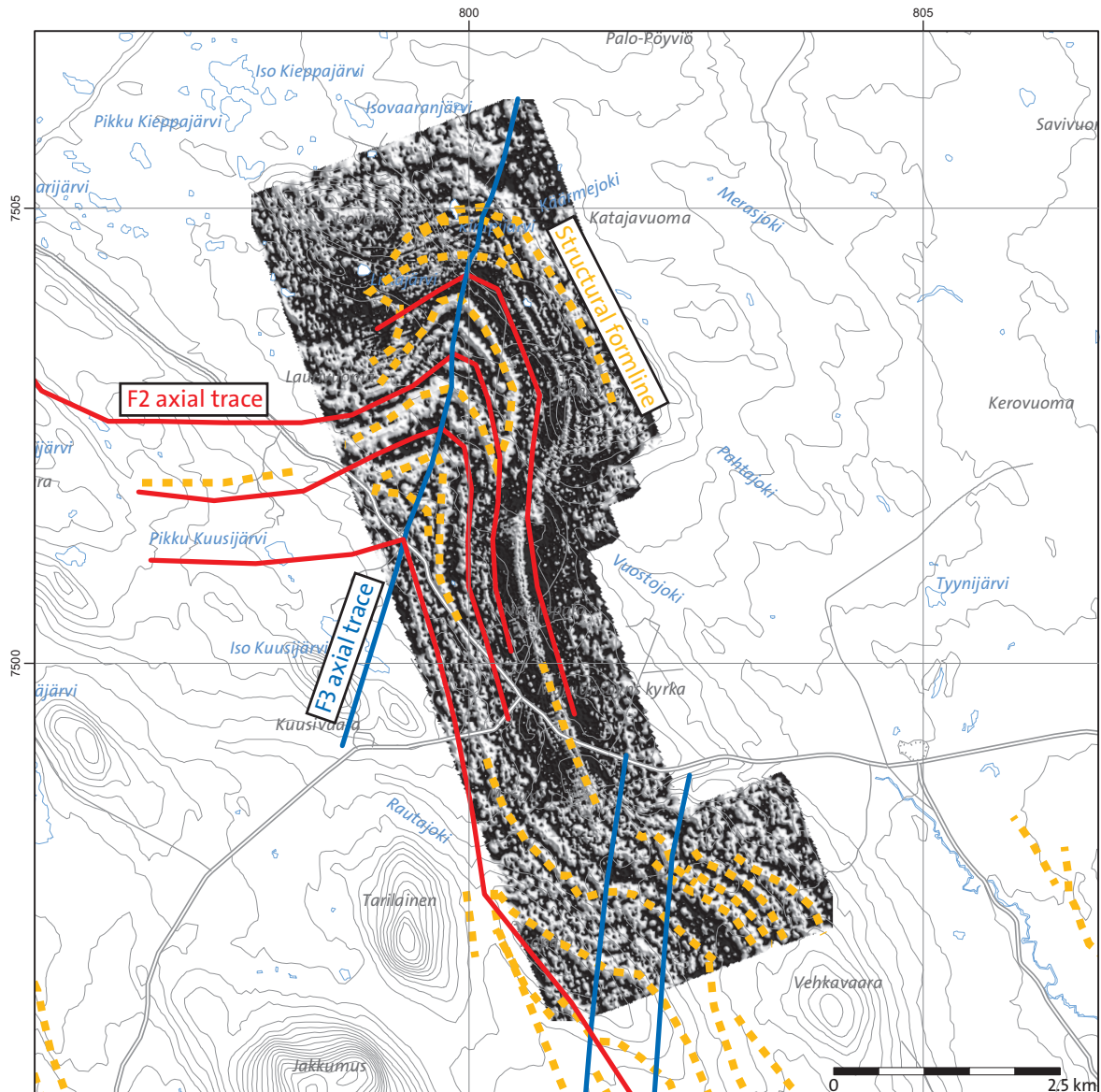


Figure 26. Fold interference created by originally E–W-striking F2 folds (red lines), being refolded by F3 folds (blue lines). The yellow lines mark magnetic connections corresponding roughly to original bedding  $S_0$  and  $S_1$  foliation.

### Unresolved questions

A major break in the orientation of magnetic markers occurs at Saarikoski (cf. Fig. 18A) at the boundary between shallowly dipping rocks of the Pahakurkio group and steeply dipping rocks of the Kalixälven group. Along the east–west-oriented part of the Kalixälven shore, mica schists and metarenites of the Pahakurkio group dip shallowly, and predominantly to the west. Stretching lineations also plunge to the west. Following these units along the river, however, it becomes clear that these rocks are folded into open, north–south-trending, doubly plunging folds, which are attributed to the F3 folding phase in this report. The “Kalixälven dome” (Padget 1970; cf. Fig. 18A) is therefore interpreted here to correspond to a culmination of a doubly plunging antiform refolding of the “Masugnsbyn syncline” (Padget, 1970). But it is unclear whether the Kalixälven dome and the Saittajärvi synform formed during the same folding

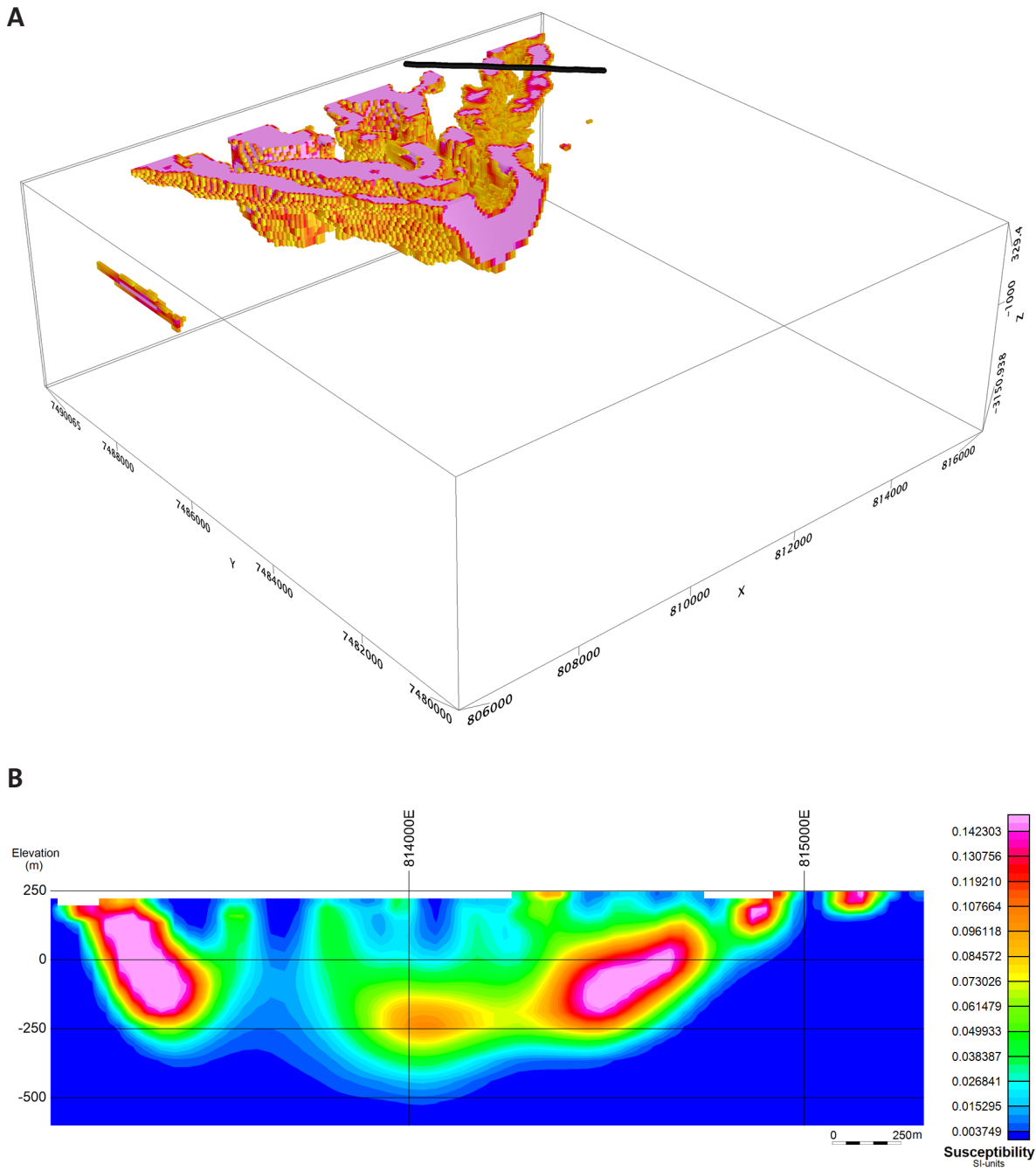


Figure 27. **A.** 3D model of the V-shaped structure at Saittajärvi using VOXEL modelling of the magnetic field. The synformal shape of the greenstone succession becomes clear when looking obliquely at the model from above towards the NE. **B.** Vertical section derived from the 3D VOXI model across the eastern limb of the Saittajärvi synform. This profile suggests that the rocks in the limb had been folded prior to formation of the synform.

event. Alternatively, the open, gently plunging folds at Kalixälven may be the result of a fourth, late folding phase F4. It is relatively unlikely though, that these flat-lying rocks reflect early thrusting in the area as was suggested by R. Rutland (pers. comm.). More detailed structural work is necessary to answer this question. A conceptual cross-section from Saarikoski to Hietajoki is presented in Figure 28.

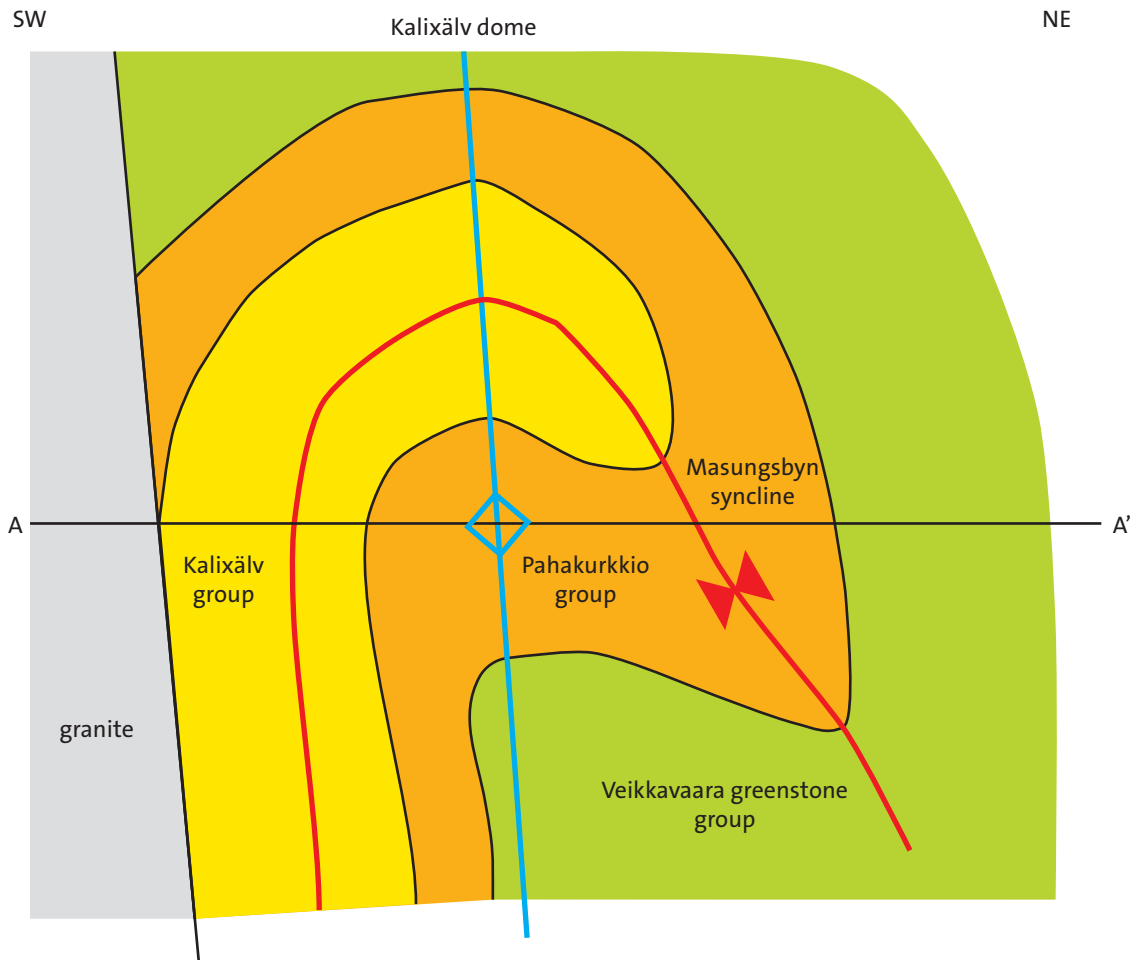


Figure 28. Conceptual cross-section (not to scale) across the Kalixälv dome. Profile line A-A' refers to the ground surface; structures above are thought to be eroded. For approximate location of the profile line see Fig. 18A.

## Käymäjärvi–Ristimella key area

### *Lithostratigraphy*

The inferred lithostratigraphy for the Käymäjärvi–Ristimella key area is predominantly based on map descriptions by Padget (1977), Lindroos & Henkel (1981) and Martinsson et al. (2013). More detailed descriptions of the lithostratigraphic sequences are given in Grigull et al. (2014), Grigull & Berggren (2015) and Martinsson et al. (2018). A simplified geological map and lithostratigraphic column are shown in Figure 29.

The oldest rocks in the area occur close to Käymäjärvi township (Fig. 29A) and consist of high-Mg, meimechitic lapilli tuffs, probably of pyroclastic origin. Meimechite belonging to the Käymäjärvi formation (Fig. 29B) of the Veikkavaara greenstone group occupies the core of an overturned anticline addressed later. The Käymäjärvi formation is overlain by rocks belonging to the Vinsa formation, a mixed unit of mafic metavolcanic and metavolcaniclastic rocks, calc-silicate rocks, dolomite, graphite-bearing schists, skarn-hosted iron ore and a banded iron formation. It is subdivided into four sub-units (Fig. 29B, cf. Martinsson et al. 2013, 2018). The lowest sub-unit of the Vinsa formation occurs within the core of the Käymäjärvi anticline and, possibly, in the far northeastern corner of the key area. Grey, fine- to medium-grained tuffites of basic composition, along with grey, fine-grained basalts, comprise the main part of the lowest sub-unit of the formation. Dark grey, very fine-grained graphite-bearing

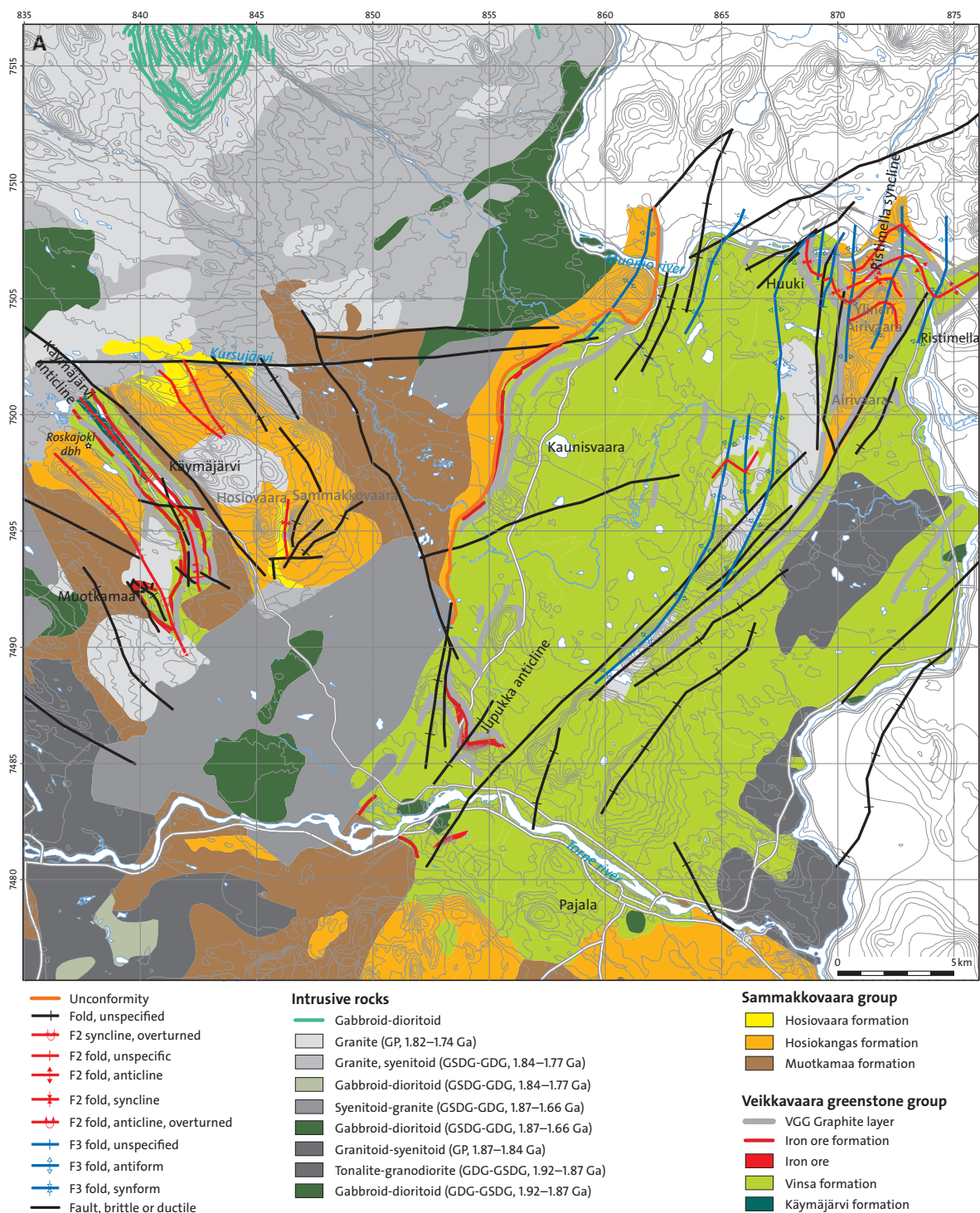


Figure 29. **A.** Simplified geological map of the Käymäjärvi–Ristimella area.

schists are intercalated with the tuffites. Schists contain sulphide mineralisations such as pyrite, chalcopyrite and pyrrhotite, leading to typical rusty weathering.

The second sub-unit of the Vinsa formation consists of a banded iron formation (BIF) with a locally developed oxide facies. These rocks are banded with 10–20 cm thick layers of recrystallised chert and silicates. The BIF occurs in limbs of both the Käymäjärvi anticline and the Jupukka anticline. Where it is magnetite-bearing, it has a strong magnetic susceptibility, which is prominent in magnetic field

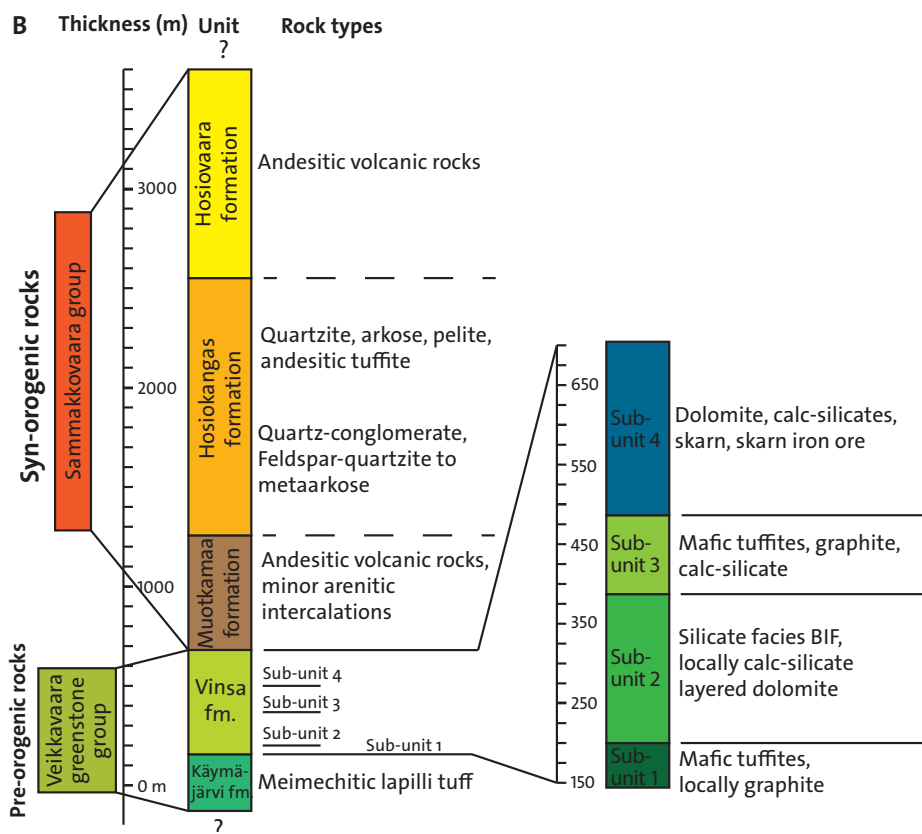


Figure 29. B. Simplified stratigraphic column for the Käymäjärvi–Ristimella key area.

(Fig. 30). The third sub-unit of the Vinsa formation consists of mafic tuffites, graphite-bearing schists and impure limestone intercalations. These rocks occur mainly to the east of the Kaunisvaara ore belt and to a lesser extent in the Käymäjärvi anticline.

Grey to green, fine-grained to very fine-grained tuffites make up the main rock volume of sub-unit 3 and are often laminated on a millimetre scale. Graded bedding and soft-sediment deformation structures, including decimetre-scale faults, slumping structures and sedimentary collapse structures, are locally preserved in the laminated tuffites. The presence of soft-sediment structures indicates that the laminated tuffites were deposited under water, either as primary volcanic metasedimentary rocks or redeposited as epiclastic metasedimentary rocks. Locally, the tuffites contain layers of massive, unbedded mafic rocks. It is unclear whether these are basaltic layers or basic sills, as the contact between the massive layers and the tuffites has not been observed in situ. Both the tuffites and the massive layers can be slightly magnetic. The impure limestones are light grey and usually coarse-grained. The limestone intercalations can reach significant thickness of approximately 100 m or more, for example in Finland just north of the river Muonioälven (Fig. 29A), where the limestone has been quarried in two open pits. Within the key area, impure limestones were observed on the shore of Muonioälven between Aarevaara and Huuki and in both limbs of the Käymäjärvi anticline. The graphite-bearing schists are probably basic tuffites enriched in graphite. These rocks are mostly very fine-grained and show typically rusty to orange weathering due to a high content of iron sulphides. Pyrite, for example, occurs disseminated throughout the graphite-bearing schist. The latter and the impure limestone intercalations usually occur close to one another.

A coarse-grained, light grey, locally calcitic dolomite forms the top of the Vinsa formation. The dolomite contains layers of more competent material (silicates?). In an outcrop near Käymäjärvi, the dolomite contains lenses and nodules of actinolite or tremolite crystals, indicating skarn alteration. A

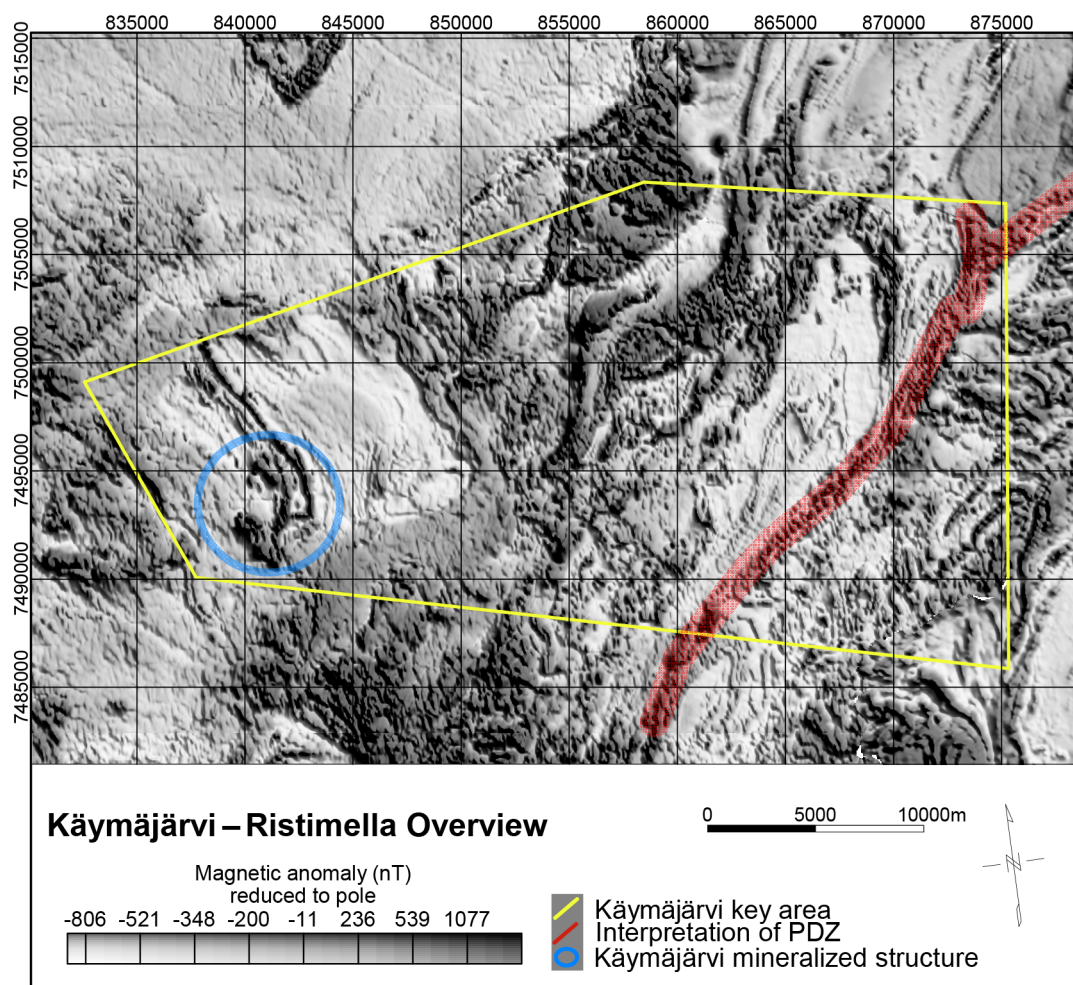


Figure 30. Magnetic anomaly map of the Käymäjärvi–Ristimella key area (yellow), based on data from airborne measurements. The blue circle marks an area modelled in 3D. The red area marks the approximate extent of the Pajala deformation belt, which is further described in the text.

banded skarn horizon underlies the dolomite lens here. At this location, the dolomite has a magnetic susceptibility ten times higher than elsewhere, indicating a higher magnetite content. The dolomite hosts the skarn iron ores in the Kaunisvaara ore belt (e.g. Tapuli and Sahavaara), which is clearly visible on the magnetic anomaly maps.

The rocks of the Veikkavaara greenstone group are overlain by syn-orogenic rocks belonging to the Sammakovaara group (Martinsson 2004, Martinsson et al. 2018). The Sammakovaara group mainly occurs in the western part of the key area, west of the Kaunisvaara ore belt. In the eastern part of the key area the group is exposed in the core of the Ristimella syncline, addressed later in the text. In Finland, immediately to the north of the key area, large amounts of clastic metasedimentary rocks occur, along with a body of an intermediate metavolcanic rock (Väänänen 1984, GTK map sheet 2713, Kolari). To the south of the key area, in the Liviöjärvi key area (Luth & Jönsson 2014), clastic metasedimentary rocks and metavolcanic rocks belonging to the Sammakovaara group are both abundant. The Sammakovaara group is divided into the Muotkamaa, Hosiokangas and Hosiovaara formations (Fig. 29B, Martinsson et al. 2018).

Andesitic metavolcanic rocks observed just east of the dolomites at Muotkamaa are interpreted as belonging to the Muotkamaa formation. The formation is poorly exposed, and other rocks belonging to it were only observed in one outcrop. However, andesitic rocks occur between a sub-unit 4 dolomite

and clastic metasedimentary rocks of the Hosiokangas formation in a borehole at Roskajoki (cf. Fig. 29A). A thin band of Muotkamaa formation is therefore included to the west of the Käymäjärvi anticline (Fig. 29A).

Rocks of the Hosiokangas formation are predominantly of clastic sedimentary origin. To the east of Käymäjärvi, the Hosiokangas formation occupies the western, overturned limb of a syncline. Light grey to pink quartzitic to arkosic and sublithic arenites occur at the bottom of the depositional succession. Heavy mineral layers in these beds trace cross-bedding on the centimetre to decimetre scale as well as horizontal lamination on the millimetre to centimetre scale. Magnetite layers occur locally and the rock has been migmatized in places. A clast-supported conglomerate has been deposited on top of the arenites or occurs as lenses. More than 95% of the clasts consist of quartz or quartzite, and the pebbles can be up to 30 cm in diameter. Less than 5% of the pebbles consist of basic volcanic rock; these are generally smaller than the quartz pebbles. The conglomerate matrix is coarse-grained. The conglomerate probably occurs as lenses within the arenites rather than as continuous layers. Arenites are overlain by sublitharenitic sandstones and siltstones with distinct hummocky cross-bedding, indicating sedimentation under tidal conditions. Pelitic siltstones were deposited on top of the arenitic sandstones and are locally laminated; ripple marks have been observed. The siltstones become richer in mafic material towards the top, and biotite content increases. White quartzites without any recognisable sedimentary structures occur as intercalations within the pelitic rocks. Migmatization of these pelites can be observed at Sammakovaara and in the Ristimella syncline (cf. Fig. 29A).

Andesitic to dacitic metavolcanic rocks of the Hosiovaara formation (Martinsson 2004) were observed in situ along the shoulders of the Kursujärvi valley in the northwest of the key area. Metavolcanic rocks with andesitic to dacitic composition are also reported to occur in the valley between Hosiovaara and Sammakovaara (Martinsson 2004).

The majority of observed intrusive rocks in the key area belong to the Granite-pegmatite association. These rocks are light red to red, locally porphyritic granites and pegmatites of variable grain size and composition. The granites locally contain magnetite patches.

A white, quartz-poor, albite-rich granite to syenite occurs in the centre of the key area. This rock usually exhibits a ductile foliation and lineation, indicating significant deformation. It may be crosscut by coarse-grained pegmatites. The lineation and parts of the foliation are sometimes traced with amphibole and biotite patches. It is unclear which magmatic suite these rocks belong to.

### *Structural inventory*

Although the rocks of the Kaunisvaara ore belt and the Käymäjärvi anticline belong to the same lithostratigraphic units, it is still unclear which structures actually connect them. A several kilometre-wide body with a relatively irregular but highly magnetic pattern, interpreted as an andesite belonging to the Sammakovaara group, separates these two ore belts (Fig. 29A and 30). No outcrop or drill core information is available for this area. Information on folding in the Kaunisvaara ore belt is particularly scarce, although small-scale folding was reported from a few drill cores near Sahavaara. Due to poor background data, this report focuses on two sub-areas: the Käymäjärvi anticline and the Ristimella syncline.

### **Käymäjärvi anticline**

The Käymäjärvi anticline is the most noticeable structure in the Käymäjärvi area (Fig. 31A, Padget 1977, Grigull et al. 2014). It contains ultramafic metavolcanic rocks (meimechite) of the Käymäjärvi formation in the core and rocks of the Vinsa formation and Sammakovaara groups in both limbs (Martinsson et al. 2013). The banded iron formation of the Vinsa formation sub-unit 2 creates a relatively continuous high magnetic anomaly, and detailed ground magnetic data make it easy to trace the BIF (Fig. 31A). The same goes for the graphitic schist of sub-unit 3, which shows up well on electromagnetic slingram maps (Fig. 31B).

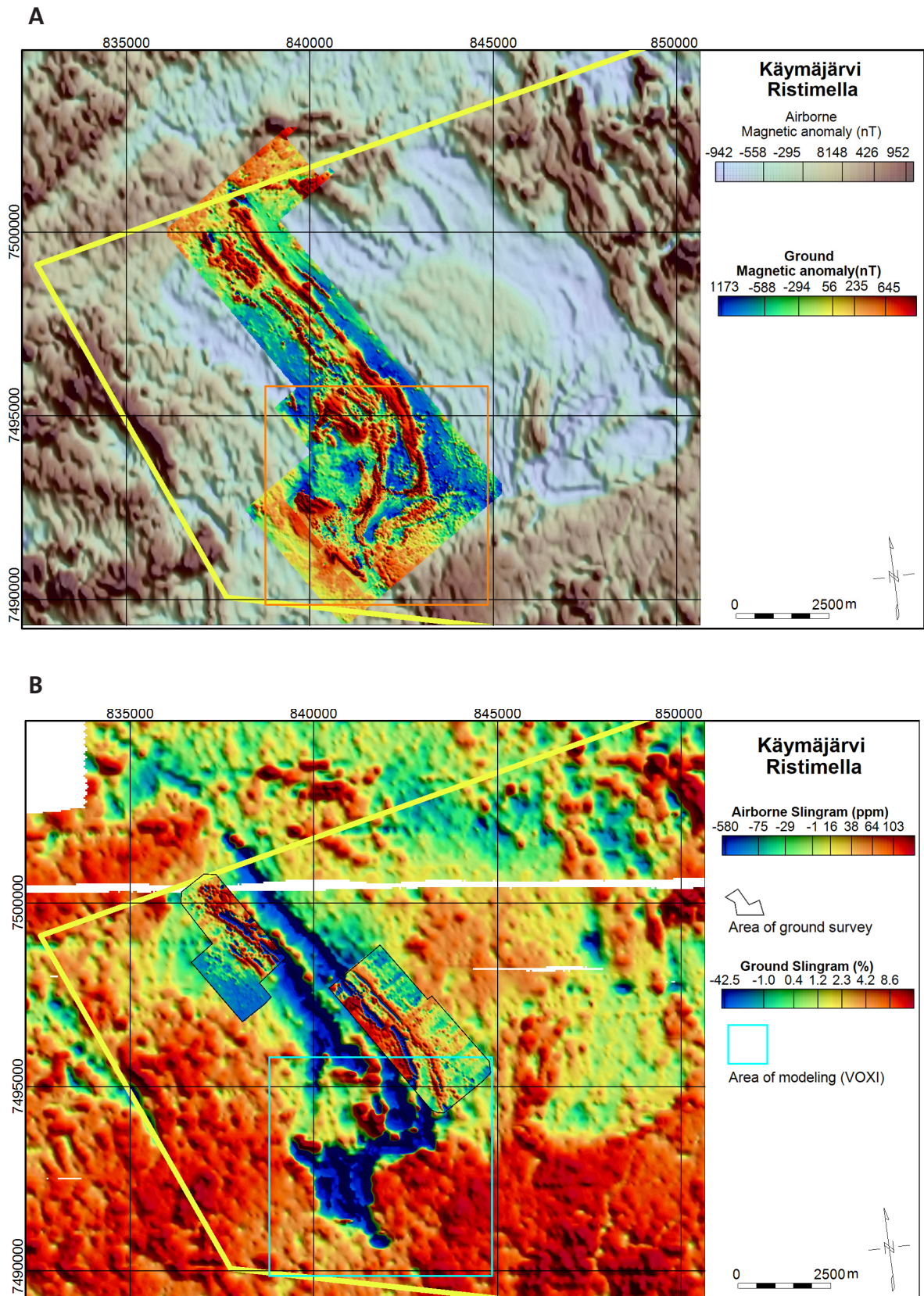


Figure 31. **A.** Airborne magnetic anomaly map of the Käymäjärvi area, based on airborne measurements with overlying ground magnetic map. The BIF and iron-rich skarn horizons of the Vinsa formation clearly stand out. The orange quadrangle refers to a 3D VOXI model of the geophysical ground data. **B.** Airborne slingram anomaly map with superposed ground slingram data. The blue areas are conducting layers and are here attributed to graphite-bearing tuffites of the Vinsa formation.

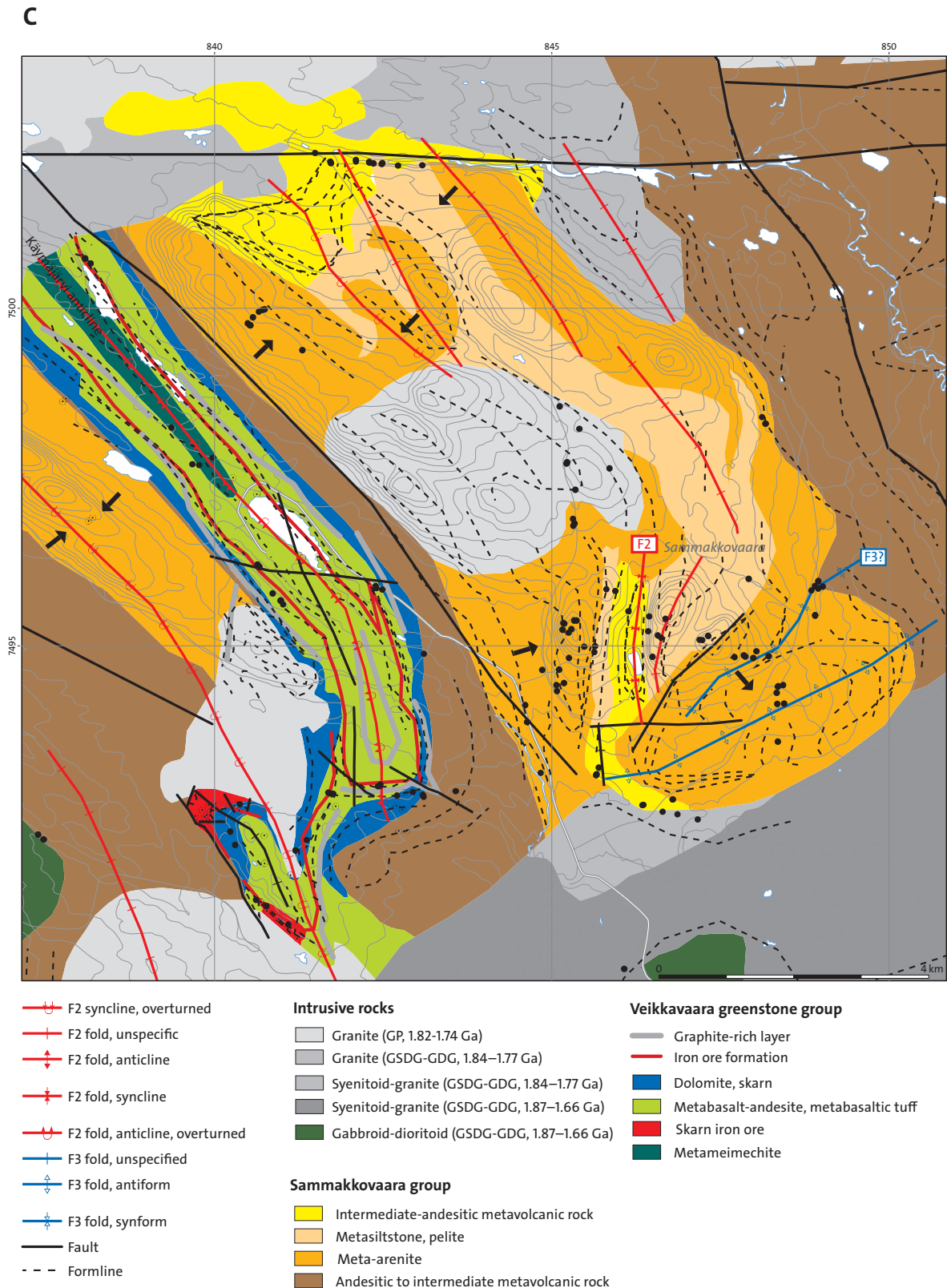


Figure 31. **C.** Simplified geological map of the area around Käymäjärvi and Sannakkovaara. The black arrows indicate younging directions. The black dots show the locations of recent outcrop observations.

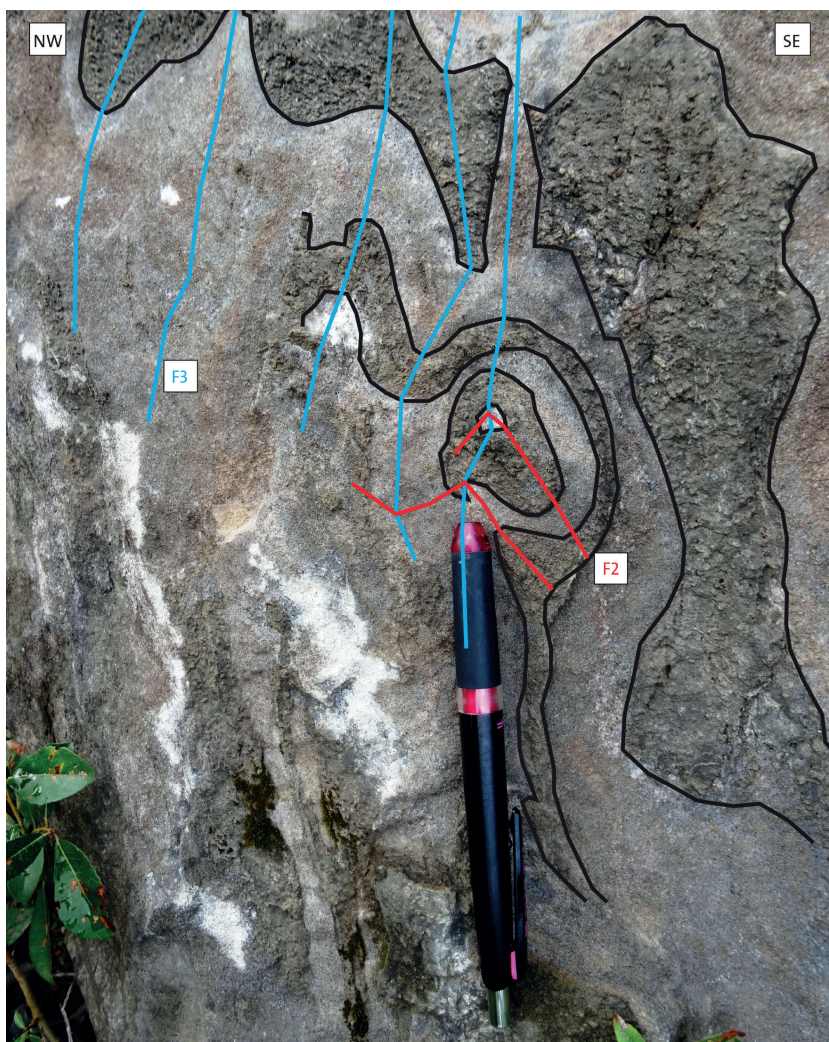


Figure 32. Potentially doubly folded impure marble belonging to the Vinsa formation sub-unit 4. Southeast of Käymäjärvi (SWEREF99 TM: N7495828, E842492).

The northern part of the anticline strikes northwest–southeast (Fig. 31C) and here the eastern limb of the anticline appears to be upright. As bedding measured in the BIF dips steeply towards the northeast, younging direction is also towards the northeast. Towards the southern part of the anticline, bedding planes in both the Veikkavaara greenstones and the Sammakkoavaara group rocks dip steeply to moderately to the west. The rocks become younger towards the east, indicating that the fold axial trace changes direction from southeast to south and the eastern fold limb is overturned.

Although the lithologies strongly resemble those in the Masugnsbyn area, indicators of multiple folding phases are hard to find in the Käymäjärvi area. An impure limestone marble in the eastern limb of the Käymäjärvi anticline has been interpreted as refolded. This was tentatively deduced from fold interference patterns in the impure layers of the marble (Fig. 32). It is questionable, however, whether this observation is representative of the larger-scale structures.

Folding of the clastic metasedimentary rocks of the Sammakkoavaara group (Hosiokangas formation) is more evident than in the greenstones, particularly on Sammakkoavaara hill (cf. Fig. 31C). Here, metapsammitic rocks of silty origin show gneissic banding (S1) that is tightly folded (F2). In other outcrops at Sammakkoavaara hill the migmatitic banding forms open folds (F3) with S-asymmetry on the western side of Sammakkoavaara hill and into Z folds further to the east. However, the outcrops where these fold shapes were observed lie too far apart to allow an interpretation of a larger-scale fold structure.

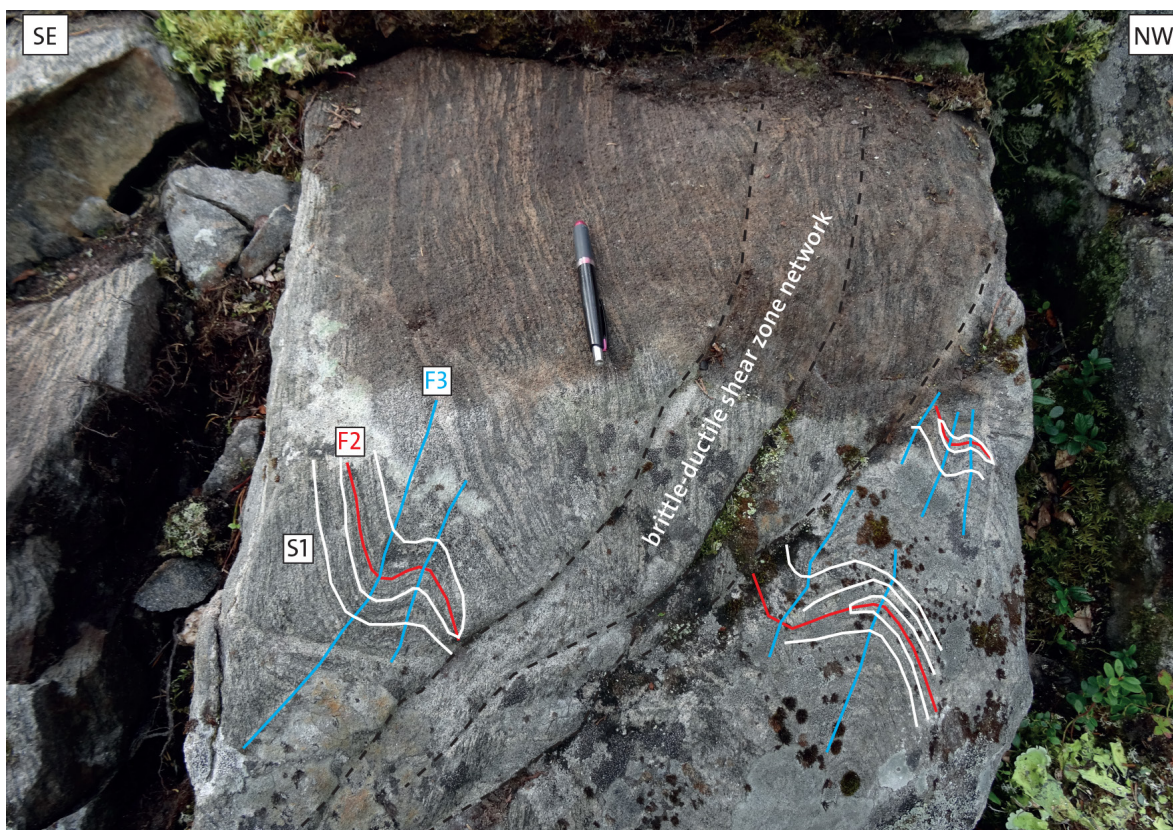


Figure 33. Isoclinal folding (F2) of migmatitic banding (S1) observed in metapelites of the Hosiokangas formation. The banding and the F2 folds are folded into open S folds (F3). Brittle-ductile shear zones cut through the banding sub-parallel to the fold axial planes of the S folds. Sammakkovaara hill (SWEREF99 TM: N7495144, E847317).

The pelitic layers in the Sammakkovaara group produce a slightly stronger magnetic signal and can therefore be used to draw form lines from the magnetic anomaly map. The form line traces, and the relatively abrupt change in strike of both bedding and foliation in the Sammakkovaara group also indicate a possible second, northeast–southwest-trending, set of folds (Fig. 31C). Migmatitic leucosomes that were isoclinally folded during F2 were observed in pelitic metasedimentary rocks at Sammakkovaara (Fig. 33). The F2 folds were refolded into open S folds (F3) with southeast-dipping axial planes (Fig. 33). These folds could be related to the development of a brittle-ductile shear zone system roughly parallel to the orientation of the F3 folds. Although further work is necessary to fully understand the structural framework, it may generally be concluded that, at least locally, the rocks in the Käymäjärvi area underwent two folding events.

The predominant structural grain in the area, seen in both geological and geophysical data, runs northwest–southeast to north–south. When projecting the area’s structural data onto a stereonet, however, many lineations and fold axes plunge steeply to moderately to the south and southwest (Fig. 34A), i.e. down-dip on the predominant foliation planes (Fig. 34B). Moreover, poles to the best-fit great circles to bedding of all units and to migmatitic banding also plunge to the south and southwest. This may indicate that the rocks were affected by a second folding event, resulting in a transposition of pre-existing linear and planar structures.

The possibility that the Käymäjärvi anticline could in fact be a synformal anticline can be discounted on the basis of 3D geophysical modelling of the ground geophysical data that is available on the southern part of the Käymäjärvi anticline (Fig. 35). The model does not show convergence of the two limbs of the fold, but instead supports an anticlinal geometry with steeply dipping fold limbs.

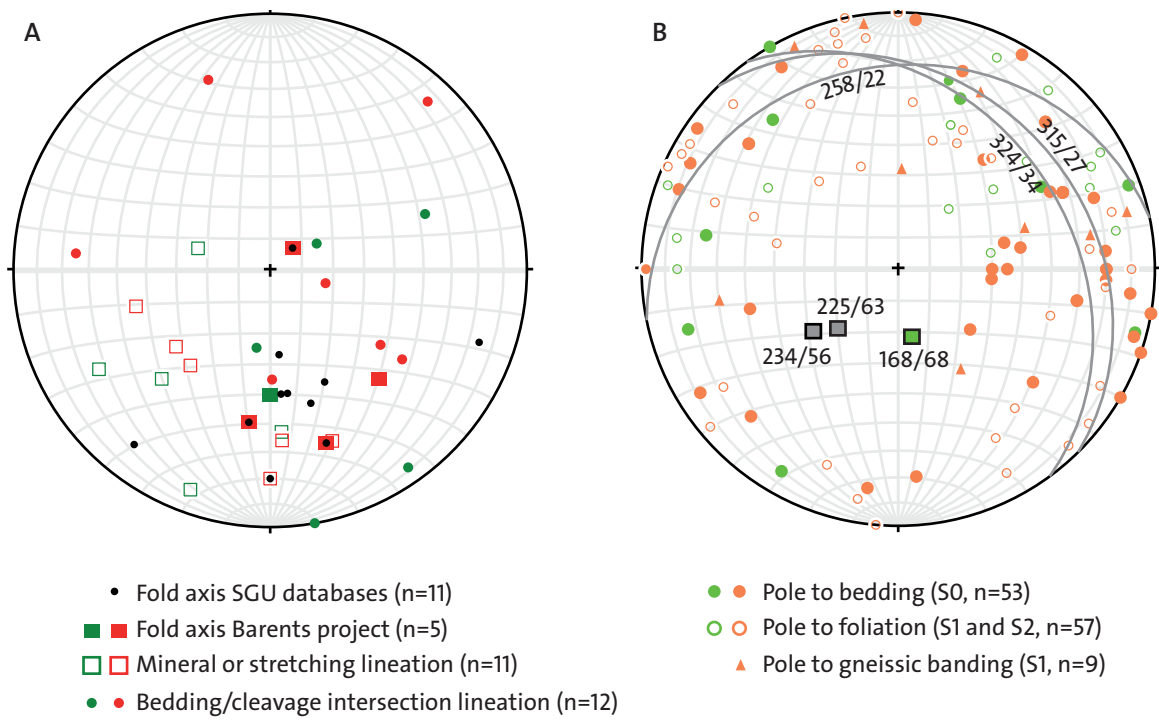


Figure 34. Stereographic projections of structural geological data from the Käymäjärvi and Sammakkoavaara area. Green: Veikkaavaara greenstone group. Red and orange: Sammakkoavaara group. **A.** Linear data. **B.** Planar data.

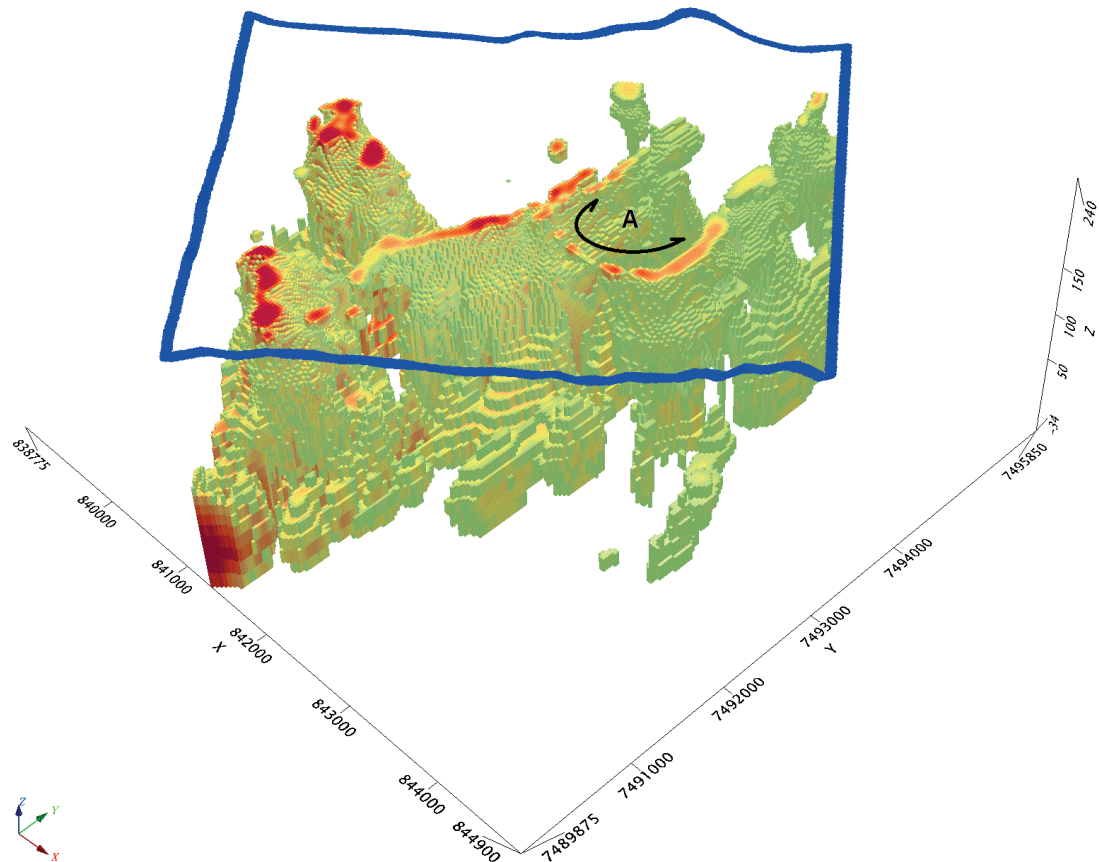


Figure 35. 3D Voxel model of ground magnetic data south of Käymäjärvi. Only high susceptibilities are plotted. Note that the steeply dipping limbs at A do not converge at depth but instead seem to diverge, indicating an anticlinal structure. For modelling area, see Figure 31A.

## Ristimella

The rocks in the area between Huuki and Ristimella, and their continuation into Finland are affected by deformation within the north–south trending Pajala deformation belt (Fig. 36, cf. Luth et al. 2018b). It is therefore important to distinguish between structures that formed before and during this event.

The most noticeable fold structure is the “Ristimella synform”, trending approximately north–south and located to the west of Ristimella (cf. Fig. 36; Grigull & Berggren 2015). The core contains pelitic and psammitic metasedimentary rocks, and is bounded by mafic metavolcanic and graphite-bearing rocks of the Veikkavaara greenstone group in both limbs. While it is not clear whether the metasedimentary rocks belong to the Sammakkoavaara group, they are assumed to be younger than the greenstones. The large difference in susceptibility between the metasedimentary rocks and the metamorphic mafic rocks of the greenstone group helps to make the synform visible in a Voxel model of aeromagnetic data (Fig. 37). A subvertical fault bounding the Ristimella syncline to the east can also be inferred from this model.

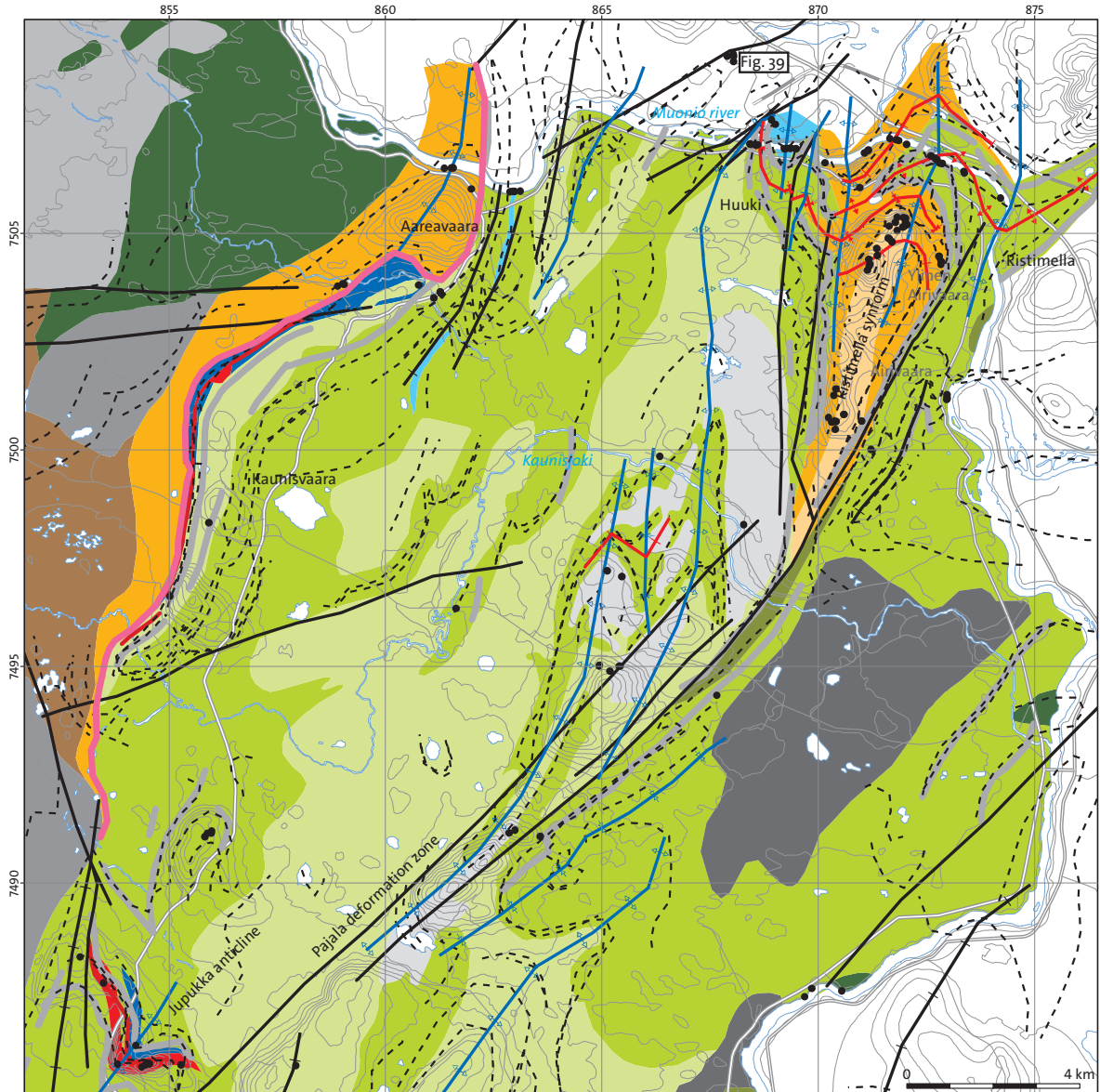
Despite regional migmatization of the metasedimentary rocks, the original bedding (S0) is often still discernible. On Airivaara and Ylinen Airivaara (Fig. 36), a first foliation (S1) developed parallel to the original bedding (S0). Locally, quartz veins are folded isoclinally with what were interpreted to be F1 fold axial planes parallel to the original bedding (Fig. 38A). A second deformation phase (D2) resulted in tight folds (F2), refolding the older structures. Locally, andalusite and sillimanite have grown parallel to the S2 foliation. A younger foliation cuts the first foliation at a high angle (Fig. 38B). It is not clear whether the younger foliation is a cleavage, indicating a second folding event that may not be easily recognisable in the field, or whether the development of this foliation is related to the northeast–southwest-trending Pajala deformation belt, in which case the surfaces would represent small-scale shear bands. Dextral movement along this foliation was mainly observed on Airivaara (Fig. 38C; cf. Grigull & Berggren 2015), where shear bands and asymmetric andalusite blasts indicate dextral kinematics. But shearing can of course also occur along cleavage planes. Since the nature of this foliation could not be determined, it is referred to here as Sx.

Direct evidence of several folding phases was documented in the area around the Ristimella synform. In a quarry in Finland, north of the river Muonioälven (cf. Fig. 36), fold interference patterns were observed in a locally derived block of impure limestone marble (Fig. 39).

Fold interference and crenulation of an earlier foliation was observed in the centre of the key area, north of the Kaunisjoki river. This outcrop lies in the core of a regional F3 antiform (cf. Fig. 36). Here, migmatitic, mica-rich (para?)gneiss shows evidence of at least three deformation events, including at least two folding events, best observed in a hand specimen (Fig. 40).

A first biotite foliation S1 developed during D1. It is possible that this foliation was originally parallel to bedding S0. During the second deformation event D2, S1 was folded about isoclinal to very tight F2 folds, and an axial planar, biotite-lined foliation S2 developed. During a third deformation event D3, the F2 folds, and both the S1 and S2 foliations were folded into open kink folds (F3). The D3 foliation is not pervasive and locally forms a spaced crenulation cleavage. The folds observed in the hand specimen are assumed to represent the large-scale structural architecture in the central part of the key area. The F3 folds are interpreted to be the result of E–W compression during dextral transpression in the Pajala deformation belt. Closer to the main northeast–southwest-striking part of the Pajala deformation belt, the F3 fold axial traces appear to have been dragged into parallelism, with the strike of the deformation zone indicating they formed before or contemporaneously with the development of this deformation zone.

Projecting all structural data from the area around Ristimella and Airivaara into a stereonet shows that bedding as well as foliations strike predominantly NE–SW (Fig. 41). The majority of mineral lineations plunge moderately to the southwest and may have formed during dextral shearing along Sx. South and southwest-plunging fold axes and crenulation lineations are probably the result of F3. The



- |  |   |   |
|--|---|---|
| <ul style="list-style-type: none"> <li><span style="color: red;">—</span> Unconformity</li> <li><span style="color: black;">—</span> fold, unspecified</li> <li><span style="color: red;">⊕</span> F2 syncline, overturned</li> <li><span style="color: red;">+</span> F2 fold, unspecified</li> <li><span style="color: red;">∩</span> F2 fold, anticline</li> <li><span style="color: red;">∪</span> F2 fold, syncline</li> <li><span style="color: red;">⊖</span> F2 fold, anticline, overturned</li> <li><span style="color: blue;">+</span> F3 fold, unspecified</li> <li><span style="color: blue;">∩</span> F3 fold, antiform</li> <li><span style="color: blue;">∪</span> F3 fold, synform</li> <li><span style="color: black;">—</span> Fault</li> <li><span style="color: black;">- -</span> Formline</li> </ul> | <p><b>Intrusive rocks</b></p> <ul style="list-style-type: none"> <li><span style="background-color: #cccccc; border: 1px solid black; display: inline-block; width: 15px; height: 10px;"></span> Granite (GP, 1.82-1.74 Ga)</li> <li><span style="background-color: #a9a9a9; border: 1px solid black; display: inline-block; width: 15px; height: 10px;"></span> Syenitoid-granite (GSDG-GDG, 1.84-1.77 Ga)</li> <li><span style="background-color: #808080; border: 1px solid black; display: inline-block; width: 15px; height: 10px;"></span> Syenitoid-granite (GSDG-GDG, 1.87-1.66 Ga)</li> <li><span style="background-color: #696969; border: 1px solid black; display: inline-block; width: 15px; height: 10px;"></span> Tonalite-granodiorite (GDG-GSDG, 1.92-1.87 Ga)</li> <li><span style="background-color: #404040; border: 1px solid black; display: inline-block; width: 15px; height: 10px;"></span> Gabbroid-dioritoid (GDG-GSDG, 1.92-1.87 Ga)</li> </ul> <p><b>Sammakkovaara group</b></p> <ul style="list-style-type: none"> <li><span style="background-color: #f5deb3; border: 1px solid black; display: inline-block; width: 15px; height: 10px;"></span> Siltstone, pelite</li> <li><span style="background-color: #ffa500; border: 1px solid black; display: inline-block; width: 15px; height: 10px;"></span> Arenite</li> <li><span style="background-color: #8b4513; border: 1px solid black; display: inline-block; width: 15px; height: 10px;"></span> Andesitic to intermediate volcanic rock</li> </ul> | <p><b>Veikkavaara greenstone group</b></p> <ul style="list-style-type: none"> <li><span style="background-color: #cccccc; border: 1px solid black; display: inline-block; width: 15px; height: 10px;"></span> Graphite layer</li> <li><span style="color: red;">—</span> Iron ore formation</li> <li><span style="background-color: #0000ff; border: 1px solid black; display: inline-block; width: 15px; height: 10px;"></span> Dolomite, skarn</li> <li><span style="background-color: #add8e6; border: 1px solid black; display: inline-block; width: 15px; height: 10px;"></span> Limestone</li> <li><span style="background-color: #90ee90; border: 1px solid black; display: inline-block; width: 15px; height: 10px;"></span> Basalt-andesite, basaltic tuff</li> <li><span style="background-color: #ff0000; border: 1px solid black; display: inline-block; width: 15px; height: 10px;"></span> Skarn iron ore</li> <li><span style="background-color: #c0c0c0; border: 1px solid black; display: inline-block; width: 15px; height: 10px;"></span> Shale, slate, graphite rich schist</li> <li><span style="background-color: #6b8e23; border: 1px solid black; display: inline-block; width: 15px; height: 10px;"></span> Arenite (?)</li> </ul> |
|--|---|---|

Figure 36. Simplified geological map of the area between Kaunisvaara and Ristimella. The form lines and all fold axial traces are based on a combination of geophysical lineaments and geological field observations. The black dots show locations of field observations.

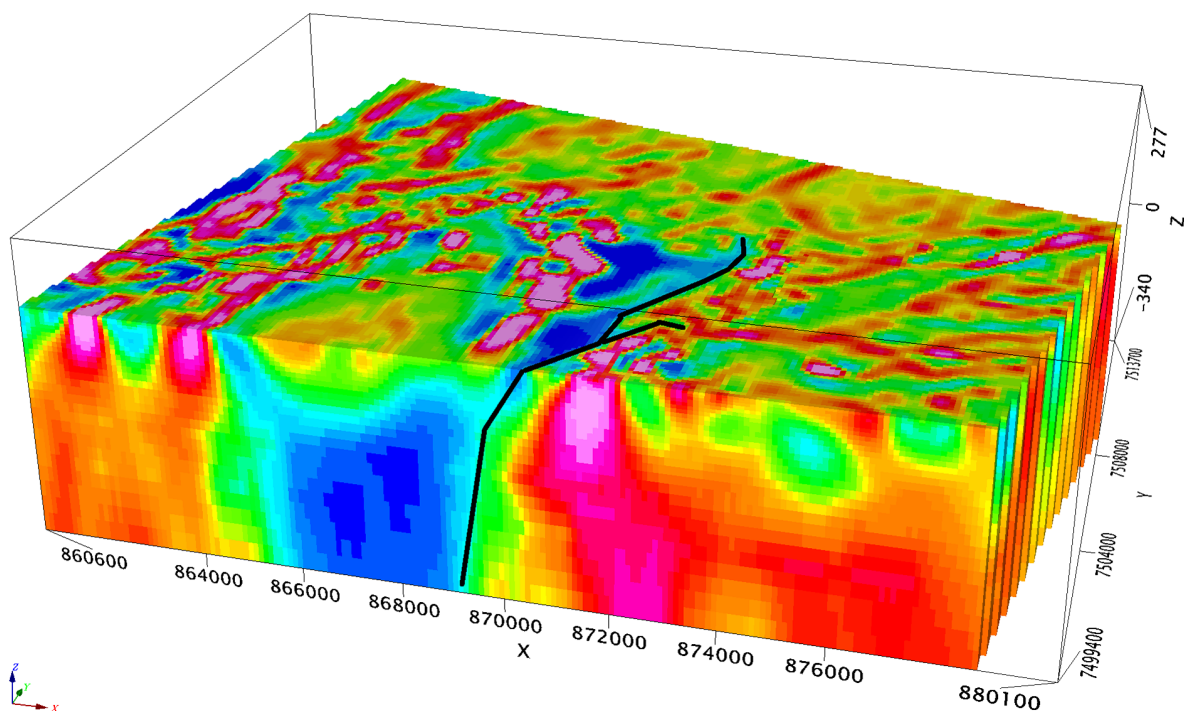


Figure 37. Voxel model based on aeromagnetic data of the Ristimella syncline. Blue represents low-magnetic rocks (e.g. meta-sedimentary rocks), red represents highly magnetic rocks.

Voxi model in Figure 37 also indicates regional-scale south to southwest-plunging antiforms and synforms for the area around the Ristimella synform.

The supracrustal rocks around Ristimella and Huuki have been folded into tight east–west-trending folds with vertical axial planes (F2), indicating north–south compression. Before or synchronously with the development of the northeast–southwest-trending step-over of the Pajala deformation belt, the rocks were folded into open, south to southwest-plunging kink folds (F3) and sheared dextrally. The sketch in Figure 42 illustrates the suggested geological model for the rocks around Ristimella.

## DISCUSSION AND CONCLUSIONS

New geological and geophysical information from key areas in the northern Fennoscandian Shield show that both pre- and syn-orogenic supracrustal rocks were affected by the same folding phases during the orogeny. But the results also indicate that deformation styles and folding phases differ distinctively from west to east. Only one folding event, probably related to contemporaneous thrusting, could be identified in the Kiruna area. The rocks in the Kiruna area are folded into a series of west-verging tight folds. Graben inversion after the deposition of the Hauki quartzite is thought to have led to a minor amount of kink folding in the Kurravaara area. However, more work is needed to support this theory. The Masugnsbyn area has undergone at least three deformation events, of which two, possibly three, are folding events. The second deformation event produced approximately E–W-trending upright, tight folds with horizontal or moderately plunging fold axes (F2) that were kinked around subvertical to moderately plunging fold axes (F3) during the third folding event, resulting in a transposition of F2 fold axial traces now trending both northwest–southeast and northeast–southwest. The Kalixälv dome, while not easily interpreted, may be part of the F3 folding event or correspond to a fourth folding phase that domed the older fold structures. The folding patterns in the Käymjärvi area are comparable to those in the Masugnsbyn key area. Evidence for vertical fold axes in Käymjärvi is

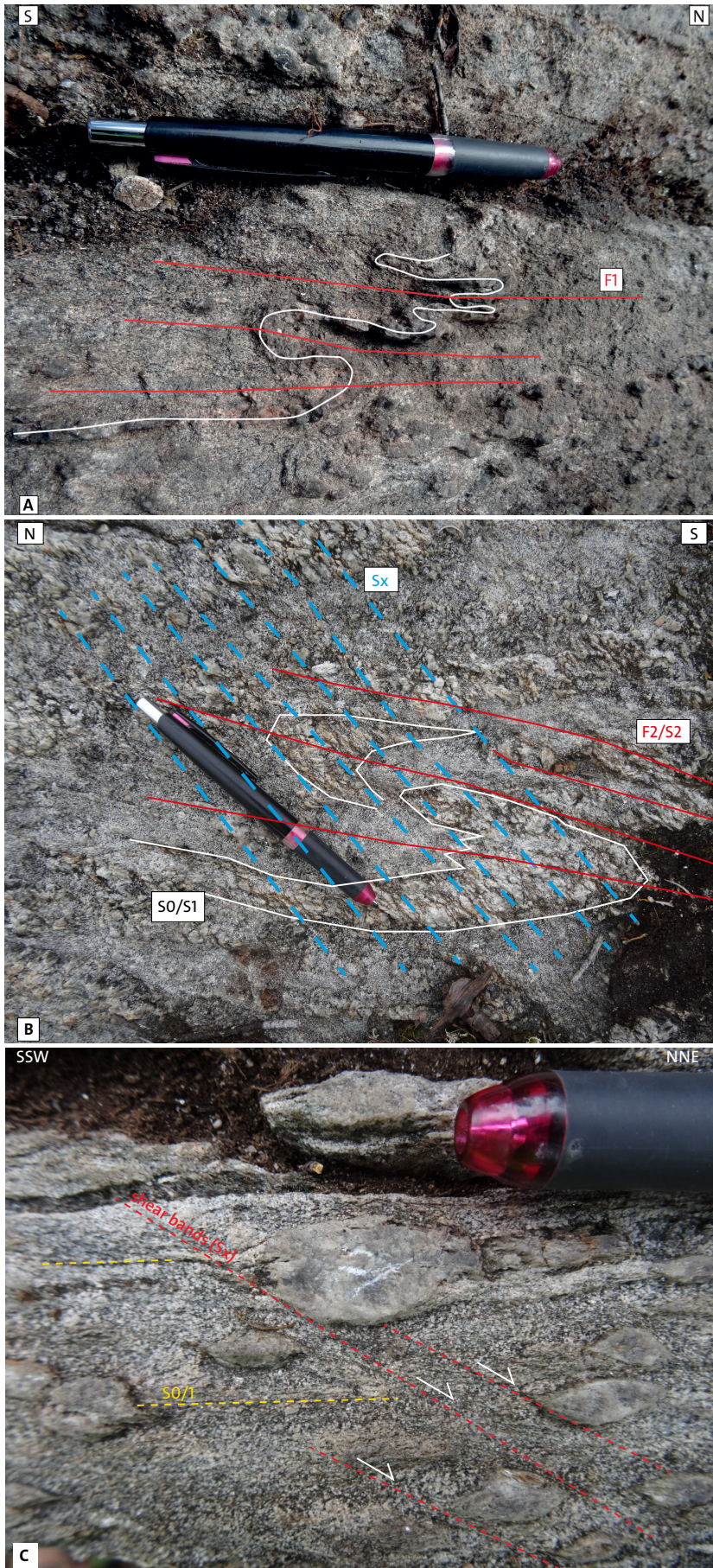


Figure 38. **A.** Migmatite vein asymmetrically folded during F1 in pelitic to psammitic metasedimentary rocks (Sammakkovaara group?). Airivaara (SWEREF99 TM: N7501253, E870365). **B.** Asymmetric F2 folds are intersected by another foliation (Sx) at a high angle. It is unclear whether this foliation is related to the F3 folding or whether it formed due to later dextral shearing within the Pajala deformation belt. Ylinen Airivaara (SWEREF99 TM: N7504142, E871137). **C.** Dextral kinematics observed along shear bands parallel to Sx. Airivaara (SWEREF99 TM: N7500640, E870405).

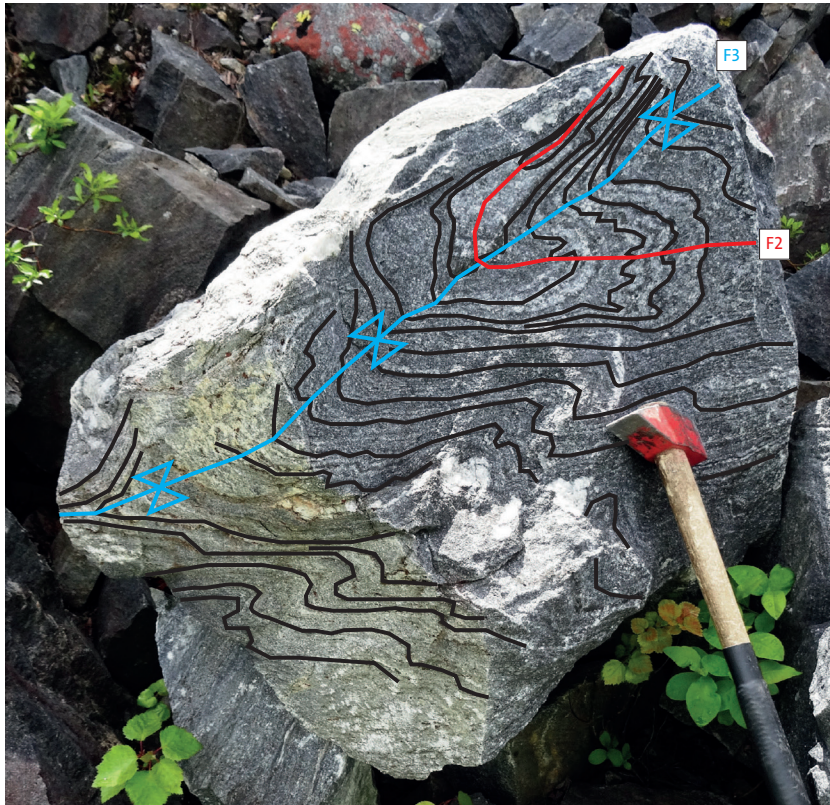


Figure 39. Fold interference observed in a block of impure limestone in a quarry in Finland (SWEREF99 TM: N7509079, E867902). Red: F2 axial trace. Blue: F3 axial trace. Black: metamorphic banding (S1).

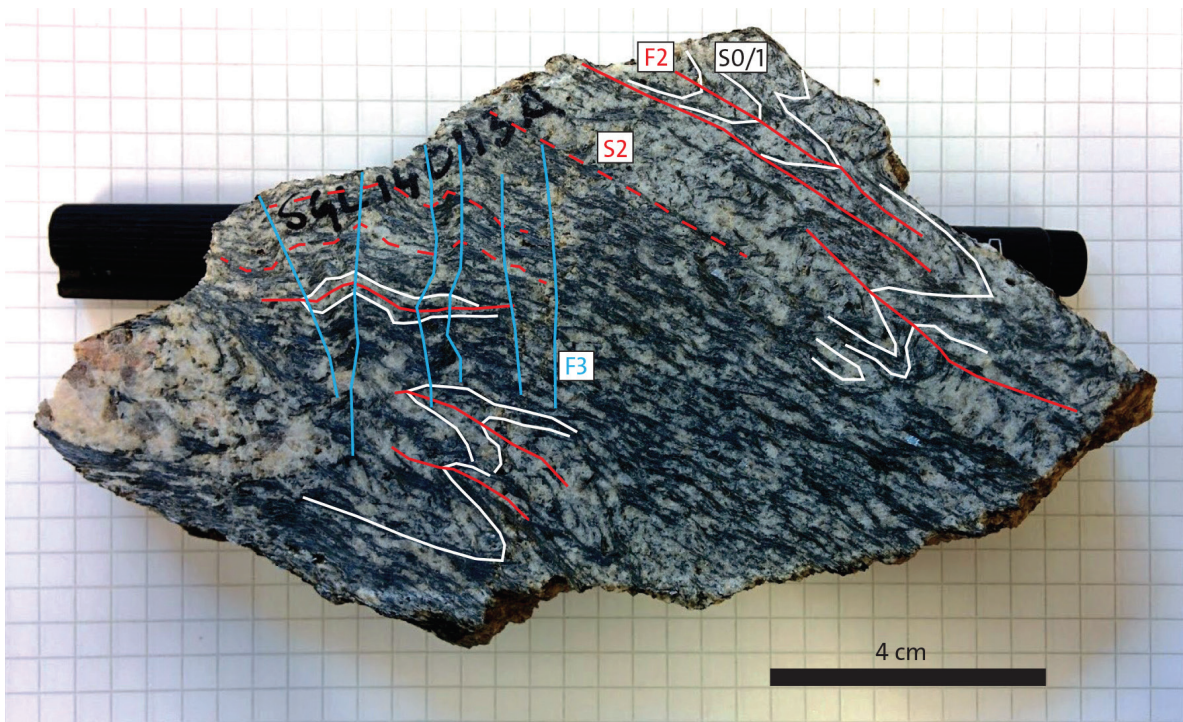


Figure 40. (Para?)gneiss from the central part of the key area (SWEREF99 TM: N7499850, E866343). F3 kink folds crenulate F2 isoclinal folds and older foliations S1 and S2.

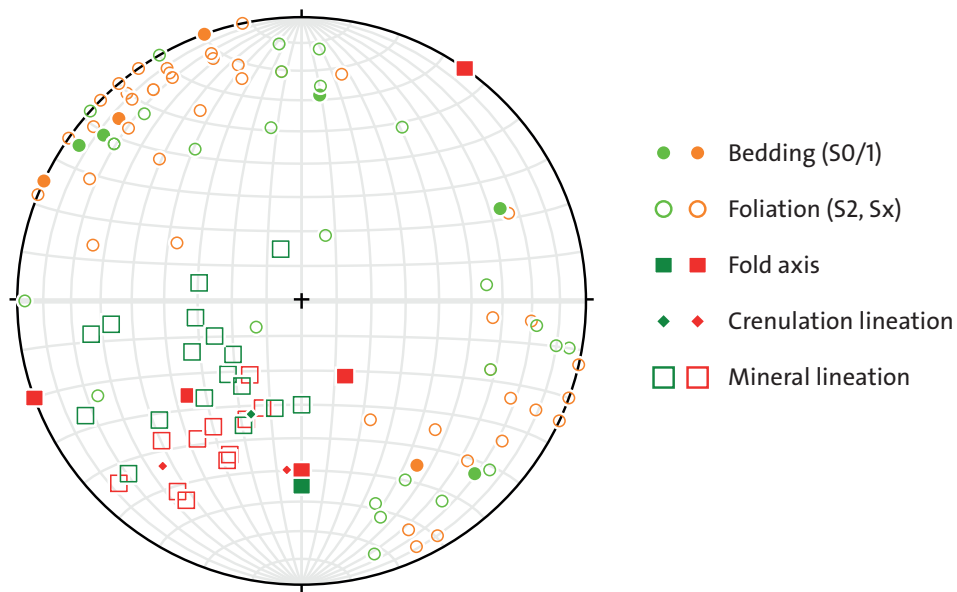


Figure 41. Stereographic projection of structural data collected in the Ristimella area. Green: Veikkavaara greenstone group. Red and orange: metasedimentary rocks, probably Sammakkoavaara group.

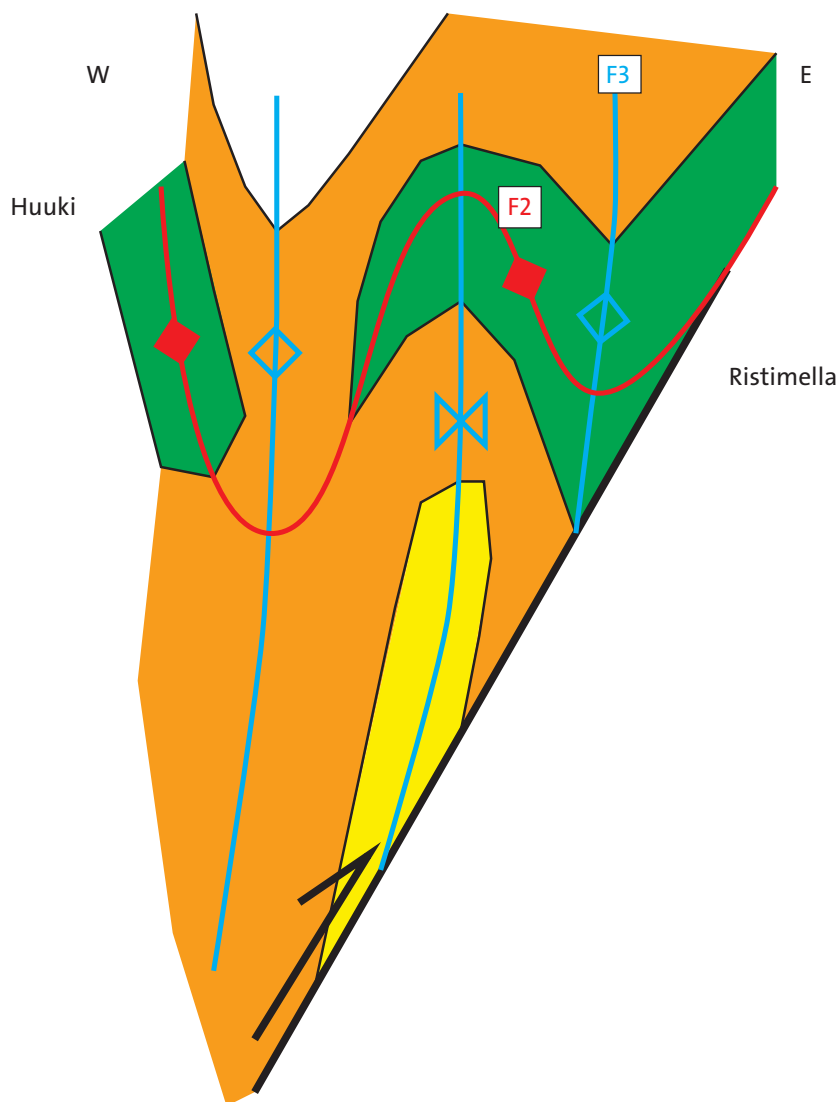


Figure 42. Geological model (map view, not to scale) of the folding pattern between Ristimella and Huuki. Green: Veikkavaara greenstone group, Orange and yellow: metasediments, possibly Sammakkoavaara group younger than the greenstones.

scarce, however. Crenulation folding, indicating a third folding event, is predominantly found along the shore of the river Muonioälven near Huuki, but open S and Z-F3 folds also exist around Sammakko-vaara. At Muonioälven, F2, and F3 axial traces can be drawn from slingram and magnetic anomaly maps. On a regional scale, F3 folds dominate the structural architecture. However, axial traces appear transposed due to dextral shearing along a NE–SW-striking step-over in the Pajala deformation belt. This may be a structure that is younger than all the previously described folding events (cf. Luth et al., 2018).

The observation of folding patterns in several key areas indicates that the rocks to the east of the Karesuando–Arjeplog deformation zone have undergone more phases of deformation than those to the west. The other key areas to the east of the Karesuando–Arjeplog deformation zone, such as Nunasvaara (Lynch et al., 2018), Svappavaara (Grigull & Jönberger 2014) and Liviöjärvi (Luth et al. 2018b), also feature a minimum of two, but potentially more folding phases. In contrast, the rocks in the key areas around Kiruna have been subjected to a single folding event.

## REFERENCES

- Bergh, S.G., Kullerud, K., Armitage, P.E.B., Zwaan, K.B., Corfu, F., Ravna, E.J.K. & Myhre, P.I. 2010: Neoarchaean to Svecofennian tectono-magmatic evolution of the West Troms Basement Complex, North Norway. *Norwegian Journal of Geology* 90, 21–48.
- Bergh, S.G., Corfu, F., Myhre, P.I., Kullerud, K., Armitage, P.E.B., Zwaan, K.B., Ravna, E.K., Holdsworth, R.E., Chattopadhyaya, A., 2012: Was the Precambrian Basement of Western Troms and Lofoten-Vesterålen in Northern Norway Linked to the Lewisian of Scotland? A Comparison of Crustal Components, Tectonic Evolution and Amalgamation History. *In: Sharkov, E. (ed.): Tectonics – Recent Advances. Earth and Planetary Sciences, Geology and Geophysics*, 283–330.
- Bergman, S., Kübler, L. & Martinsson, O., 2001: Description of regional geological and geophysical maps of northern Norrbotten County (east of the Caledonian orogen). *Sveriges geologiska undersökning Ba 56*, 110 pp.
- Bergman, S., Billström, K., Persson, P.-O., Skiöld, T., Evins, P., 2006: U-Pb age evidence for repeated Palaeoproterozoic metamorphism and deformation near the Pajala shear zone in the northern Fennoscandian Shield. *GFF* 128, 7–20.
- Bergman, S., Stephens, M.B., Andersson, J., Kathol, B., Bergman, T., 2012: Sveriges berggrund 1:1 miljon. *Sveriges geologiska undersökning K 423*.
- Berthelsen, A., Marker, M. 1986: 1.9-1.8 Ga old strike-slip megashears in the Baltic shield, and their plate tectonic implications. *Tectonophysics* 128, 163–181.
- Boynton, W.V., 1984: Cosmochemistry of the rare earth elements: meteorite studies. *In: Henderson, P. (ed.): Rare Earth Element Geochemistry. Elsevier, Amsterdam*, 63–114.
- Forsell, P., 1987: The stratigraphy of the Precambrian rocks of the Kiruna district, Northern Sweden. *Sveriges geologiska undersökning C 812*, 36 pp.
- Geijer, P., 1910: Igneous rocks and iron ores of Kiirunavaara, Luossavaara and Tuolluvaara. *Economic Geology* 5, 699–718.
- Grigull, S. & Antal Lundin, I., 2013: Kartering Barents. Background information Kiruna-Jukkasjärvi key area. *SGU-rapport 2013:08*, Sveriges geologiska undersökning. 43 pp.
- Grigull, S. & Jönberger, J., 2014: Geological and geophysical field work in the Kiruna-Jukkasjärvi and Svappavaara key areas, Norrbotten. *Sveriges geologiska undersökning SGU-rapport 2014:10*, 30 pp.
- Grigull, S., Berggren, R. & Jönsson, C., 2014: Background information Käymjärvi-Ristimella key area. *SGU-rapport 2014:30*, Sveriges geologiska undersökning. 37 pp.
- Grigull, S. & Berggren, R., 2015: Geological and geophysical field work in the Käymjärvi-Ristimella key area. *Sveriges geologiska undersökning SGU-rapport 2015:29*, 31 pp.
- Gustafsson, B. & Carlson, L., 1992: Kallosalmi Diamantborrning 1992. Sveriges Geologiska AB Prospekteringsrapport, PRAP92013, 93 pp.

- Hellström, F.A., 2018: Early Svecokarelian migmatization west of the Pajala Deformation Belt, north-eastern Norrbotten Province, northern Sweden. *In: Bergman, S. (ed): Geology of the Northern Norrbotten ore province, northern Sweden. Rapport och Meddelanden 141, Sveriges geologiska undersökning. This volume pp 361–379.*
- Hellström, F. & Jönsson, C., 2014: Summary of geological and geophysical information of the Masugnsbyn key area. *SGU-rapport 2014:21, Sveriges geologiska undersökning. 84 pp.*
- Hellström, F.A., Kumpulainen, R., Jönsson, C., Thomsen, T.B., Huhma, H. & Martinsson, O., 2018: Age and lithostratigraphy of Svecofennian volcanosedimentary rocks at Masugnsbyn, northernmost Sweden – host rocks to Zn-Pb-Cu- and Cu ±Au sulphide mineralisations. *In: Bergman, S. (ed): Geology of the Northern Norrbotten ore province, northern Sweden. Rapport och Meddelanden 141, Sveriges geologiska undersökning. This volume pp 151–203.*
- Henkel, H., 1991: Magnetic crustal structures in northern Fennoscandia. *Tectonophysics 192, 57–79.*
- Irvine, T. N. & Baragar, W. R. A., 1971: A guide to the chemical classification of the common volcanic rocks. *Canadian Journal of Earth Sciences 8, 523–548.*
- Korja, A., Lahtinen, R. & Nironen, M., 2006: The Svecofennian orogen: a collage of microcontinents and island arcs. *In: Gee, D.G. & Stephenson, R.A. (eds.): European Lithosphere Dynamics. Geological Society, London, Memoirs, 32, 561–578.*
- Kumpulainen, R., 2000: The Palaeoproterozoic sedimentary record of northernmost Norrbotten, Sweden. Unpublished report. *Sveriges geologiska undersökning BRAP 200030, 45 pp.*
- Kärki, A., Laajoki, K. & Luukas, J., 1993: Major Paleoproterozoic shear zones of the central Fennoscandian Shield. *Precambrian Research 64, 207–223.*
- Lahtinen, R., Korja, A., Nironen, M. & Heikkinen, P., 2009: Paleoproterozoic accretionary processes in Fennoscandia. *In: Cawood, P.A., Kröner, A. (eds.) Earth Accretionary Systems in Space and Time. Geol. Soc. London Special Publication, 318, 237–256.*
- Lahtinen, R., Huhma, H., Lahaye, Y., Jönsson, E., Manninen, T., Lauri, L.S., Bergman, S., Hellström, F., Niiranen, T. & Nironen, M., 2015a: New geochronological and Sm-Nd constraints across the Pajala shear zone of northern Fennoscandia: Reactivation of a Paleoproterozoic suture. *Precambrian Research 256, 102–119.*
- Lahtinen, R., Sayab, M. & Karell, F., 2015b: Near-orthogonal deformation successions in the poly-deformed Paleoproterozoic Martimo belt: Implications for the tectonic evolution of Northern Fennoscandia. *Precambrian Research 270, 22–28.*
- LeBas, M.J., LeMaitre, R.W., Streckeisen, A. & Zanettin, B., 1986: A chemical classification of volcanic rocks based on the total alkali-silica diagram. *Journal of Petrology 27, 745–750.*
- Lindroos, H., Henkel, H. & 1981: Beskrivning till berggrundskartorna och geofysiska kartorna Huuki NV/NO, SV, SO och Muonionalusta NV, SV/SO. *Sveriges geologiska undersökning Af35–39.*
- Luth, S. & Jönsson, C., 2014: Summary report on the geological and geophysical characteristics of the Liviöjärvi key area. *SGU rapport 2014:29, Sveriges geologiska undersökning. 34 pp.*
- Luth, S., Jönsson, C. & Jönberger, J., 2015: Integrated geological and geophysical studies in the Liviöjärvi key area, Pajala region. *SGU rapport 2015:12, Sveriges geologiska undersökning. 29 pp.*
- Luth, S., Jönberger, J. & Grigull, S., 2018a: The Vakko and Kovo greenstone belts north of Kiruna: Integrating structural geological mapping and geophysical modelling. *In: Bergman, S. (ed): Geology of the Northern Norrbotten ore province, northern Sweden. Rapport och Meddelanden 141, Sveriges geologiska undersökning. This volume pp 287–309.*
- Luth, S., Jönsson, C., Jönberger, J., Grigull, S., Berggren, R., van Assema, B., Smoor, W. & Djuly, T., 2018b: The Pajala Deformation Belt in northeast Sweden: Structural geological mapping and 3D modelling around Pajala. *In: Bergman, S. (ed): Geology of the Northern Norrbotten ore province, northern Sweden. Rapport och Meddelanden 141, Sveriges geologiska undersökning. This volume pp 259–285.*
- Lynch, E.P., Hellström, F.A., Huhma, H., Jönberger, J., Persson, P.-O. & Morris, G.A., 2018: Geology, lithostratigraphy and petrogenesis of c. 2.14 Ga greenstones in the Nunasvaara and Masugnsbyn areas, northernmost Sweden. *In: Bergman, S. (ed): Geology of the Northern Norrbotten ore province, northern Sweden. Rapport och Meddelanden 141, Sveriges geologiska undersökning. This volume pp 19–77.*

- Martinsson, O., 1995: Greenstone and porphyry hosted ore deposits in northern Norrbotten. Report, NUTEK, Project nr. 9200752-3, Div. of Applied Geology, Luleå University of Technology.
- Martinsson, O., 1997: Tectonic setting and metallogeny of the Kiruna greenstones. *Doctoral thesis 1997:19*. Luleå University of Technology.
- Martinsson, O., 1999: Berggrundskartan 30J Rensjön SO. *Sveriges geologiska undersökning Ai 133*.
- Martinsson, O., 2004: Geology and Metallogeny of the Northern Norrbotten Fe-Cu-Au Province. In: R.L. Allen, O. Martinsson & P. Weihed (eds.): Svecofennian ore-forming environments. Volcanic-Associated Zn-Cu-Au-Ag, Intrusion-Associated Cu-Au, Sediment-Hosted Pb-Zn, and Magnetite-Apatite Deposits of Northern Sweden. *Society of Economic Geologists Guidebook Series 33*, 131–148.
- Martinsson, O. & Perdahl, J.-A., 1995: Paleoproterozoic extensional and compressional magmatism in northern Sweden. In: J.-A. Perdahl: Svecofennian volcanism in northern Sweden, *Doctoral thesis 1995:169D, Paper II*, 1–13. Luleå University of Technology.
- Martinsson, O., Allan, Å. & Denisová, N., 2013: Day 2. Skarn iron ores in the Pajala area. In: O. Martinsson & C. Wanhainen (Eds.): Fe oxide and Cu-Au deposits in the northern Norrbotten ore district. Excursion guidebook SWE5, 12th Biennial SGA Meeting, Uppsala, Sweden.
- Martinsson, O. Billström, K., Broman, C., Weihed, P., Wanhainen, C., 2016: Metallogeny of the Northern Norrbotten Ore Province, northern Fennoscandian Shield with emphasis on IOCG and apatite-iron ore deposits. *Ore Geology Reviews* 78, 447–492.
- Martinsson, O., Bergman, S., Persson, P.-O., Schöberg, H., Billström, K. & Shumlyansky, L., 2018: Stratigraphy and ages of Palaeoproterozoic metavolcanic and metasedimentary rocks at Käymäjärvi, northern Sweden. In: Bergman, S. (ed): Geology of the Northern Norrbotten ore province, northern Sweden. *Rapporter och Meddelanden 141*, Sveriges geologiska undersökning. This volume pp 79–105.
- Niiniskorpi, V., 1986: Kurkkionvaara – En Zn-Pb-Cu-mineralisering i norra Sverige en case-studie. LKAB Prospektering, K 86–56, 90 pp.
- Niiranen, T., Poutianen, M. & Mänttari, I., 2007: Geology, geochemistry, fluid inclusion characteristics, and U–Pb age studies on iron oxide–Cu–Au deposits in the Kolari region, northern Finland. *Ore Geology Reviews* 30, 75–105.
- Nironen, M., 1997: The Svecofennian Orogen: a tectonic model. *Precambrian Research* 86, 21–44.
- Offerberg, J., 1967: Beskrivning till Berggrundskartbladen Kiruna NV, NO, SV, SO. *Sveriges geologiska undersökning Af1–4*, 147 pp.
- Olesen, O. & Sandstad, J.S., 1993: Interpretation of the Proterozoic Kautokeino Greenstone Belt, Finnmark, Norway from combined geophysical and geological data. *NGU Bulletin* 425, 43–64.
- Padget, P., 1970: Beskrivning till berggrundskartbladen Tärenö NV, NO, SV, SO. *Sveriges geologiska undersökning Af5–8*, 95 pp.
- Padget, P., 1977: Beskrivning till berggrundskartbladen Pajala NV, NO, SV, SO. *Sveriges geologiska undersökning Af21–24*, 73 pp.
- Parák, T., 1975: The origin of the Kiruna iron ores. *Sveriges geologiska undersökning C 709*, 209 pp.
- Talbot, C.J. & Koyi, H., 1995: Paleoproterozoic intraplate exposed by resultant gravity overturn near Kiruna, northern Sweden. *Precambrian Research* 72, 199–225.
- Vollmer, F.W., Wright, S.F. & Hudleston, P.J., 1984: Early deformation in the Svecokarelian greenstone belt of the Kiruna iron district, northern Sweden. *GFF* 106, 109–118.
- Väänänen, J., 1984: Kolari. Kallioperäkarta 1:100 000 – Maps of Pre-Quaternary Rocks. Geological survey of Finland GTK Map sheet 2713, Kolari.
- Witschard, F., 1984: The geological and tectonic evolution of the Precambrian of northern Sweden – a case for basement reactivation? *Precambrian Research* 23, 273–315.
- Wood, D.A., Joron, J.-L., Treuil, M., Norry, M. & Tarney, J., 1979: Elemental and Sr isotope variations in basic lavas from Iceland and the surrounding ocean floor. *Contributions to Mineralogy and Petrology* 70, 319–339.
- Wright, S.F., 1988: Early Proterozoic deformational history of the Kiruna district, northern Sweden. *Unpublished PhD thesis, University of Minnesota*, 170 pp.



Geological Survey of Sweden  
Box 670  
SE-751 28 Uppsala  
Phone: +46 18 17 90 00  
Fax: +46 18 17 92 10  
[www.sgu.se](http://www.sgu.se)

Uppsala 2018  
ISSN 0349-2176  
ISBN 978-91-7403-393-9  
Tryck: Elanders Sverige AB